Identification and characterization of genes associated with congenital intestinal disease

Désirée Y. van Haaften-Visser

Identification and characterization of genes associated with congenital intestinal disease
Genetische oorzaken van congenitale intestinale aandoeningen

Thesis with a summary in Dutch
Proefschrift met een samenvatting in het Nederlands

Author	Désirée Y. van Haaften-Visser
Cover design	Désirée Y. van Haaften-Visser
Layout	ProefschriftMaken || www.proefschriftmaken.nl
Printing	ProefschriftMaken || www.proefschriftmaken.nl
ISBN	978-94-6295-766-4

Publication of this thesis was financially supported by the Wilhelmina Children's Hospital, Infection & Immunity Utrecht and ChipSoft.

Identification and characterization of genes associated with congenital intestinal disease

Genetische oorzaken van congenitale intestinale aandoeningen

(met een samenvatting in het Nederlands)

Proefschrift

ter verkrijging van de graad van doctor aan de Universiteit Utrecht
op gezag van de rector magnificus, prof. dr. G.J. van der Zwaan,
ingevolge het besluit van het college voor promoties
in het openbaar te verdedigen op
dinsdag 28 november 2017 des middags te 2.30 uur

door

Désirée Yvonne van Haaften – Visser
geboren op 22 januari 1985 te Den Helder

Promotoren: Prof. dr. R.H.J. Houwen
Prof. dr. P.J. Coffer

Table of contents

Chapter 1

General introduction

A proper function of the intestine is essential for normal growth and function of the human body. Disturbance of this function can lead to severe illness, both due to local disease and malnutrition. Treatment can be challenging, since current therapies are often unable to offer a cure, but at best ameliorate symptoms. To improve the therapy of diseases of the gastrointestinal tract a better understanding of the pathogenesis of these disorders is essential.

This thesis focusses on genetically determined intestinal diseases that become symptomatic in the first few months of life. For this group of diseases progress in next-generation sequencing analyses has enabled the identification of the underlying genetic defect in many cases and has improved diagnostics, while the development of better treatment options seems to be just around the corner.

The function of the intestine

Absorptive function of the intestine

The main function of the intestine is digestion and absorption of nutrients [1–3]. Digestion is mediated by intraluminal enzymes, such as the lipase, amylase and trypsin released by the pancreas [2]. Absorption of nutrients is performed by enterocytes [2,4–6], which are the most abundant cell type in the epithelium of the small intestine. For a proper absorptive function, enterocytes are polarized. Their apical membrane contains specific transporters, channels, receptors and enzymes, which enable digestion and absorption of nutrients from the intestinal lumen [7,8]. The surface area and thus the absorptive capacity of the small intestine is maximized by villi, which are finger-like projections of the intestinal mucosa in the lumen of the gut [1–4], and by microvilli, which are microscopic projections of the apical membrane of the enterocytes [2,4,9]. After processing at the apical surface of the enterocyte nutrients are transported to the basolateral membrane, where they are delivered to lymph and blood [7,8]. To this effect some intracellular metabolic modification of the absorbed nutrients can be necessary.

The intestinal immune system

Apart from its role in the digestion and absorption of nutrients, the intestine also has an important immunological function [1–3]. The intestinal immune system tolerates the large amount of intraluminal non-pathogenic, commensal bacteria, which together are called the microbiota. The microbiota has several functions, including digestion of specific dietary components, such as plant polysaccharides, the prevention of colonization with pathogens and the modulation of gastrointestinal motility [10–13]. Furthermore, the microbiota modifies and affects the intestinal immune system, for example by increasing the expression of antimicrobial peptides, stimulating IgA transport and regulating differ-

entiation of Th1 and Th17 effector T-lymphocytes and regulatory T-lymphocytes [13–15]. Both IgA and regulatory T-lymphocytes are key players in the tolerance against microbiota [11].

The intestinal immune system is also the primary defense against the large numbers of pathogens that enter the lumen of the intestine each day. This defense is made up of different layers. Mucus and antimicrobial peptides prevent pathogens reaching the epithelial layer [10,12,13]. Passage through the epithelial layer is hindered by tight junctions and the different epithelial cells [12,13]. Epithelial cells also have immunological functions themselves. Enterocytes, for example, express receptors that recognize pathogens and act as antigen presenting cell by expressing class I and II MHC molecules [6,9]. The different types of immune cells, including dendritic cells, macrophages, T-lymphocytes and B-lymphocytes, that are located in the gut-associated lymphoid tissue in the lamina propria are responsible for antigen sampling and immune responses [12–14].

Congenital diarrhea and malabsorption

Disruption of the absorptive function of the enterocytes, of the interplay between enterocytes and the intestinal immune system, or of the interaction between the intestine and its microbiota may lead to diarrhea, malabsorption or a combination of these two. While diarrhea and malabsorption can occur at any moment in life, patients who present with these disorders in the neonatal period are more likely to have an underlying genetic cause. Studying these patients in detail will not only contribute to a deeper insight into the pathophysiology of the specific disease, but also to a better understanding of the pathophysiology of diarrhea and malabsorption in general, as well as of the normal intestinal physiology. This thesis contributes to these efforts in three different disorders: infantile-onset inflammatory bowel disease, microvillus inclusion disease and a hereditary cause of severe fat intolerance. In addition a novel diagnostic method for identifying disease-causing mutations in patients with congenital diarrhea is described.

Infantile-onset inflammatory bowel disease

Inflammatory bowel disease (IBD) is a severe disease that comprises both Crohn's disease and ulcerative colitis and is characterized by chronic inflammation of the intestine. The main symptoms are chronic diarrhea and abdominal pain. Furthermore, IBD can be associated with rectal bleeding, weight loss, perianal disease and extra-intestinal manifestations [16]. Therapy is dependent on final diagnosis, severity of symptoms and disease course and includes nutritional therapy, immunosuppressive drugs, immunomodulating drugs, biologicals and surgery [16].

The pathogenesis of IBD is still not fully understood. At the center is a disturbance of the balance between the microbiota and the host defense at the level of the intestinal mucosa, caused by genetic and environmental factors [17–20]. The specific defects contributing to this problem are only partly understood. Mechanisms of the pathobiology include, but are probably not limited to, a changed composition of the commensal bacteria (dysbiosis) [21–23], disrupted signalling of pattern recognition receptors [17,24], dysfunction of the unfolded protein response [25–27], inhibition of anti-inflammatory pathways [28–32], defects in the autophagy pathway [17,24,33,34], an impaired epithelial integrity leading to an increased translocation of microorganisms through the epithelium [35,36], and a decreased reactive oxygen species production resulting in a defective host resistance to specific bacteria [37].

Genetic defects are especially important in the pathogenesis of infantile-onset IBD (IO IBD) [20,38,39], which is defined by a presentation in the first two years of life [40] and associated with a more severe disease course and resistance to current therapies [20,36,39,41,42]. In this patient group IBD can even be a monogenic disorder, as opposed to IBD seen in older patients, where a genetic component is obviously important, but which is probably multifactorial [17–20]. Recently disease-causing mutations have been identified in several genes in patients with IO IBD, including *IL10RA*, *IL10RB*, *IL10*, *XIAP*, *ADAM17* and *TTC7A*, and the identification of such genetic mutations is ongoing [28,29,43–45]. The mechanisms by which the disease-causing mutations cause IO IBD can be divided in several subgroups: [20,39,41,42,46,47]

- Epithelial barrier and epithelial response defects, leading to translocation of bacteria and subsequently a physiological inflammatory immune response, for example *ADAM17* mutations causing ADAM17 deficiency [20,39,42,44]
- Dysfunction of neutrophil granulocytes, leading to an increased number of bacteria in the lamina propria and subsequently hyperinflammation, for example *CYBA* mutations causing chronic granulomatous disease [20,39,42]
- Hyper- and auto-inflammation as result of a defective response on intracellular bacterial handling, for example *XIAP* mutations causing X-linked lymphoproliferative syndrome 2 [20,39,42,43]
- Defective T- and B-cell selection and activation, for example *LRBA* mutations causing common variable immune deficiency type 8 [20,39,42]
- Dysfunctional regulatory T cell and IL10 signaling, for example *IL10, IL10RA* and *IL10RB* mutations causing IL10 and IL10 receptor defects [20,28,29,42,48]

Microvillus inclusion disease

Microvillus inclusion disease (MVID) is a severe, autosomal recessively inherited enteropathy that presents with life-threatening, profuse, watery diarrhea. Children with MVID develop intestinal failure and require total parenteral nutrition, often life-long,

or intestinal transplantation. Many MVID patients do not survive the first few years of life [49–51]. The disease is classified in early-onset MVID and late-onset MVID, where symptoms arise either in the first days of life or in the first months of life. Late-onset MVID is often associated with a less severe disease course. Some patients with late-onset MVID may tolerate a small amount of enteral feeding [49,51]. Histologically MVID is characterized by microvillus atrophy at the apical membrane of the mature enterocyte, the accumulation of subapical granules in these cells and the presence of microvillus inclusion bodies in immature enterocytes (**Figure 1**) [49–51].

The great majority of patients with MVID have mutations in *MYO5B*, which encodes the motor protein myosin Vb [52–56]. Myosin Vb consists of two heads and a tail. The heads contain a motor domain that is highly conserved in all classes of myosins. They bind to actin and walk along this filament by a process driven by ATP hydrolysis [50].

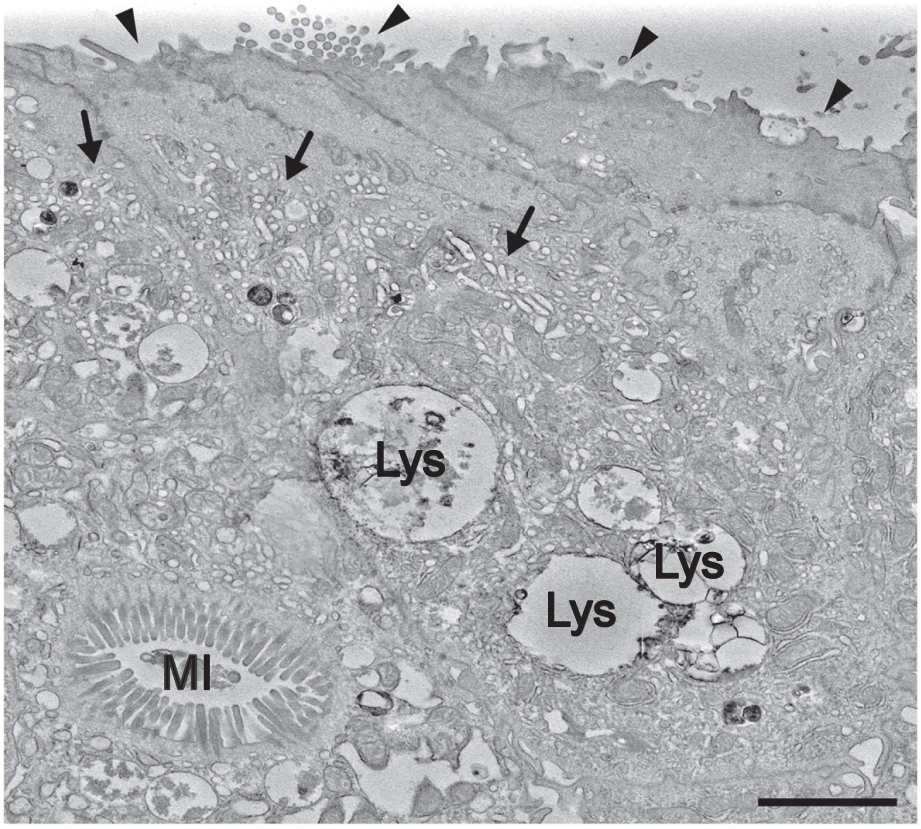

Figure 1. Hallmarks of microvillus inclusion disease (Adapted from [51]). Histologically MVID is characterized by microvillus atrophy (arrow heads), the accumulation of subapical granules (arrows) and microvillus inclusion bodies (MI). Lys = lysosome. Scale bar = 2 µm.

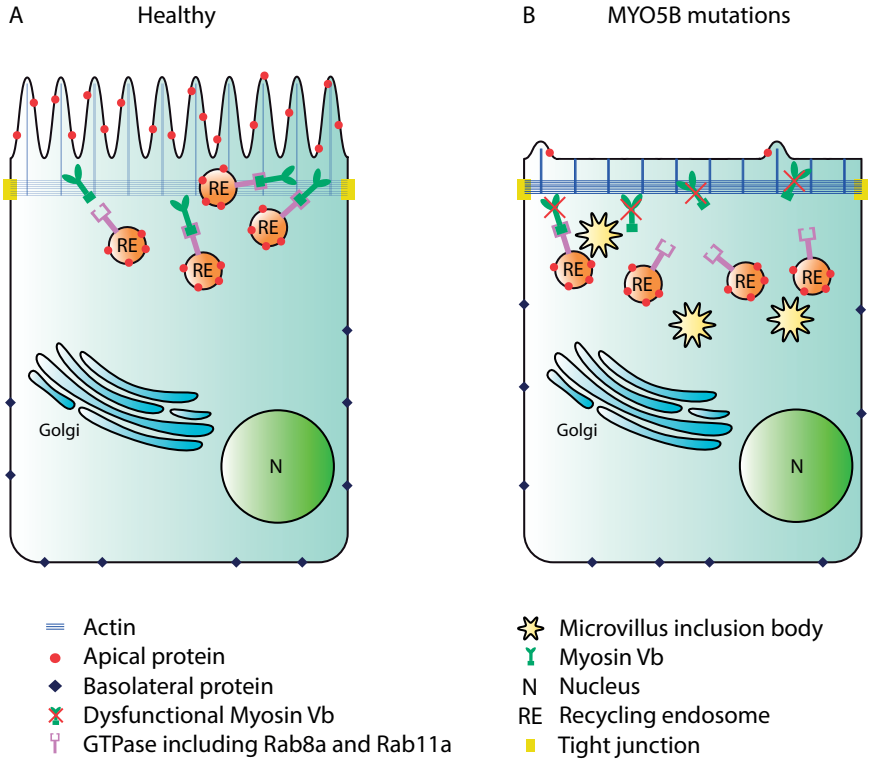

Figure 2. Myosin Vb is essential for transporting recycling endosomes to the apical plasma membrane. Myosin Vb consists of two heads which bind to actin and one tail that binds to specific GTPases on recycling endosomes. By walking along actin myosin Vb transports recycling endosomes to the apical plasma membrane (**A**). When myosin Vb is dysfunctional, this process is disrupted, leading to MVID (**B**).

The tail is responsible for substrate specificity. By binding to small GTPases such as Rab8a and Rab11a on the surface of recycling endosomes, myosin Vb is responsible for trafficking of these vesicles to the apical plasma membrane (**Figure 2**) [57,58]. Mutations in *MYO5B* lead to mislocalization of apical and basolateral membrane proteins resulting in a disruption of the polarity of the cell (**Figure 2**) [54,55,57,59,60]. It is unclear whether microvillus inclusion bodies are a direct result of *MYO5B* mutations or due to disrupted cell polarity. Hypotheses range from endocytosed apical cell membrane to de novo formed intracellular apical domains [51]. Some patients, especially with late-onset MVID, were known to have the classical histological hallmarks of the disease, but no mutations in *MYO5B* [54,61], suggesting that MVID can also be the result of mutations in other genes.

Fat intolerance

Triacylglycerols are the predominant lipids in our diet. In the small intestine triacylglycerol is emulsified by bile salts, subsequently hydrolysed by pancreatic lipases to fatty acids and monoacylglycerol and then absorbed into the enterocyte, both through passive diffusion and through transporters [62,63]. In the endoplasmic reticulum (ER) of the enterocyte fatty acids and monoacylglycerol are combined to diacylglycerol by the enzyme monoacylglycerol O-acyltransferase. Diacylglycerol is either converted to triacylglycerol by diacylglycerol O-acyltransferase 1 (DGAT1) or used to generate phospholipids. [62,63]. Triacylglycerol is stored in lipid droplets or packaged into chylomicrons for secretion. Chylomicrons are large, spherical particles containing triacylglycerol and cholesteryl esters covered by phospholipids and free cholesterol. After release from the ER, chylomicrons are transported to the Golgi system for further modifications and subsequently secreted at the basolateral side of the enterocytes into the lymphatic system (**Figure 3**) [62,63].

Several diseases are known to affect this process, causing fat malabsorption and fat intolerance. Examples of hereditary diseases are chylomicron retention disease, abetalipoproteinemia and homozygous hypobetalipoproteinemia. Clinical manifestations of these diseases are steatorrea, vomiting, abdominal distension and failure to thrive

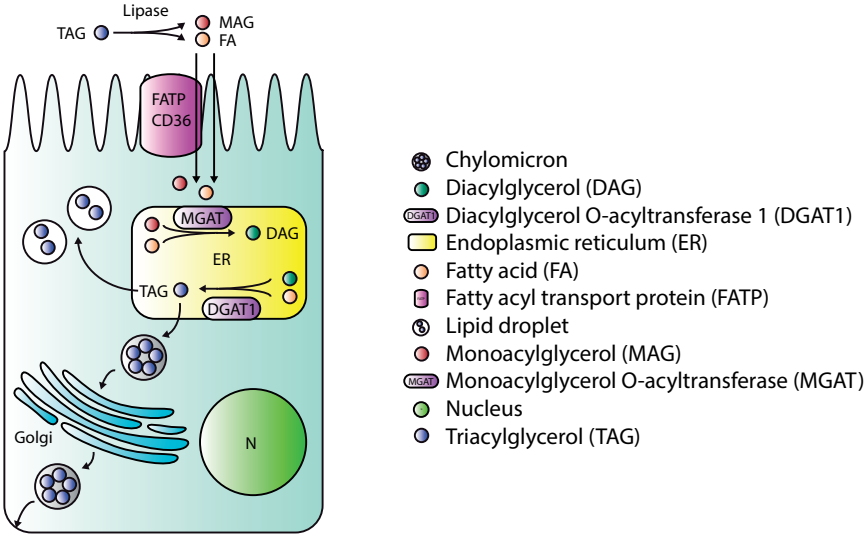

Figure 3. Intestinal triacylglycerol absorption. In the intestinal lumen triacylglycerol is hydrolysed to monoacylglycerol and fatty acids, which are absorbed in the enterocyte by both passive and active transport. In the endoplasmic reticulum monoacylglycerol and fatty acids are converted to diacylglycerol by MGAT, which is subsequently converted to triacylglycerol by DGAT1. Triacylglycerol is either stored in lipid droplets or packaged into chylomicrons and, via the Golgi apparatus, secreted in the lymphatic system.

due to fat malabsorption. The latter can give a deficiency of lipids and lipid soluble vitamins leading to severe complications, including ophthalmological and neurological abnormalities. Current treatment includes a fat-restriced diet and lipid-soluble vitamin suppletion [64–68].

Next-generation sequencing

Although the genetic background of many hereditary causes of congenital diarrhea and malabsorption has already been unravelled, there are still genes in this realm to be identified. Formerly, ie at the beginning of the current millennium, this was done through positional cloning [69–75]. The identification of *SLC26A3*, the gene mutated in congenital chloride diarrhea, is a good example of this approach [76]. Its major drawback is that large or multiple families are required [70,71,73,75]. Although in consanguineous families this process can be facilitated by homozygosity mapping, this process remains tedious and time consuming [70,71,73–75,77].

A major step forward in identifying disease-causing mutations in genetic disorders has been the development of next-generation sequencing (NGS). NGS is a high-throughput sequencing technique, that allows parallel sequencing of many different genes [78–80]. In contrast to positional cloning NGS is also successful in identifying an underlying gene defect when only one or a few patients are available. Furthermore, with NGS a large number of genes can be sequenced in a much shorter time period and with lower costs than with traditional capillary sequencing [75,78,79]. Currently, three different NGS methods are known: whole genome sequencing (WGS), whole exome sequencing (WES) and targeted NGS (TNGS) [81]. With WGS the entire genome is sequenced, both introns and exons. With WES only the coding part of the genome is sequenced. This is currently the method of choice when NGS is used to identify novel disease-causing mutations, since it is known that about 85% of the disease-causing mutations are located in the exome and WES provides far less data than the alternative WGS, which makes interpretation easier [71,74,81,82]. With TNGS a specific set of genes known to be associated with the disorder of interest is investigated. This method is frequently used in the diagnostics of genetically heterogeneous diseases [81,83,84]. TNGS can be performed by sequencing only a fixed set of genes known to be associated with a specific disorder, or by sequencing the whole exome (WES) but analysing only this specific set of genes. One of the first intestinal disease related genes that has been identified using NGS is *XIAP*, which causes X-linked lymphoproliferative syndrome 2 [43].

Aim of this thesis

This thesis aims to understand the pathogenesis of a few rare hereditary intestinal diseases through the use of molecular genetic methods, including next-generation sequencing, followed by *in vitro* functional assays. This approach of 'functional genomics' has the ultimate goal to improve the therapy of these diseases.

Outline of this thesis

Chapter 2 describes the association of mutations in *ANKZF1* with infantile-onset IBD. ANKZF1 is an essential protein in the mitochondrial response to cellular stress and ANKZF1 deficiency leads to mitochondrial dysfunction. Out of thirteen IO IBD patients two patients were found to have two mutated *ANKZF1* alleles. In both patients *ANKZF1* mutations resulted in dysfunctional ANKZF1.

Chapter 3 reports the identification of mutations in *STX3* as a novel cause of microvillus inclusion disease. *STX3* encodes syntaxin 3, which is a target N-ethylmaleimide-sensitive factor attachment protein receptor (t-SNARE) on the apical plasma membrane of several cell types. By binding to SNARE proteins on vesicles (v-SNAREs) syntaxin 3 is responsible for the fusion of these vesicles with the apical plasma membrane. The mutations identified in two unrelated patients with MVID result in a deficiency of syntaxin 3 leading to mislocalization of apical cargo and subsequently a disturbed polarity of the enterocyte and MVID.

Chapter 4 describes a novel mutation in *DGAT1* as cause of severe congenital fat intolerance. In two brothers with congenital fat intolerance a homozygous mutation in *DGAT1* was found which results in an increased ubiquitin-mediated proteasomal degradation of DGAT1. Presumably DGAT1 deficiency leads to a decreased conversion of diacylglycerol to triacylglycerol and subsequently fat malabsorption.

Chapter 5 introduces next-generation sequencing as a novel tool in the diagnostics of congenital diarrhea. Furthermore it describes a novel diagnostic approach, where the whole exome is sequenced and the subsequent analysis is performed in two steps. First, all genes known to be associated with congenial diarrhea are sequenced. When no underlying mutation is identified, the analysis is extended to the whole exome.

Chapter 6 discusses the results described in this thesis and the clinical implications.

This thesis contributes to the unravelling of the pathogenesis of a few rare congenital intestinal diseases, which is crucial to develop novel treatment options for these patients.

References

1. Kliegman RM, Behrman RE, Jenson HB, Stanton BF. Nelson Textbook of Pediatrics. 18th ed. 2007
2. Young B, Heath JW. Wheater's Functional Histology. 4th ed. 2000
3. Cotran RS, Kumar V, Colling T. Robbins Pathologic basis of disease. 6th ed. 1999
4. Barker N, van de Wetering M, Clevers H. The intestinal stem cell. *Genes Dev* 2008;22:1856–1864
5. Shifrin DA, Tyska MJ. Ready…aim…fire into the lumen: a new role for enterocyte microvilli in gut host defense. *Gut Microbes* 2012;3:460–462
6. Miron N, Cristea V. Enterocytes: active cells in tolerance to food and microbial antigens in the gut. *Clin Exp Immunol* 2012;167:405–412
7. Massey-Harroche D. Epithelial cell polarity as reflected in enterocytes. *Microsc Res Tech* 2000;49: 353–362
8. Rodriguez-Boulan E, Macara IG. Organization and execution of the epithelial polarity programme. *Nat Rev Mol Cell Biol* 2014;15:225–242
9. Snoeck V, Goddeeris B, Cox E. The role of enterocytes in the intestinal barrier function and antigen uptake. *Microbes Infect* 2005;7:997–1004
10. Kato LM, Kawamoto S, Maruya M, Fagarasan S. The role of the adaptive immune system in regulation of gut microbiota. *Immunol Rev* 2014;260:67–75
11. Elson CO, Alexander KL. Host-microbiota interactions in the intestine. *Dig Dis* 2015;33:131–136
12. Viggiano D, Ianiro G, Vanella G, Bibbò S, Bruno G, Simeone G, Mele G. Gut barrier in health and disease: focus on childhood. *Eur Rev Med Pharmacol Sci* 2015;19:1077–1085
13. Kunisawa J, Kiyono H. Immune regulation and monitoring at the epithelial surface of the intestine. *Drug Discov Today* 2013;18:87–92
14. Tomkovich S, Jobin C. Microbiota and host immune responses: a love-hate relationship. *Immunology* 2015;147:1-10
15. Caricilli AM, Castoldi A, Câmara NOS. Intestinal barrier: A gentlemen's agreement between microbiota and immunity. *World J Gastrointest Pathophysiol* 2014;5:18–32
16. Gijsbers CFM, Groeneweg M, Kneepkens CMF, Kokke FTM, Koot BGP RE. Werkboek kinder-maag-darm-leverziekten. 2014
17. Khor B, Gardet A, Xavier RJ. Genetics and pathogenesis of inflammatory bowel disease. *Nature* 2011;474:307–317
18. Xavier RJ, Podolsky DK. Unravelling the pathogenesis of inflammatory bowel disease. *Nature* 2007; 448:427–434
19. Kaser A, Zeissig S, Blumberg RS. Inflammatory bowel disease. *Annu Rev Immunol* 2010;28:573–621
20. Uhlig HH, Schwerd T, Koletzko S, Shah N, Kammermeier J, Elkadri A, Ouahed J, Wilson DC, Travis SP, Turner D, Klein C, Snapper SB, Muise AM. The diagnostic approach to monogenic very early onset inflammatory bowel disease. *Gastroenterology* 2014;147:990–1007
21. Sartor RB. Microbial influences in inflammatory bowel diseases. *Gastroenterology* 2008;134: 577–594
22. Knights D, Lassen KG, Xavier RJ. Advances in inflammatory bowel disease pathogenesis: linking host genetics and the microbiome. *Gut* 2013;62:1505–1510

23. Round JL, Mazmanian SK. The gut microbiota shapes intestinal immune responses during health and disease. *Nat Rev Immunol* 2009;9:313–323
24. Fritz T, Niederreiter L, Adolph T, Blumberg RS, Kaser A. Crohn's disease: NOD2, autophagy and ER stress converge. *Gut* 2011;60:1580–1588
25. Kaser A, Lee A-H, Franke A, Glickman JN, Zeissig S, Tilg H, Nieuwenhuis EES, Higgins DE, Schreiber S, Glimcher LH, Blumberg RS. XBP1 links ER stress to intestinal inflammation and confers genetic risk for human inflammatory bowel disease. *Cell* 2008;134:743–756
26. Kaser A, Martínez-Naves E, Blumberg RS. Endoplasmic reticulum stress: implications for inflammatory bowel disease pathogenesis. *Curr Opin Gastroenterol* 2010;26:318–326
27. Adolph T-E, Niederreiter L, Blumberg RS, Kaser A. Endoplasmic reticulum stress and inflammation. *Dig Dis* 2012;30:341–346
28. Glocker E-O, Frede N, Perro M, Sebire N, Elawad M, Shah N, Grimbacher B. Infant colitis--it's in the genes. *Lancet* 2010;376:1272
29. Glocker E-O, Kotlarz D, Boztug K, Gertz EM, Schäffer AA, Noyan F, Perro M, Diestelhorst J, Allroth A, Murugan D, Hätscher N, Pfeifer D, Sykora K-W, Sauer M, Kreipe H, Lacher M, Nustede R, Woellner C, Baumann U, Salzer U, Koletzko S, Shah N, Segal AW, Sauerbrey A, Buderus S, Snapper SB, Grimbacher B, Klein C. Inflammatory bowel disease and mutations affecting the interleukin-10 receptor. *N Engl J Med* 2009;361:2033–2045
30. Begue B, Verdier J, Rieux-Laucat F, Goulet O, Morali A, Canioni D, Hugot J-P, Daussy C, Verkarre V, Pigneur B, Fischer A, Klein C, Cerf-Bensussan N, Ruemmele FM. Defective IL10 signaling defining a subgroup of patients with inflammatory bowel disease. *Am J Gastroenterol* 2011;106:1544–1555
31. Lee CH, Hsu P, Nanan B, Nanan R, Wong M, Gaskin KJ, Leong RW, Murchie R, Muise AM, Stormon MO. Novel de novo mutations of the interleukin-10 receptor gene lead to infantile onset inflammatory bowel disease. *J Crohns Colitis* 2014;8:1551–1556
32. Shim JO, Hwang S, Yang HR, Moon JS, Chang JY, Ko JS, Park SS, Kang G-H, Kim WS, Seo JK. Interleukin-10 receptor mutations in children with neonatal-onset Crohn's disease and intractable ulcerating enterocolitis. *Eur J Gastroenterol Hepatol* 2013;25:1235–1240
33. Parkes M, Barrett JC, Prescott NJ, Tremelling M, Anderson CA, Fisher SA, Roberts RG, Nimmo ER, Cummings FR, Soars D, Drummond H, Lees CW, Khawaja SA, Bagnall R, Burke DA, Todhunter CE, Ahmad T, Onnie CM, McArdle W, Strachan D, Bethel G, Bryan C, Lewis CM, Deloukas P, Forbes A, Sanderson J, Jewell DP, Satsangi J, Mansfield JC, Cardon L, Mathew CG. Sequence variants in the autophagy gene IRGM and multiple other replicating loci contribute to Crohn's disease susceptibility. *Nat Genet* 2007;39:830–832
34. Hampe J, Franke A, Rosenstiel P, Till A, Teuber M, Huse K, Albrecht M, Mayr G, De La Vega FM, Briggs J, Günther S, Prescott NJ, Onnie CM, Häsler R, Sipos B, Fölsch UR, Lengauer T, Platzer M, Mathew CG, Krawczak M, Schreiber S. A genome-wide association scan of nonsynonymous SNPs identifies a susceptibility variant for Crohn disease in ATG16L1. *Nat Genet* 2007;39:207–211
35. Wallace KL, Zheng L-B, Kanazawa Y, Shih DQ. Immunopathology of inflammatory bowel disease. *World J Gastroenterol* 2014;20:6–21
36. Bianco AM, Girardelli M, Tommasini A. Genetics of inflammatory bowel disease from multifactorial to monogenic forms. *World J Gastroenterol* 2015;21:12296–12310

37. Hayes P, Dhillon S, O'Neill K, Thoeni C, Hui KY, Elkadri A, Guo CH, Kovacic L, Aviello G, Alvarez LA, Griffiths AM, Snapper SB, Brant SR, Doroshow JH, Silverberg MS, Peter I, McGovern DPB, Cho J, Brumell JH, Uhlig HH, Bourke B, Muise AA, Knaus UG. Defects in NADPH Oxidase Genes NOX1 and DUOX2 in Very Early Onset Inflammatory Bowel Disease. *Cell Mol Gastroenterol Hepatol* 2015;1:489–502
38. Kelsen JR, Dawany N, Moran CJ, Petersen B-S, Sarmady M, Sasson A, Pauly-Hubbard H, Martinez A, Maurer K, Soong J, Rappaport E, Franke A, Keller A, Winter HS, Mamula P, Piccoli D, Artis D, Sonnenberg GF, Daly M, Sullivan KE, Baldassano RN, Devoto M. Exome sequencing analysis reveals variants in primary immunodeficiency genes in patients with very early onset inflammatory bowel disease. *Gastroenterology* 2015;149:1415–1424
39. Kelsen JR, Baldassano RN, Artis D, Sonnenberg GF. Maintaining intestinal health: the genetics and immunology of very early onset inflammatory bowel disease. *Cell Mol Gastroenterol Hepatol* 2015;1: 462–476
40. Levine A, Griffiths A, Markowitz J, Wilson DC, Turner D, Russell RK, Fell J, Ruemmele FM, Walters T, Sherlock M, Dubinsky M, Hyams JS. Pediatric modification of the Montreal classification for inflammatory bowel disease: the Paris classification. *Inflamm Bowel Dis* 2011;17:1314–1321
41. Kammermeier J, Dziubak R, Pescarin M, Drury S, Godwin H, Reeve K, Chadokufa S, Huggett B, Sider S, James C, Acton N, Cernat E, Gasparetto M, Noble-Jamieson G, Kiparissi F, Elawad M, Beales PL, Sebire NJ, Gilmour K, Uhlig HH, Bacchelli C, Shah N. Phenotypic and Genotypic Characterisation of Inflammatory Bowel Disease Presenting Before the Age of 2 years. *J Crohn's Colitis* 2017;11:60–69
42. Uhlig HH. Monogenic diseases associated with intestinal inflammation: implications for the understanding of inflammatory bowel disease. *Gut* 2013;62:1795–1805
43. Worthey EA, Mayer AN, Syverson GD, Helbling D, Bonacci BB, Decker B, Serpe JM, Dasu T, Tschannen MR, Veith RL, Basehore MJ, Broeckel U, Tomita-Mitchell A, Arca MJ, Casper JT, Margolis DA, Bick DP, Hessner MJ, Routes JM, Verbsky JW, Jacob HJ, Dimmock DP. Making a definitive diagnosis: successful clinical application of whole exome sequencing in a child with intractable inflammatory bowel disease. *Genet Med* 2011;13:255–262
44. Blaydon DC, Biancheri P, Di W-L, Plagnol V, Cabral RM, Brooke MA, van Heel DA, Ruschendorf F, Toynbee M, Walne A, O'Toole EA, Martin JE, Lindley K, Vulliamy T, Abrams DJ, MacDonald TT, Harper JI, Kelsell DP. Inflammatory skin and bowel disease linked to ADAM17 deletion. *N Engl J Med* 2011;365:1502–1508
45. Avitzur Y, Guo C, Mastropaolo LA, Bahrami E, Chen H, Zhao Z, Elkadri A, Dhillon S, Murchie R, Fattouh R, Huynh H, Walker JL, Wales PW, Cutz E, Kakuta Y, Dudley J, Kammermeier J, Powrie F, Shah N, Walz C, Nathrath M, Kotlarz D, Puchaka J, Krieger JR, Racek T, Kirchner T, Walters TD, Brumell JH, Griffiths AM, Rezaei N, Rashtian P, Najafi M, Monajemzadeh M, Pelsue S, McGovern DPB, Uhlig HH, Schadt E, Klein C, Snapper SB, Muise AM. Mutations in tetratricopeptide repeat domain 7A result in a severe form of very early onset inflammatory bowel disease. *Gastroenterology* 2014;146:1028–1039
46. Uhlig HH, Schwerd T. From Genes to Mechanisms. *Inflamm Bowel Dis* 2016;22:202–212

47. Ashton JJ, Andreoletti G, Coelho T, Haggarty R, Batra A, Afzal NA, Beattie RM, Ennis S. Identification of Variants in Genes Associated with Single-gene Inflammatory Bowel Disease by Whole-exome Sequencing. *Inflamm Bowel Dis* 2016;22:2317–2327
48. Kelsen JR, Dawany N, Moran CJ, Petersen B-S, Sarmady M, Sasson A, Pauly-Hubbard H, Martinez A, Maurer K, Soong J, Rappaport E, Franke A, Keller A, Winter HS, Mamula P, Piccoli D, Artis D, Sonnenberg GF, Daly M, Sullivan KE, Baldassano RN, Devoto M. Exome Sequencing Analysis Reveals Variants in Primary Immunodeficiency Genes in Patients With Very Early Onset Inflammatory Bowel Disease. *Gastroenterology* 2015;149:1415–1424
49. Ruemmele FM, Schmitz J, Goulet O. Microvillous inclusion disease (microvillous atrophy). *Orphanet J Rare Dis* 2006;1:22
50. van der Velde KJ, Dhekne HS, Swertz MA, Sirigu S, Ropars V, Vinke PC, Rengaw T, van den Akker PC, Rings EHHM, Houdusse A, van IJzendoorn SCD. An overview and online registry of microvillus inclusion disease patients and their MYO5B mutations. *Hum Mutat* 2013;34:1597–1605
51. Vogel GF, Hess MW, Pfaller K, Huber LA, Janecke AR, Müller T. Towards understanding microvillus inclusion disease. *Mol Cell Pediatr* 2016;3:3
52. Erickson RP, Larson-Thomé K, Valenzuela RK, Whitaker SE, Shub MD. Navajo microvillous inclusion disease is due to a mutation in MYO5B. *Am J Med Genet A* 2008;146A:3117–3119
53. Ruemmele FM, Müller T, Schiefermeier N, Ebner HL, Lechner S, Pfaller K, Thöni CE, Goulet O, Lacaille F, Schmitz J, Colomb V, Sauvat F, Revillon Y, Canioni D, Brousse N, de Saint-Basile G, Lefebvre J, Heinz-Erian P, Enninger A, Utermann G, Hess MW, Janecke AR, Huber LA. Loss-of-function of MYO5B is the main cause of microvillus inclusion disease: 15 novel mutations and a CaCo-2 RNAi cell model. *Hum Mutat* 2010;31:544–551
54. Müller T, Hess MW, Schiefermeier N, Pfaller K, Ebner HL, Heinz-Erian P, Ponstingl H, Partsch J, Röllinghoff B, Köhler H, Berger T, Lenhartz H, Schlenck B, Houwen RJ, Taylor CJ, Zoller H, Lechner S, Goulet O, Utermann G, Ruemmele FM, Huber LA, Janecke AR. MYO5B mutations cause microvillus inclusion disease and disrupt epithelial cell polarity. *Nat Genet* 2008;40:1163–1165
55. Szperl AM, Golachowska MR, Bruinenberg M, Prekeris R, Thunnissen A-MWH, Karrenbeld A, Dijkstra G, Hoekstra D, Mercer D, Ksiazyk J, Wijmenga C, Wapenaar MC, Rings EHHM, van IJzendoorn SCD. Functional characterization of mutations in the myosin Vb gene associated with microvillus inclusion disease. *J Pediatr Gastroenterol Nutr* 2011;52:307–313
56. Wiegerinck CL, Janecke AR, Schneeberger K, Vogel GF, van Haaften-Visser DY, Escher JC, Adam R, Thöni CE, Pfaller K, Jordan AJ, Weis C-A, Nijman IJ, Monroe GR, van Hasselt PM, Cutz E, Klumperman J, Clevers H, Nieuwenhuis EES, Houwen RHJ, van Haaften G, Hess MW, Huber LA, Stapelbroek JM, Müller T, Middendorp S. Loss of syntaxin 3 causes variant microvillus inclusion disease. *Gastroenterology* 2014;147:65–68
57. Roland JT, Bryant DM, Datta A, Itzen A, Mostov KE, Goldenring JR. Rab GTPase-Myo5B complexes control membrane recycling and epithelial polarization. *Proc Natl Acad Sci U S A* 2011;108:2789–2794
58. Lapierre LA, Kumar R, Hales CM, Navarre J, Bhartur SG, Burnette JO, Provance DW, Mercer JA, Bähler M, Goldenring JR. Myosin vb is associated with plasma membrane recycling systems. *Mol Biol Cell* 2001;12:1843–1857

59. Thoeni CE, Vogel GF, Tancevski I, Geley S, Lechner S, Pfaller K, Hess MW, Müller T, Janecke AR, Avitzur Y, Muise A, Cutz E, Huber LA. Microvillus inclusion disease: loss of Myosin vb disrupts intracellular traffic and cell polarity. *Traffic* 2014;15:22–42
60. Knowles BC, Roland JT, Krishnan M, Tyska MJ, Lapierre LA, Dickman PS, Goldenring JR, Shub MD. Myosin Vb uncoupling from RAB8A and RAB11A elicits microvillus inclusion disease. *J Clin Invest* 2014;124:2947–2962
61. Perry A, Bensallah H, Martinez-Vinson C, Berrebi D, Arbeille B, Salomon J, Goulet O, Marinier E, Drunat S, Samson-Bouma M-E, Gérard B, Hugot J-P. Microvillous atrophy: atypical presentations. *J Pediatr Gastroenterol Nutr* 2014;59:779–785
62. Hussain MM. Intestinal lipid absorption and lipoprotein formation. *Curr Opin Lipidol* 2014;25: 200–206
63. Abumrad NA, Davidson NO. Role of the gut in lipid homeostasis. *Physiol Rev* 2012;92:1061–1085
64. Hooper AJ, Burnett JR. Update on primary hypobetalipoproteinemia. *Curr Atheroscler Rep* 2014; 16:423
65. Lee J, Hegele RA. Abetalipoproteinemia and homozygous hypobetalipoproteinemia: a framework for diagnosis and management. *J Inherit Metab Dis* 2014;37:333–339
66. Zamel R, Khan R, Pollex RL, Hegele RA. Abetalipoproteinemia: two case reports and literature review. *Orphanet J Rare Dis* 2008;3:19
67. Cefalù AB, Norata GD, Ghiglioni DG, Noto D, Uboldi P, Garlaschelli K, Baragetti A, Spina R, Valenti V, Pederiva C, Riva E, Terracciano L, Zoja A, Grigore L, Averna MR, Catapano AL. Homozygous familial hypobetalipoproteinemia: two novel mutations in the splicing sites of apolipoprotein B gene and review of the literature. *Atherosclerosis* 2015;239:209–217
68. Peretti N, Sassolas A, Roy CC, Deslandres C, Charcosset M, Castagnetti J, Pugnet-Chardon L, Moulin P, Labarge S, Bouthillier L, Lachaux A, Levy E. Guidelines for the diagnosis and management of chylomicron retention disease based on a review of the literature and the experience of two centers. *Orphanet J Rare Dis* 2010;5:24
69. Xu L, Li Y. Positional cloning. *Methods Mol Biol* 2000;136:285–296
70. Sheffield VC, Nishimura DY, Stone EM. Novel approaches to linkage mapping. *Curr Opin Genet Dev* 1995;5:335–341
71. Rabbani B, Mahdieh N, Hosomichi K, Nakaoka H, Inoue I. Next-generation sequencing: impact of exome sequencing in characterizing Mendelian disorders. *J Hum Genet* 2012;57:621–632
72. Papadopoulos N. Introduction to positional cloning. *Clin Exp Allergy* 1995;25 Suppl 2:116–118
73. Fuchs SA, Harakalova M, van Haaften G, van Hasselt PM, Cuppen E, Houwen RHJ. Application of exome sequencing in the search for genetic causes of rare disorders of copper metabolism. *Metallomics* 2012;4:606–613
74. Botstein D, Risch N. Discovering genotypes underlying human phenotypes: past successes for mendelian disease, future approaches for complex disease. *Nat Genet* 2003;33 Suppl:228–237
75. Kuhlenbäumer G, Hullmann J, Appenzeller S. Novel genomic techniques open new avenues in the analysis of monogenic disorders. *Hum Mutat* 2011;32:144–151
76. Mäkelä S, Kere J, Holmberg C, Höglund P. SLC26A3 mutations in congenital chloride diarrhea. *Hum Mutat* 2002;20:425–438

77. Lander ES, Botstein D. Homozygosity mapping: a way to map human recessive traits with the DNA of inbred children. *Science* 1987;236:1567–1570
78. Mardis ER. Next-generation DNA sequencing methods. *Annu Rev Genomics Hum Genet* 2008;9: 387–402
79. Metzker ML. Sequencing technologies - the next generation. *Nat Rev Genet* 2010;11:31–46
80. Shendure J, Ji H. Next-generation DNA sequencing. *Nat Biotechnol* 2008;26:1135–45
81. de Koning TJ, Jongbloed JDH, Sikkema-Raddatz B, Sinke RJ. Targeted next-generation sequencing panels for monogenetic disorders in clinical diagnostics: the opportunities and challenges. *Expert Rev Mol Diagn* 2015;15:61–70
82. Majewski J, Schwartzentruber J, Lalonde E, Montpetit A, Jabado N. What can exome sequencing do for you? *J Med Genet* 2011;48:580–589
83. Nijman IJ, van Montfrans JM, Hoogstraat M, Boes ML, van de Corput L, Renner ED, van Zon P, van Lieshout S, Elferink MG, van der Burg M, Vermont CL, van der Zwaag B, Janson E, Cuppen E, Ploos van Amstel JK, van Gijn ME. Targeted next-generation sequencing: a novel diagnostic tool for primary immunodeficiencies. *J Allergy Clin Immunol* 2014;133:529–534
84. Lemke JR, Riesch E, Scheurenbrand T, Schubach M, Wilhelm C, Steiner I, Hansen J, Courage C, Gallati S, Bürki S, Strozzi S, Simonetti BG, Grunt S, Steinlin M, Alber M, Wolff M, Klopstock T, Prott EC, Lorenz R, Spaich C, Rona S, Lakshminarasimhan M, Kröll J, Dorn T, Krämer G, Synofzik M, Becker F, Weber YG, Lerche H, Böhm D, Biskup S. Targeted next generation sequencing as a diagnostic tool in epileptic disorders. *Epilepsia* 2012;53:1387–1398

Chapter 2

Ankyrin repeat and zinc-finger domain-containing 1 mutations are associated with infantile-onset inflammatory bowel disease

Désirée Y. van Haaften - Visser, Magdalena Harakalova*, Enric Mocholi*, Joris M. van Montfrans, Abdul Elkadri, Ester Rieter, Karoline Fiedler, Peter M. van Hasselt, Emily M.M. Triffaux, Mieke M. van Haelst, Isaac J. Nijman, Wigard P. Kloosterman, Edward E.S. Nieuwenhuis, Aleixo M. Muise, Edwin Cuppen, Roderick H.J. Houwen, Paul J. Coffer

* These authors contributed equally

J Biol Chem 2017;292:7904–7920

Abstract

Infantile-onset inflammatory bowel disease (IO IBD) is an invalidating illness with an onset before two years of age and has a complex pathophysiology in which genetic factors are important. Homozygosity mapping and whole exome sequencing in an IO IBD patient and subsequent sequencing of the candidate gene in twelve additional IO IBD patients revealed two patients with two mutated *Ankyrin Repeat and Zinc-Finger Domain-containing 1 (ANKZF1)* alleles (homozygous *ANKZF1* R585Q mutation and compound heterozygous *ANKZF1* E152K and V32_Q87del mutations respectively) and two patients with one mutated *ANKZF1* allele. While the function of ANKZF1 in mammals had not been previously evaluated, we show that ANKZF1 has an indispensible role in the mitochondrial response to cellular stress. ANKZF1 is located diffusely in the cytoplasm and translocates to the mitochondria upon cellular stress. ANKZF1 depletion reduces mitochondrial integrity and mitochondrial respiration under conditions of cellular stress. The *ANKZF1* mutations identified in IO IBD patients with two mutated *ANKZF1* alleles result in dysfunctional ANKZF1, as shown by an increased level of apoptosis in patients' lymphocytes, a decrease in mitochondrial respiration in patient fibroblasts with a homozygous *ANKZF1* R585Q mutation and an inability of ANKZF1 R585Q and E152K to rescue the phenotype of yeast deficient in Vms1, the yeast homologue of ANKZF1. These data indicate that loss-of-function mutations in *ANKZF1* result in deregulation of mitochondrial integrity and this may play a pathogenic role in the development of IO IBD.

Introduction

Inflammatory bowel disease (IBD) is a heterogeneous group of disorders, encompassing both Crohn's disease and ulcerative colitis, characterized by chronic inflammation of the gastrointestinal tract [1–3]. The pathogenesis of IBD is complex and still largely unknown. It involves a disturbance of the intestinal mucosal homeostasis, which is an interplay of genetic factors, the intestinal microbiome, the immune system and environmental factors [1–3]. Genetic factors are especially important in infantile-onset IBD (IO IBD, defined as an onset before two years of age) [4], making this patient group particularly interesting to investigate the genetic defects underlying IBD [5–7].

Next-generation sequencing (NGS) has been shown to be a valuable tool for increasing understanding of the genetic basis of human diseases and disease-causing pathways [8–10]. For IO IBD patients NGS has also led to the identification of several novel disease-causing mutations in genes including *IL10RA* [11], *IL10RB* [11], *IL10* [12], *XIAP* [13], *ADAM17* [14] and *TTC7A* [15]. Using a combination of homozygosity mapping and whole exome sequencing we identified a homozygous mutation in the *Ankyrin Repeat and Zinc-Finger Domain-containing 1 (ANKZF1)* gene in one IO IBD patient. We also defined compound heterozygous *ANKZF1* mutations in one additional IO IBD patient and a single heterozygous *ANKZF1* mutation in two additional IO IBD patients. While the function of ANKZF1 in humans has not been previously described, Valosin-containing protein (VCP)/Cell division cycle 48 (Cdc48)-associated mitochondrial stress responsive (Vms1), the yeast homologue of ANKZF1, has been demonstrated to be essential for mitochondrial protein degradation under stress conditions. Upon cellular stress a complex containing Vms1 and Cdc48, a protein which has a role in endoplasmic reticulum-associated protein degradation (ERAD), translocates from the cytoplasm to the mitochondria, where it regulates the degradation of damaged, misfolded and ubiquitinated proteins. Vms1 deficiency results in decreased ubiquitin-dependent mitochondrial protein degradation leading to accumulation of damaged and misfolded mitochondrial proteins causing mitochondrial dysfunction and subsequently apoptosis [16].

Here we show for the first time that mammalian ANKZF1 has a role in the mitochondrial response to cellular stress. ANKZF1 depletion reduces mitochondrial integrity and mitochondrial respiration under conditions of cellular stress, and mutations identified in the IO IBD patients with two mutated *ANKZF1* alleles also result in loss of ANKZF1 function. Although mitochondrial pathology has been previously observed in IBD patients, this is the first time that underlying mutations have been identified that provide evidence for a link between mitochondrial stress and the pathogenesis of IBD. These findings provide a novel molecular mechanism in the pathophysiology of IO IBD.

Results

Mutation of *ANKZF1* in four patients with infantile-onset inflammatory bowel disease

The female index patient presented at the age of six weeks with loose stools containing blood and mucus as well as severe ulcerative skin lesions at the perioral and perianal regions and extremities (**Figure 1A and 1B**). At endoscopy, extensive ulcerating lesions were found in the mouth and the entire colon, including the rectosigmoid (**Figure 1B**). Histology of colonic biopsies showed extensive lymphocytic infiltration of the lamina propria without distortion of crypt architecture. A biopsy of a skin lesion showed an epidermis distorted by lymphocytic and granulocytic infiltrate. Immunological investigations of peripheral blood showed severe lymphopenia in T cells, B cells and NK cells with typical total lymphocyte counts $<0.5{\cdot}10^9$/l, however with normal percentages of naïve $CD4^+$ and $CD8^+$ T cells. Based on the clinical signs and histological abnormalities in combination with the exclusion of an infectious or allergic cause, the diagnosis IO IBD was made. Although the clinical phenotype resembled the phenotype of patients with IL10 deficiency, no mutations were found in *IL10*, *IL10RA* and *IL10RB*, as well as in several other genes known to be associated with IBD (including *RAG1*, *RAG2*, *DOCK8* and CGD related genes). Immunosuppressive treatment with corticosteroids was started with a marked response on both ulcerating skin lesions and colitis. After complete resolution of symptoms azathioprine was started (2 mg/kg/day) and corticosteroids were tapered, however skin lesions recurred, although with a milder (non-ulcerating) phenotype (**Figure 1C**). During follow up until the age of five years, low grade ulcerative skin lesions as well as signs of residual gut inflammation persisted, with frequent periods of non-infectious diarrhea containing mucus and continuous elevations of fecal calprotectin levels. Concurrent with the lymphopenia, hypogammaglobulinemia was noted and prophylactic antibiotics were prescribed. No severe or opportunistic infections were noted.

Since the parents are second cousins, an autosomal recessive inherited cause of the IBD was suspected. Homozygosity mapping resulted in 6 regions larger than 2 Mb. With whole exome sequencing only one novel homozygous mutation was identified that was not present in our in-house database: g.220100258G>A (c.1754G>A, p.R585Q, NM_018089.2) in *ANKZF1*. This mutation, as well as its segregation, was confirmed by Sanger sequencing (**Figure 1D and 1F**). Twelve additional patients with IO IBD, of which three had a disease onset before six months of age, were screened for mutations in *ANKZF1*. In all three patients in which symptoms initiated before six months of age *ANKZF1* mutations were identified, while no *ANKZF1* mutations were found in the patients with a disease onset between six and 24 months of age. One boy carried compound heterozygous *ANKZF1* mutations: g.220096885G>A, resulting in skipping of half of exon 2 and exon 3 (p.V32_Q87del), and g.220097301G>A (c.454G>A,

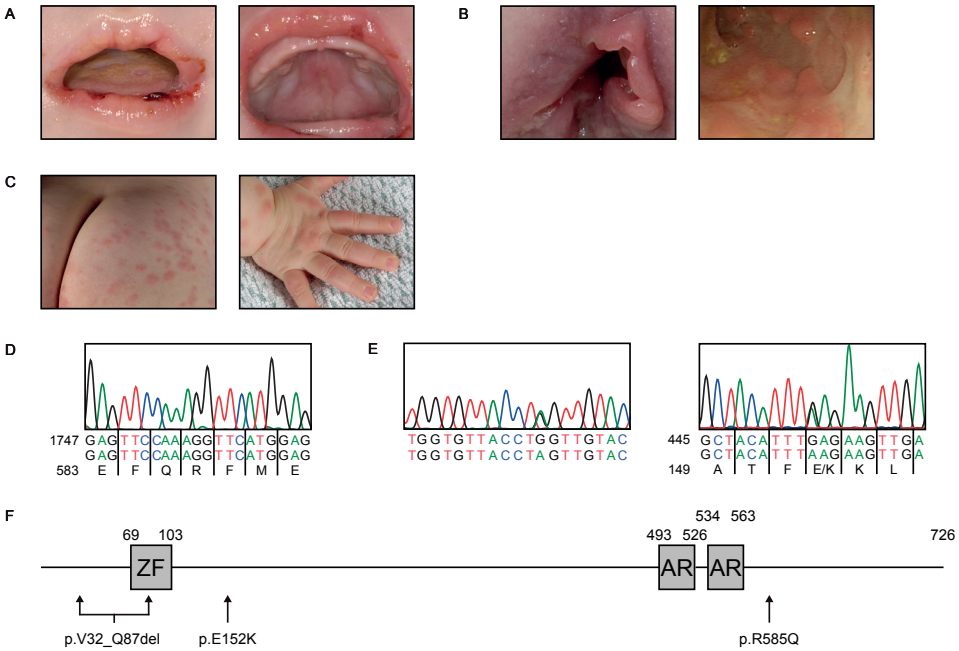

Figure 1. Two mutated *ANKZF1* alleles in two patients with infantile-onset inflammatory bowel disease. (A) Perioral and oral inflammation of patient with homozygous *ANKZF1* R585Q mutation at 2 months of age. **(B)** Perianal and colonic inflammation of patient with homozygous *ANKZF1* R585Q mutation at 2 months of age. **(C)** Skin anomalies of patient with homozygous *ANKZF1* R585Q mutation at 10 months of age. **(D)** Sanger sequencing of *ANKZF1* in peripheral blood derived genomic DNA from patient with homozygous *ANKZF1* R585Q mutation. **(E)** Sanger sequencing of *ANKZF1* in peripheral blood derived genomic DNA from patient with compound heterozygous *ANKZF1* V32_Q87del and E152K mutations. **(F)** Schematic diagram of ANKZF1 protein structure, including one zinc-finger (ZF) and two ankyrin repeats (AR). *ANKZF1* mutations identified in patients with two mutated *ANKZF1* alleles are indicated.

p.E152K) (**Figure 1E and 1F**). This patient presented in the first six months of life with a pancolitis. In this boy no skin inflammation or lymphopenia was present. Two other patients were found to have a single heterozygous *ANKZF1* mutation: g.220094405C>T, located in the promotor of *ANKZF1*, and g.220100539A>C (c.1913A>C, p.Q638P) respectively. Taken together, two IO IBD patients carried a mutation on both *ANKZF1* alleles and two additional patients were found to have a single mutated *ANKZF1* allele.

ANKZF1 mRNA and protein expression are reduced in IO IBD patient with homozygous *ANKZF1* R585Q mutation

First, it was determined whether *ANKZF1* mutations may influence ANKZF1 mRNA and protein expression. In fibroblasts and peripheral blood mononuclear cells (PBMCs)

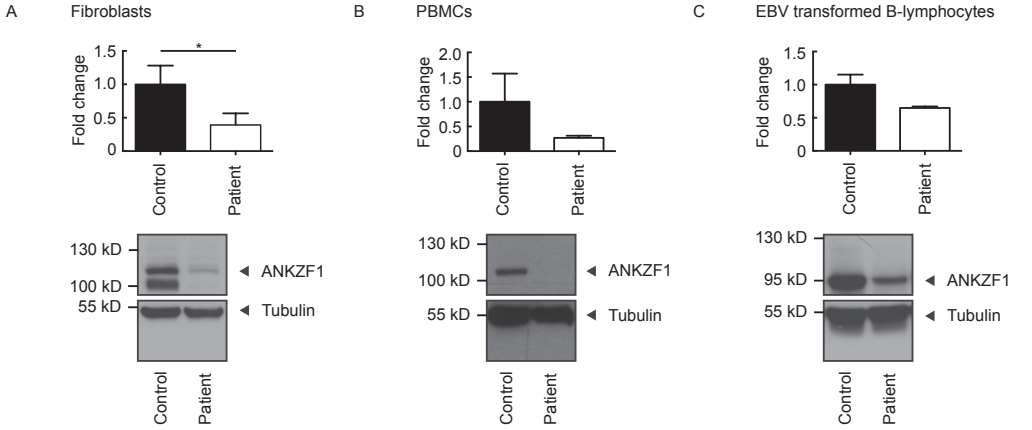
A
Fibroblasts
Fold change
1.5
1.0
0.5
0
*
Control
Patient
130 kD
100 kD
55 kD
ANKZF1
Tubulin
B
PBMCs
2.0
1.5
1.0
0.5
0
C
EBV transformed B-lymphocytes
95 kD

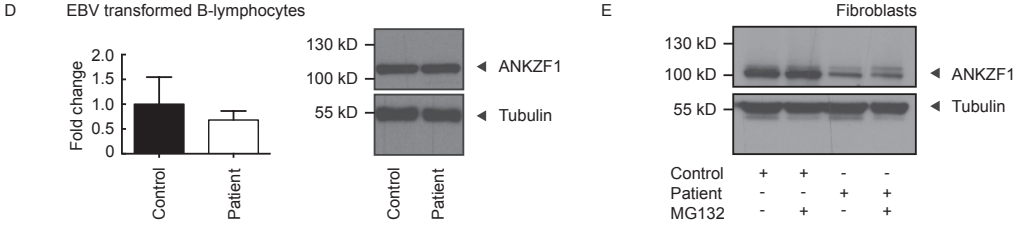
D
EBV transformed B-lymphocytes
E
Fibroblasts
Control + + - -
Patient - - + +
MG132 - + - +

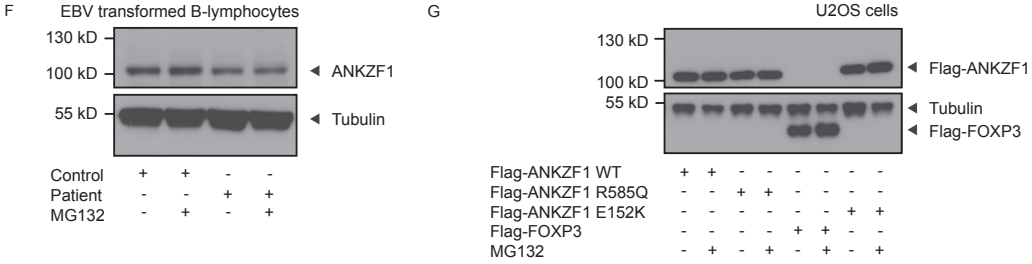
F
EBV transformed B-lymphocytes
Control + + - -
Patient - - + +
MG132 - + - +
G
U2OS cells
Flag-ANKZF1
Tubulin
Flag-FOXP3
Flag-ANKZF1 WT + + - - - - - -
Flag-ANKZF1 R585Q - - + + - - - -
Flag-ANKZF1 E152K - - - - - - + +
Flag-FOXP3 - - - - + + - -
MG132 - + - + - + - +

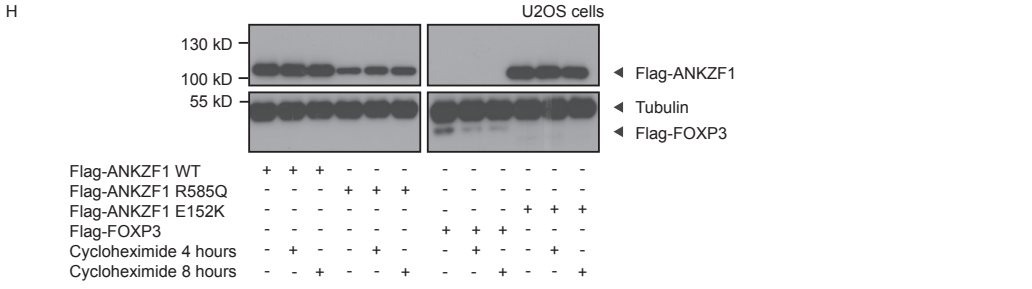
H
U2OS cells
130 kD
100 kD
55 kD
Flag-ANKZF1
Tubulin
Flag-FOXP3
Flag-ANKZF1 WT + + + - - - - - - - - -
Flag-ANKZF1 R585Q - - - + + + - - - - - -
Flag-ANKZF1 E152K - - - - - - - - - + + +
Flag-FOXP3 - - - - - - + + + - - -
Cycloheximide 4 hours - + - - + - - + - - + -
Cycloheximide 8 hours - - + - - + - - + - - +

from the patient with a homozygous *ANKZF1* R585Q mutation, *ANKZF1* mRNA expression levels were clearly reduced (**Figure 2A and 2B**), while in EBV transformed B-lymphocytes reduced expression was also evident (**Figure 2C**). All three cell types also exhibited reduced ANKZF1 protein expression (**Figure 2A-2C**). In EBV transformed B-lymphocytes from the patient with the compound heterozygous *ANKZF1* V32_Q87del and E152K mutations ANKZF1 mRNA and protein expression were equal to the ANKZF1 levels in control cells (**Figure 2D**).

To test whether the decline in protein expression in the patient with a homozygous *ANKZF1* R585Q mutation may also be due to an increased proteasomal degradation of ANKZF1, fibroblasts and EBV transformed B-lymphocytes were left untreated or treated with the proteasome inhibitor MG132 and ANKZF1 protein levels were analyzed. Treatment with MG132 did not affect ANKZF1 protein expression levels (**Figure 2E and 2F**). Subsequently, U2OS cells transfected with Flag-ANKZF1 wild-type (WT), Flag-ANKZF1 R585Q or Flag-ANKZF1 E152K were incubated with or without MG132 and ANKZF1 protein levels were evaluated. Cells transfected with Flag-FOXP3 were used as positive control, since we have previously shown FOXP3 levels to increase upon MG132 treatment [17]. Again no change in ANKZF1 protein level was detected (**Figure 2G**). These data suggest that the reduced ANKZF1 protein expression is not due to increased proteasomal degradation. To further confirm that the stability of ANKZF1 is not influenced by R585Q or E152K mutations, cells transfected with Flag-ANKZF1 WT, Flag-ANKZF1 R585Q or Flag-ANKZF1 E152K were incubated with or without cycloheximide, an inhibitor of protein translation, and ANKZF1 protein levels were determined. Again cells transfected with Flag-FOXP3 were used as positive control, since treatment with cycloheximide decreases FOXP3 levels [17]. In cells transfected with WT or with mutated ANKZF1, no change in ANKZF1 protein expression was observed between the untreated and treated cells, indicating a similar turnover of WT and mutated ANKZF1 (**Figure 2H**).

Figure 2. ANKZF1 mRNA and protein expression are reduced in IO IBD patient with homozygous *ANKZF1* R585Q mutation. (A-C) qRT-PCR and Western blot analysis of ANKZF1 mRNA and protein expression respectively in fibroblasts (A), PBMCs (B) and EBV transformed B-lymphocytes (C) healthy control and patient with homozygous *ANKZF1* R585Q mutation. **(D)** qRT-PCR and Western blot analysis of ANKZF1 mRNA and protein expression respectively in EBV transformed B-lymphocytes healthy control and patient with compound heterozygous *ANKZF1* V32_Q87del and E152K mutations. **(E-F)** Fibroblasts (E) and EBV transformed B-lymphocytes (F) healthy control and patient with homozygous *ANKZF1* R585Q mutation were left untreated or treated with 2 μM MG132 for 16 hours. Protein expression was determined by Western blot analysis using anti-ANKZF1 and anti-tubulin antibodies. **(G-H)** U2OS cells were transfected with indicated constructs. Cells were left untreated, treated with 2 μM MG132 for 16 hours (G) or treated with 5 μg/ml cycloheximide for 4 or 8 hours (H). Protein expression was determined by Western blot analysis using anti-Flag and anti-tubulin antibodies. For qRT-PCR analyses average and standard deviation of three independent experiments are shown. For Western blot analyses results are representative of three independent experiments. * $p \leq 0.05$.

Taken together, these data show that the *ANKZF1* R585Q mutation causes reduced ANKZF1 mRNA and protein expression, while ANKZF1 protein stability is unaffected. However, *ANKZF1* mutations do not *per se* affect ANKZF1 mRNA and protein expression, as illustrated by the IO IBD patient with compound heterozygous *ANKZF1* V32_87del and E152K mutations.

ANKZF1 R585Q mutation exhibits reduced stress-induced mitochondrial translocation

A recent study has shown that the yeast ANKZF1 homologue, Vms1, constitutively interacts with Cdc48, the yeast orthologue of human VCP. Under conditions of cellular stress this complex translocates to mitochondria, where it regulates the degradation of damaged, misfolded and ubiquitinated proteins [16]. To investigate whether cellular stress may also regulate mitochondrial translocation of ANKZF1, and whether this is maybe influenced by R585Q and E152K mutations, U2OS cells were first left untreated or exposed to hydrogen peroxide (H_2O_2). ANKZF1 localization was determined by confocal microscopy. In untreated cells, ANKZF1 was localized diffusely in the cytoplasm. However, upon exposure to H_2O_2 a translocation towards the mitochondria was observed (**Figure 3A**). To evaluate the consequences of the *ANKZF1* R585Q and E152K mutation, cells co-transfected with HA-VCP and Flag-ANKZF1 WT, Flag-ANKZF1 R585Q or Flag-ANKZF1 E152K were untreated or exposed to H_2O_2. Localization of ANKZF1 and VCP was visualized by confocal microscopy. In untreated cells VCP and both WT and mutant ANKZF1 were located diffusely in the cytoplasm. Exposure of the cells to H_2O_2 resulted in translocation of ANKZF1 and VCP towards the mitochondria. This translocation was reduced in cells transfected with ANKZF1 R585Q, but not in cells transfected with ANKZF1 E152K (**Figure 3B**).

To determine whether this reduced translocation of ANKZF1 R585Q upon exposure to H_2O_2 is the result of a disrupted interaction between ANKZF1 R585Q and VCP, cells co-transfected with HA-VCP and Flag-ANKZF1 WT, Flag-ANKZF1 R585Q or Flag-ANKZF1 E152K were left untreated or exposed to H_2O_2. Flag-ANKZF1 was immunoprecipitated, after which the VCP and ANKZF1 protein association was visualized by Western blot. In cells which were not exposed to H_2O_2 ANKZF1 was already associated with VCP, indicating that interaction was independent of levels of cellular stress. Association of ANKZF1 and VCP was unaffected in ANKZF1 R585Q and E152K mutants. Furthermore, both in cells transfected with WT or mutated ANKZF1 exposure to H_2O_2 did not influence association between VCP and ANKZF1 (**Figure 3C**). To further validate these results, cells co-transfected with HA-VCP and Flag-ANKZF1 WT, Flag-ANKZF1 R585Q or Flag-ANKZF1 E152K were untreated or exposed to H_2O_2 and an *in situ* proximity ligation assay (PLA) was performed. This technique allows visualization of protein-protein interactions, since a PLA signal is only obtained when proteins are in very close proximity to each other. Interaction was

observed between Flag-ANKZF1 WT and VCP in both treated and untreated cells and this interaction was similar for ANKZF1 R585Q and E152K mutants (**Figure 3D**).

Taken together, these data show that, similar to the yeast Cdc48-Vms1 complex, the VCP-ANKZF1 complex translocates towards the mitochondria under conditions of cellular stress. This translocation is reduced in the ANKZF1 R585Q mutant, while interaction between VCP and ANKZF1 is unaffected.

ANKZF1 depletion reduces mitochondrial integrity and mitochondrial respiration under conditions of cellular stress

In yeast, deficiency of the ANKZF1 homologue Vms1 causes accumulation of damaged mitochondrial proteins and subsequently mitochondrial dysfunction [16]. To determine the effect of deficiency of ANKZF1 on mitochondrial integrity and mitochondrial function, an ANKZF1 knockdown cell line was generated resulting in a reduction of ANKZF1 protein expression by approximately 60%. A control line was also generated by transduction of U2OS cells with a lentiviral construct containing scrambled shRNA (**Figure 4A**). To investigate mitochondrial integrity, cells with and without ANKZF1 knockdown were left untreated or exposed to H_2O_2, after which they were stained with rhodamine-123 and analyzed by FACS. Rhodamine-123 selectively accumulates in mitochondria in a mitochondrial membrane potential-dependent manner. Under basal conditions mitochondrial integrity was similar between cells with or without ANKZF1 knockdown. However, induction of cellular stress by H_2O_2 treatment caused a time-dependent decrease in mitochondrial integrity when ANKZF1 levels were reduced (**Figure 4B and 4C**).

To investigate the effect of ANKZF1 depletion on mitochondrial function, cells were left untreated or exposed to H_2O_2 and oxygen consumption rates (OCR) and extracellular acidification rates (ECAR) were determined using Seahorse metabolic flux analyzer technology, both at baseline and after treatment of the cells with drugs affecting mitochondrial respiration. In untreated cells the basal mitochondrial respiration was similar between ANKZF1 knockdown and control cells. However, the observed reduction in basal OCR after induction of cellular stress, was more pronounced in ANKZF1 knockdown cells than in control cells (**Figure 4D**). This leads to a decreased ATP production in ANKZF1 knockdown cells under stress conditions, as shown by a more pronounced reduction in ATP-linked mitochondrial respiration in these cells compared to control cells (**Figure 4E**), as evaluated after oligomycin treatment to block the mitochondrial H^+-ATP synthase. To investigate whether the decrease in mitochondrial respiration in ANKZF1 knockdown cells also influences glycolysis, ECAR was determined, which was increased in ANKZF1 knockdown cells exposed to H_2O_2 (**Figure 4F**). This indicates that in ANKZF1 knockdown cells treated with H_2O_2, glycolytic activity is increased, most likely to compensate for the decrease in mitochondrial respiration (**Figure 4G**).

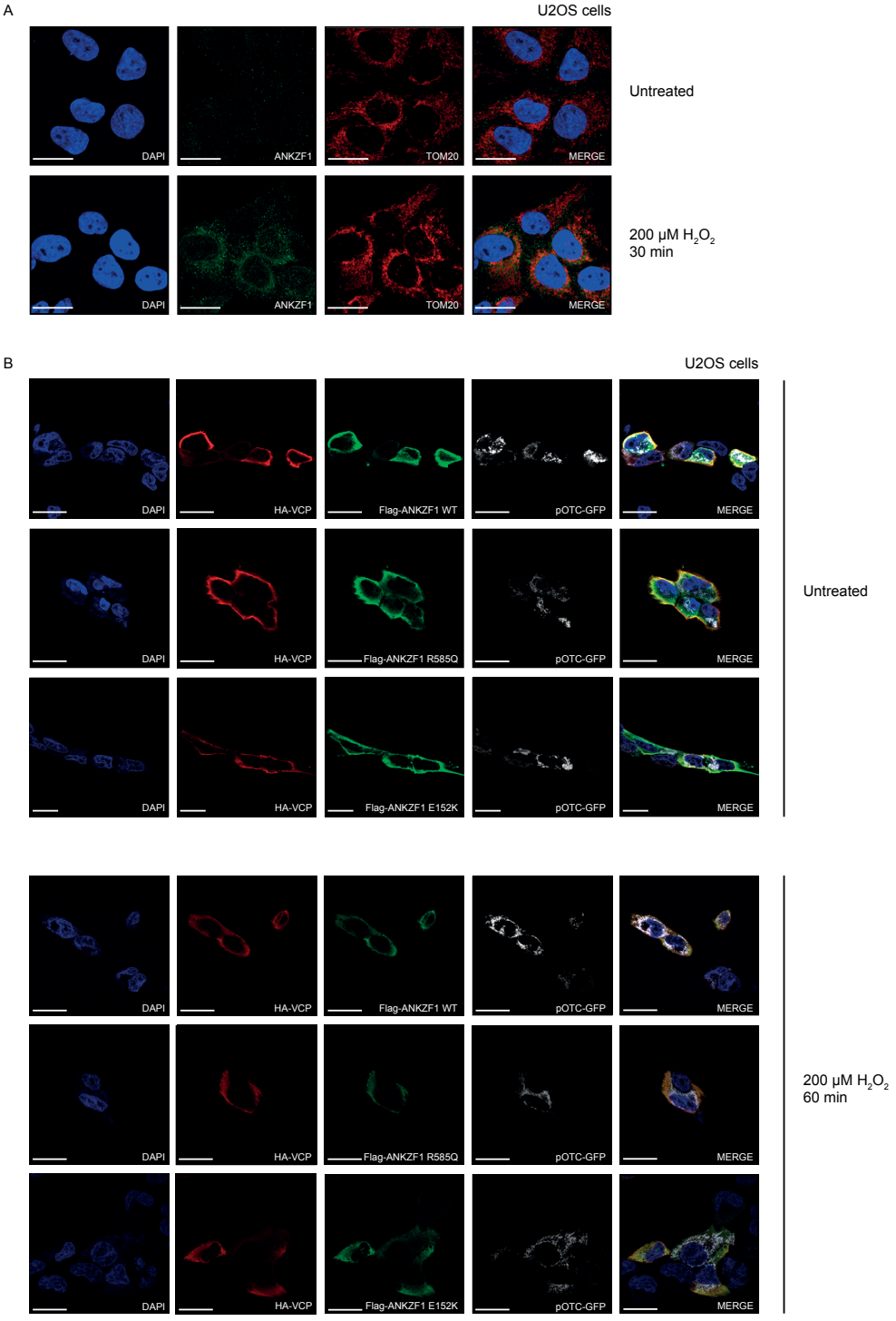
A
U2OS cells
DAPI
ANKZF1
TOM20
MERGE
Untreated
200 μM H_2O_2
30 min
B
U2OS cells
DAPI
HA-VCP
Flag-ANKZF1 WT
pOTC-GFP
MERGE
Flag-ANKZF1 R585Q
Flag-ANKZF1 E152K
Untreated
200 μM H_2O_2
60 min

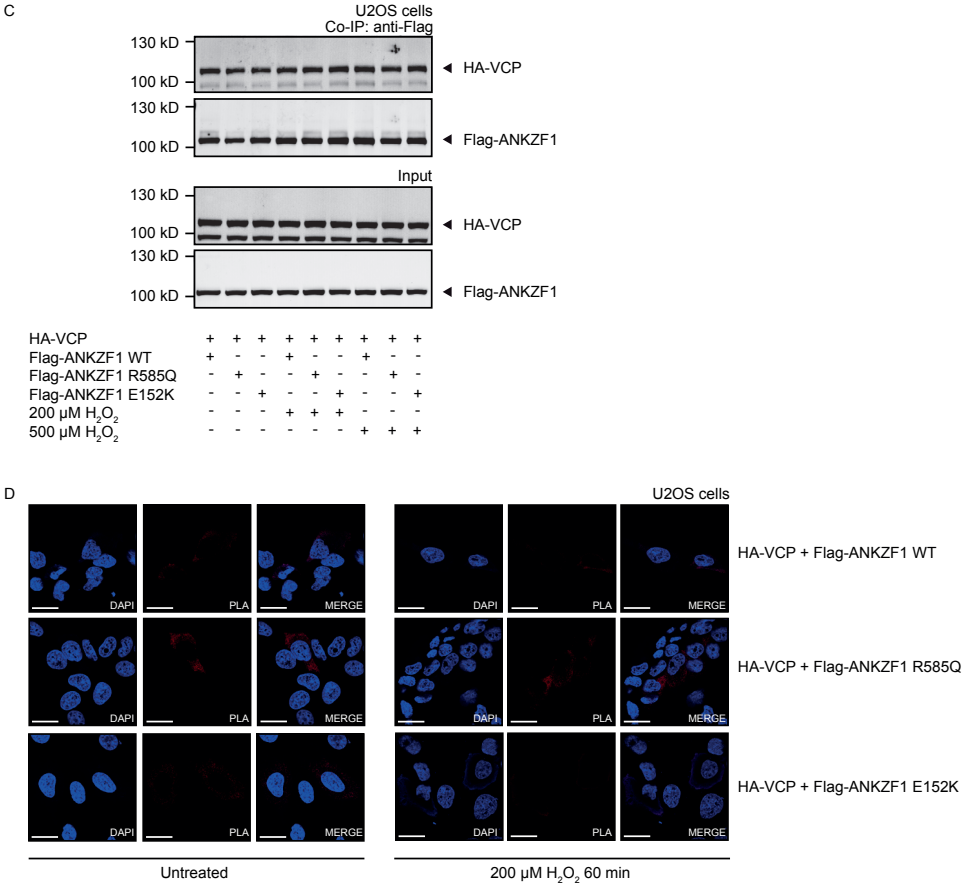

Figure 3. *ANKZF1* R585Q mutation exhibits reduced stress-induced mitochondrial translocation. (A) U2OS cells were left untreated or treated with 200 µM H_2O_2 for 30 minutes. ANKZF1 and TOM20 were visualized by immunofluorescence microscopy using anti-ANKZF1 and anti-TOM20 antibodies. TOM20 was used as a mitochondrial marker. DAPI was used to visualize the nuclei. Scale bars, 25 µm. **(B)** U2OS cells were co-transfected with indicated constructs and left untreated or treated with 200 µM H_2O_2 for 60 minutes. HA-VCP and Flag-ANKZF1 were visualized by immunofluorescence microscopy using anti-HA and anti-Flag antibodies. pOTC-GFP was used as mitochondrial marker. DAPI was used to visualize the nuclei. Scale bars, 25 µm. **(C)** U2OS cells were co-transfected with indicated constructs and left untreated or treated with 200 µM or 500 µM H_2O_2 for 90 minutes. A co-immunoprecipitation was performed using anti-Flag beads. ANKZF1-VCP interaction was determined by Western blot analysis using anti-Flag and anti-HA antibodies. **(D)** U2OS cells were co-transfected with indicated constructs and exposed to 0 or 200 µM H_2O_2 for 60 minutes. A proximity ligation assay (PLA) was performed. Punctate staining (red) indicates a VCP-ANKZF1 interaction. DAPI was used to visualize the nuclei. Scale bars, 25 µm. Results are representative of three independent experiments.

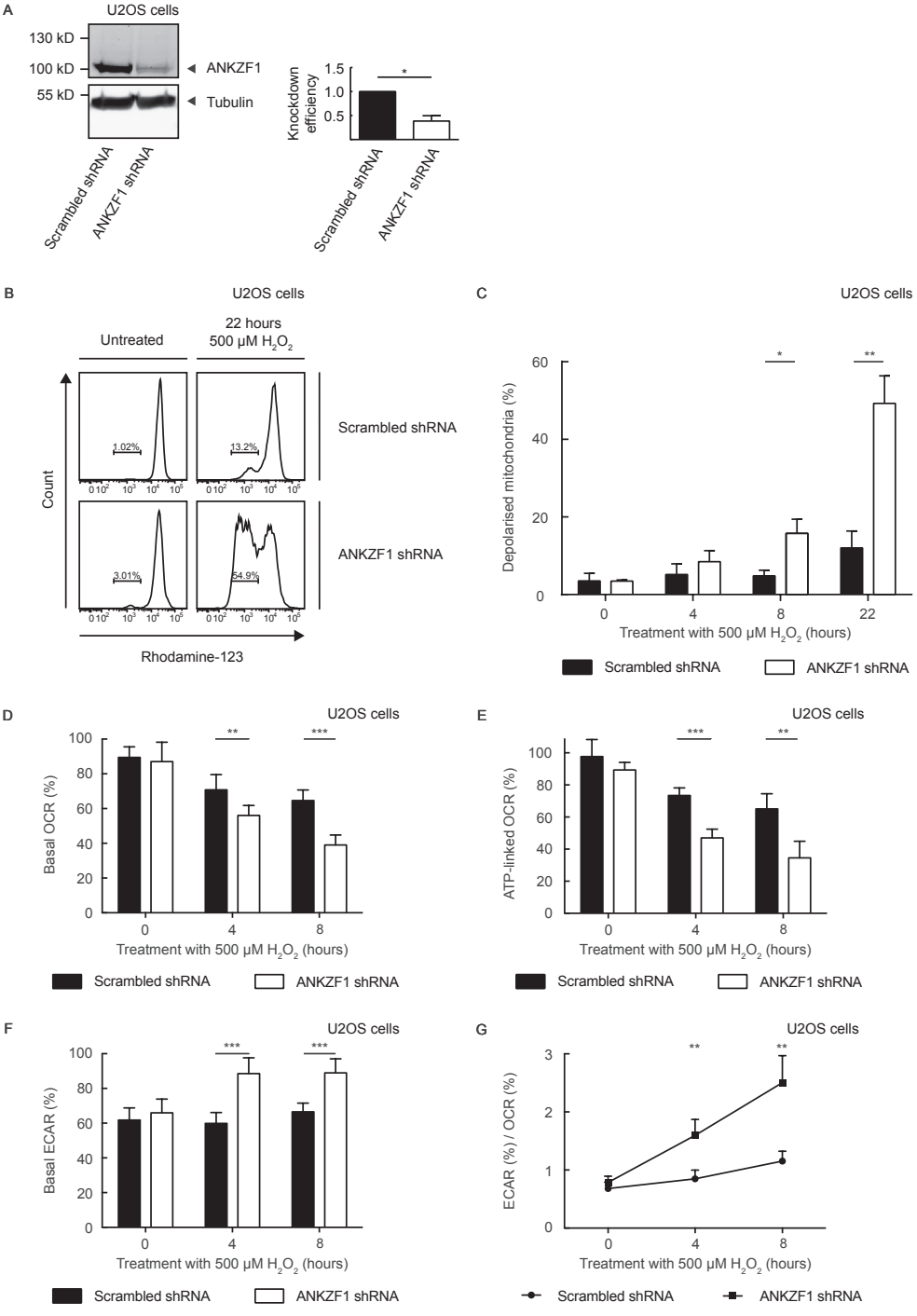
A
U2OS cells
130 kD
100 kD
55 kD
ANKZF1
Tubulin
Scrambled shRNA
ANKZF1 shRNA
Knockdown efficiency
1.5
1.0
0.5
*
Scrambled shRNA
ANKZF1 shRNA
B
U2OS cells
Untreated
22 hours
500 μM H2O2
Scrambled shRNA
ANKZF1 shRNA
1.02%
13.2%
3.01%
54.9%
Count
Rhodamine-123
C
U2OS cells
Depolarised mitochondria (%)
60
40
20
0
*
**
0
4
8
22
Treatment with 500 μM H2O2 (hours)
Scrambled shRNA
ANKZF1 shRNA
D
U2OS cells
Basal OCR (%)
100
80
60
40
20
0
**
***
0
4
8
Treatment with 500 μM H2O2 (hours)
Scrambled shRNA
ANKZF1 shRNA
E
U2OS cells
ATP-linked OCR (%)
100
80
60
40
20
0
***
**
0
4
8
Treatment with 500 μM H2O2 (hours)
Scrambled shRNA
ANKZF1 shRNA
F
U2OS cells
Basal ECAR (%)
100
80
60
40
20
0
***
***
0
4
8
Treatment with 500 μM H2O2 (hours)
Scrambled shRNA
ANKZF1 shRNA
G
U2OS cells
ECAR (%) / OCR (%)
3
2
1
0
**
**
0
4
8
Treatment with 500 μM H2O2 (hours)
Scrambled shRNA
ANKZF1 shRNA

Figure 4. ANKZF1 depletion reduces mitochondrial integrity and mitochondrial respiration under conditions of cellular stress. (A) U2OS ANKZF1 knockdown and control cell lines were generated. Knockdown efficiency of ANKZF1 was determined by Western blot analysis and quantified relatively to control cell line. Differences in loading were compensated. Average and standard deviation of three independent experiments are shown. **(B)** U2OS ANKZF1 knockdown and control cell line were left untreated or exposed to 500 μM H_2O_2 for 4, 8 or 22 hours. Percentage of cells with depolarized mitochondria was determined by FACS using rhodamine-123. Graphs of untreated U2OS cells and U2OS cells treated for 22 hours are shown. Results are representative of three independent experiments. **(C)** Percentage of U2OS ANKZF1 knockdown and control cells with depolarized mitochondria as determined by FACS after treatment with 500 μM H_2O_2 as indicated and staining with rhodamine-123. Average and standard deviation of three independent experiments are shown. **(D-G)** U2OS ANKZF1 knockdown and control cell line were left untreated or exposed to 500 μM H_2O_2 for 4 or 8 hours. Basal oxygen consumption rate (OCR) (D), ATP-linked OCR (E), extracellular acidification rate (ECAR) (F) and ratio of basal ECAR and basal OCR (G) were determined using the XF-24 Extracellular Flux Analyzer. OCR and ECAR are shown as percentage of highest rate. Average and standard deviation of two independent experiments are shown. * $p \leq 0.05$, ** $p \leq 0.01$, *** $p \leq 0.001$.

These data demonstrate that ANKZF1 deficiency results in both a loss of mitochondrial integrity and a decrease in mitochondrial respiration under conditions of cellular stress.

Increased apoptosis in lymphocytes harboring *ANKZF1* mutations

It is known that mitochondrial dysfunction can ultimately lead to apoptosis [18,19]. To investigate whether the *ANKZF1* mutations identified in patients with two mutated *ANKZF1* alleles cause dysfunction of ANKZF1, the effect of the mutations on apoptosis was studied. First, to determine whether cell expansion is influenced by the *ANKZF1* mutations, EBV transformed B-lymphocytes from both IO IBD patients with two mutated *ANKZF1* alleles and a healthy control were cultured and cell numbers determined daily. Decreased proliferative capacity of EBV transformed B-lymphocytes from both patients was observed (**Figure 5A**).

To investigate whether decreased cell numbers were due to increased apoptosis, patient-derived EBV transformed B-lymphocytes were left untreated or treated with H_2O_2 and numbers of apoptotic cells were determined. EBV transformed B-lymphocytes from both patients exposed to H_2O_2 exhibited a higher level of apoptosis compared to control EBV transformed cell lines. Interestingly, in untreated EBV transformed B-lymphocytes the initial level of apoptosis was also higher in the patients' cells, which suggests increased basal levels of cellular stress (**Figure 5B and 5C**).

Subsequently, it was investigated whether the *ANKZF1* R585Q mutation also causes increased levels of apoptosis in patient lymphocytes. PBMCs were left untreated or treated with H_2O_2 and numbers of apoptotic T- and B-lymphocytes were determined. Apoptosis was significantly higher in both T-lymphocytes and B-lymphocytes from the

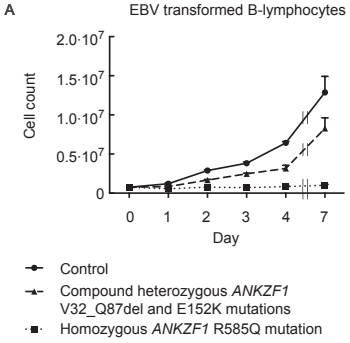
A
EBV transformed B-lymphocytes
Cell count
2.0·10^7
1.5·10^7
1.0·10^7
0.5·10^7
0
0 1 2 3 4 7
Day
Control
Compound heterozygous ANKZF1 V32_Q87del and E152K mutations
Homozygous ANKZF1 R585Q mutation

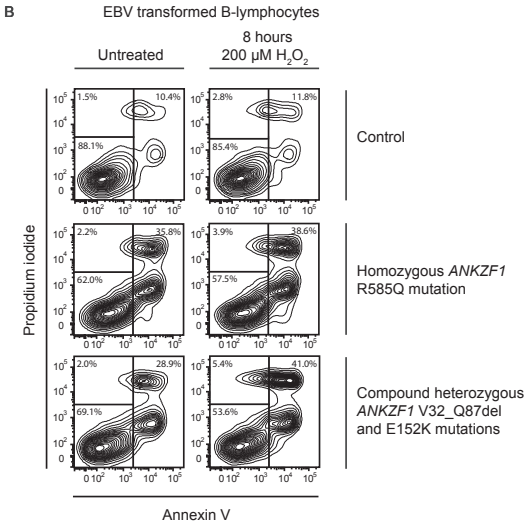
B
EBV transformed B-lymphocytes
Untreated
8 hours 200 μM H2O2
Propidium iodide
Annexin V
Control
Homozygous ANKZF1 R585Q mutation
Compound heterozygous ANKZF1 V32_Q87del and E152K mutations

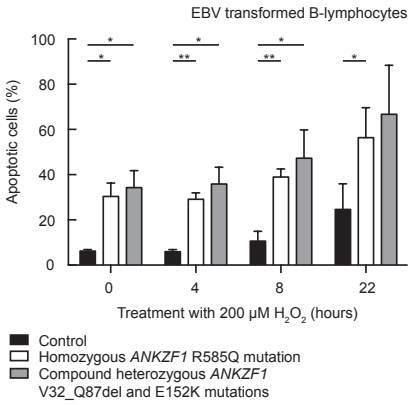
C
EBV transformed B-lymphocytes
Apoptotic cells (%)
Treatment with 200 μM H2O2 (hours)
Control
Homozygous ANKZF1 R585Q mutation
Compound heterozygous ANKZF1 V32_Q87del and E152K mutations

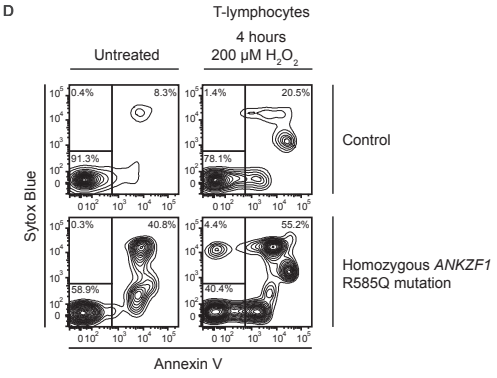
D
T-lymphocytes
Untreated
4 hours 200 μM H2O2
Sytox Blue
Annexin V
Control
Homozygous ANKZF1 R585Q mutation

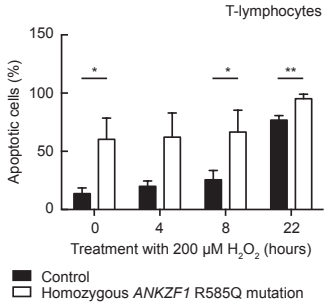
E
T-lymphocytes
Apoptotic cells (%)
Treatment with 200 μM H2O2 (hours)
Control
Homozygous ANKZF1 R585Q mutation

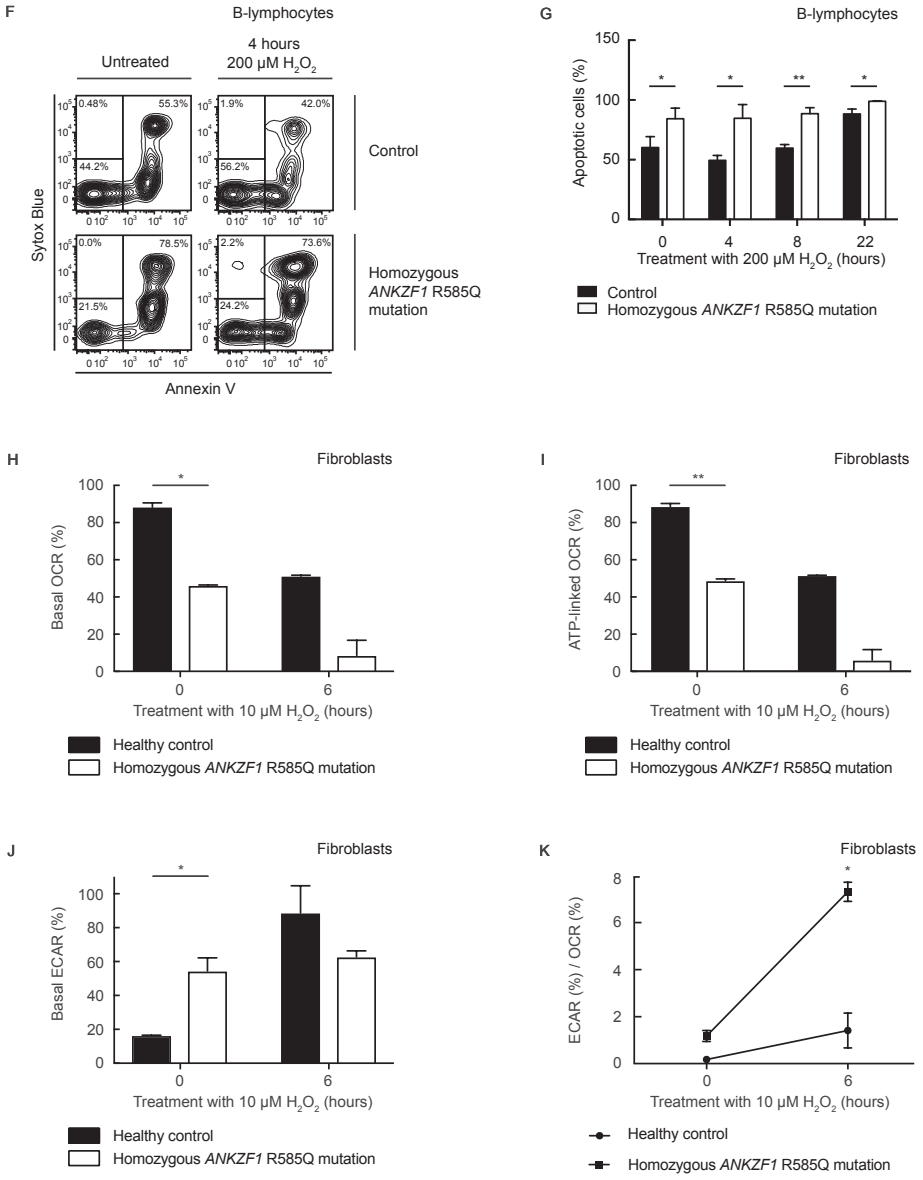

Figure 5. Increased apoptosis in lymphocytes harboring *ANKZF1* mutations. (A) Amplification of $7.5 \bullet 10^5$ EBV transformed B-lymphocytes from healthy control, patient with homozygous *ANKZF1* R585Q mutation and patient with compound heterozygous *ANKZF1* V32_Q87del and E152K mutations was determined on indicated days. **(B-C)** EBV transformed B-lymphocytes from two healthy controls, patient with homozygous *ANKZF1* R585Q mutation and patient with compound heterozygous *ANKZF1* V32_Q87del and E152K mutations were left untreated or treated with 200 μM H_2O_2 for 4, 8 or 22 hours. Percentage apoptotic cells was determined by FACS after staining with Annexin V and propidium iodide. **(D-G)** PBMCs isolated from healthy controls and patient with homozygous *ANKZF1*

Figure 5 (*continued*)
R585Q mutation were left untreated or treated with 200 μM H_2O_2 for 4, 8 or 22 hours. Percentage apoptotic cells was determined by FACS using Annexin V and Sytox Blue. T-lymphocytes were identified using anti-CD3 antibodies (D and E). B-lymphocytes were identified using anti-CD19 antibodies (F and G). Results are representative of three independent experiments. Average and standard deviation are shown. **(H-K)** Fibroblasts healthy control and patient with homozygous *ANKZF1* R585Q mutation were left untreated or exposed to 10 μM H_2O_2 for 6 hours. OCR (H), ATP-linked OCR (I), ECAR (J) and ratio of basal ECAR and basal OCR (K) were determined using the XF-24 Extracellular Flux Analyzer. OCR and ECAR are shown as percentage of highest rate. Average and standard deviation of triplicates of one experiment are shown. Results are representative of three independent experiments. * $p \leq 0.05$, ** $p \leq 0.01$.

IO IBD patient compared to healthy controls, either when the cells were left untreated or when they were exposed to H_2O_2 (**Figure 5D-5G**).

To investigate whether this increased level of apoptosis could be the result of decreased mitochondrial respiration, fibroblasts from the patient with a homozygous *ANKZF1* R585Q mutation were left untreated or treated with H_2O_2 and OCR and ECAR were determined. In untreated cells the basal OCR was significantly decreased in patient fibroblasts compared to control fibroblasts (**Figure 5H**) resulting in a decreased ATP production (**Figure 5I**), a trend which was also present after treatment with H_2O_2 (**Figure 5H and 5I**). ECAR was increased in untreated patient fibroblasts (**Figure 5J**). These data suggest that the *ANKZF1* R585Q mutation results in an increased glycolytic activity (**Figure 5K**) to compensate for the decrease in mitochondrial respiration, even in cells not treated with H_2O_2.

To determine whether decreased mitochondrial respiration could be coupled with changes in autophagic flux, fibroblasts from the patient with a homozygous *ANKZF1* R585Q mutation were left untreated or treated with hydroxychloroquine and protein expression of autophagy markers LC3-II and p62 was determined by Western blot. However, no differences in autophagic flux were observed between patient and control cells (data not shown).

Taken together these data demonstrate that *ANKZF1* mutations found in the patients with two mutated *ANKZF1* alleles may result in increased lymphocyte apoptosis and the *ANKZF1* R585Q mutation causes a decrease in mitochondrial respiration but does not affect autophagy.

ANKZF1 R585Q and E152K are unable to functionally rescue Vms1-deficient yeast

Our data suggest that human ANKZF1 has a similar function to Vms1 in yeast. *ANKZF1* mutations found in the IO IBD patients with two mutated *ANKZF1* alleles lead to an increased level of apoptosis, suggesting that these mutations result in loss of ANKZF1 function. To confirm this, the ability of WT and mutant ANKZF1 to rescue

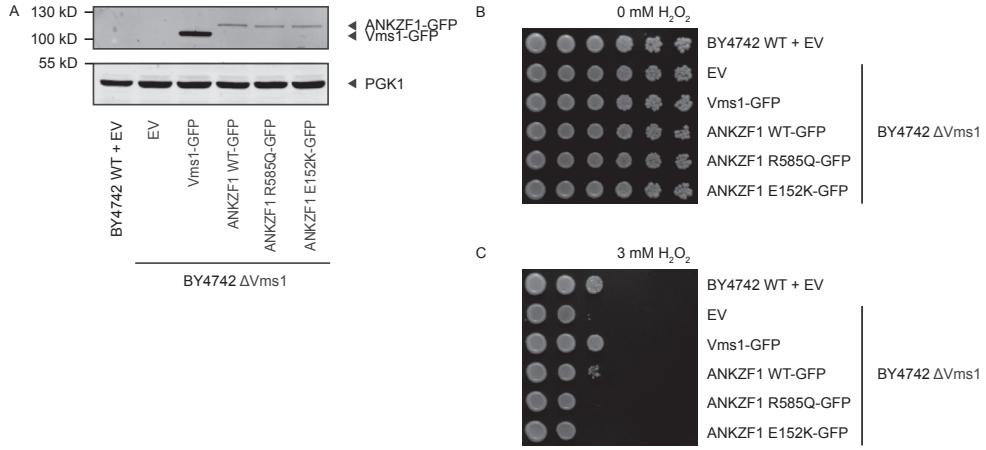

Figure 6. ANKZF1 R585Q and E152K are unable to functionally rescue Vms1-deficient yeast. (A) Protein expression of Vms1-GFP and ANKZF1-GFP in BY4742 WT and BY4742 ΔVms1 yeast strains transformed with indicated constructs determined by Western blot analysis using anti-GFP and anti-PGK1 antibodies. **(B-C)** Indicated yeast strains were grown overnight in SMD without uracil at 30°C. Serial five-fold dilutions of 0.4 OD600 of each strain were grown on SMD plates without uracil and without H_2O_2 (B) or with 3 mM H_2O_2 (C) for 2 days at 30°C. Results are representative of three independent experiments.

the loss of Vms1 in yeast was studied. A BY4742 Δ*Vms1* yeast strain was transformed with a pRS416 vector containing GFP-tagged Vms1, ANKZF1 WT, ANKZF1 R585Q or ANKZF1 E152K. Expression of all ANKZF1 constructs was equal, although levels were reduced compared with Vms1 (**Figure 6A**). These yeast strains, together with a BY4742 WT and a BY4742 Δ*Vms1* yeast strain transformed with pRS416 empty vector, were grown on synthetic minimal medium (SMD) plates without uracil with or without 3 mM H_2O_2. Under normal growth conditions no difference in growth of the different yeast strains was observed (**Figure 6B**). However, treatment with 3 mM H_2O_2 resulted in a reduction of BY4742 Δ*Vms1* yeast growth compared to BY4742 WT yeast growth. This inability to grow of the Δ*Vms1* yeast strain could be completely rescued by transformation of a construct containing Vms1 and partially but reproducibly rescued by transformation of a construct containing WT ANKZF1. However, ANKZF1 R585Q and ANKZF1 E152K were unable to rescue *Vms1* deletion (**Figure 6C**). Taken together, these data show that while ANKZF1 WT is able to functionally rescue BY4742 Δ*Vms1* yeast, both ANKZF1 R585Q and E152K are not, confirming that ANKZF1 R585Q and E152K impair ANKZF1 function, likely leading to loss of mitochondrial integrity and apoptosis.

Discussion

In this study we, for the first time, link mutations in *ANKZF1* to IO IBD and provide the first functional characterization of this gene in mammals. Using a combination of homozygosity mapping and whole exome sequencing we identified a homozygous g.220100258G>A (*ANKZF1* p.R585Q) mutation in one IO IBD patient. In an additional IO IBD patient we found compound heterozygous g.220096885G>A (*ANKZF1* p.V32_Q87del) and g.220097301G>A (*ANKZF1* p.E152K) mutations. Furthermore, two IO IBD patients carried a single heterozygous *ANKZF1* mutation: g.220094405C>T (located in the promotor) and g.220100539A>C (p.Q638P). Except for the g.220100258G>A mutation in the NHLBI ESP Exome Variant Server (EVS) and dbSNP databases none of these mutations are described or no frequency data are known. In the ExAC Browser Beta database for the g.220097301G>A mutation an A allele frequency of $5{\cdot}10^{-5}$ is described. For the g.220100258G>A mutation in humans from European descent the A allele frequency varies between 0.004 (dbSNP database, mutation added to NCBI dbSNP Build 135) and 0.01 (NHLBI ESP EVS and ExAC Browser Beta databases). This A allele frequency suggests that humans homozygous for the *ANKZF1* R585Q mutation can be free of symptoms, as no IBD patients with this mutation have been described before. Nevertheless, in our population of thirteen IO IBD patients, four patients carried *ANKZF1* mutations on one or two alleles. When we only consider IBD with an onset before six months of age the frequency of *ANKZF1* mutations in our study population is even 100%, suggesting that ANKZF1 is indeed important in the pathogenesis of IO IBD. We suggest that modifier genes may protect individuals with *ANKZF1* mutations against the development of IO IBD [20–22], explaining the low number of IO IBD patients with *ANKZF1* mutations found to date.

While so far uncharacterized in mammalian cells, here we show that the function of ANKZF1 resembles the function of Vms1 in yeast. Vms1, the yeast homologue of ANKZF1, interacts with Cdc48, the yeast orthologue of VCP. In conditions of cellular stress this complex is recruited to the mitochondrial membrane [16]. We show that ANKZF1 also interacts with VCP and that this complex translocates to the mitochondria after exposure to H_2O_2 (**Figure 3A-3D**). Here, Vms1 has a role in the degradation of mitochondrial proteins and deficiency results in the accumulation of damaged and misfolded mitochondrial proteins causing mitochondrial dysfunction and subsequently apoptosis [16]. We propose that ANKZF1 has a similar function, since we found that ANKZF1 depletion leads to both a reduced mitochondrial integrity and mitochondrial respiration under conditions of cellular stress (**Figure 4B-4G**). Furthermore mammalian ANKZF1 was able to functionally replace yeast Vms1 in complementation assays, suggesting evolutionary conservation (**Figure 6C**).

ANKZF1 mutations identified in both IO IBD patients with two mutated *ANKZF1* alleles cause impairment of ANKZF1 function, as shown by an increased level of apoptosis in patients' lymphocytes (**Figure 5B-5G**), a decrease in mitochondrial respiration in patient fibroblasts with a homozygous *ANKZF1* R585Q mutation (**Figure 5H-5K**) and an inability of ANKZF1 R585Q and E152K to rescue the phenotype of Vms1-deficient yeast (**Figure 6C**). Dysfunction of ANKZF1 R585Q is the result of both reduced ANKZF1 mRNA and protein levels (**Figure 2A-2C**) and a decreased translocation of ANKZF1 R585Q to the mitochondria in response to cellular stress (**Figure 3B**). In contrast, in cells with compound heterozygous *ANKZF1* V32_Q87del and E152K mutations ANKZF1 function is disturbed after recruitment of the VCP-ANKZF1 complex to the mitochondria, since mRNA and protein levels are unaffected in these cells (**Figure 2D**) as well as interaction of ANKZF1 E152K with VCP and translocation of this complex to the mitochondria after induction of cellular stress (**Figure 3B-3D**). Although it is unclear how the *ANKZF1* E152K mutation causes dysfunction, the *ANKZF1* V32_Q87del mutation occurs within an *in silico*-defined zinc-finger, located near the N-terminus of ANKZF1 (**Figure 1F**). The exact function of this potential zinc-finger has not been investigated yet, but it is highly conserved among several species. Normally associated with DNA-binding, potentially disruption of the ANKZF1 zinc-finger motif disrupts protein-protein interactions critical for ANKZF1 localization or function.

We demonstrate that loss-of-function mutations in *ANKZF1* are related to IO IBD and dysfunction of ANKZF1 causes mitochondrial stress. Although mitochondrial stress has not previously been linked to the development of IO IBD, increased ER stress plays an important role in the pathogenesis of IBD [23–25]. The unfolded protein response (UPR) is a pathway activated by ER stress that facilitates the removal of unfolded and misfolded ER proteins [26]. Dysfunction of the UPR leads to increased ER stress and the development of intestinal inflammation [23–25]. Our data strongly suggest that besides ER stress, mitochondrial stress induced by loss of ANKZF1 function is also involved in the pathogenesis of IO IBD. However, further research is required to clarify the exact mechanism.

Although the pathway described in this paper has not previously been associated with IBD, mitochondrial pathology has been observed in IBD patients, including electron transport chain complex dysfunction [27–29], diminished mitochondrial membrane potential [30] and changed mitochondrial morphology [31]. Thus far, it has remained enigmatic whether these mitochondrial anomalies are a consequence of the disease, or indeed contribute to pathology. However, in combination with the known link between mitochondrial stress and the development of a number of other immune diseases, this strongly suggests a role for mitochondrial stress in the pathogenesis of IBD. The genetic

defect described in this paper for the first time provides a direct link between mitochondrial stress and the pathogenesis of IBD.

Taken together, we show that loss-of-function mutations in *ANKZF1* likely play a novel role in the pathogenesis of IO IBD. Furthermore, we characterize for the first time the function of ANKZF1 in mammals. These observations increase our understanding of the pathophysiology of IO IBD and underline the value of using modern sequencing techniques in this patient group. It also further highlights the potential role of mitochondrial stress in immunological disorders. Additional research is needed to further characterize the molecular pathway by which loss of ANKZF1 function causes intestinal inflammation.

Materials and Methods

Homozygosity mapping

Peripheral blood genomic DNA samples from the index patient and both parents were analyzed using Illumina HumanCytoSNP-12v2 arrays according to the manufacturer's protocol (Illumina Inc., San Diego, California, United States of America (USA)). Regions of homozygosity were determined using the BeadStudio® as well as our in-house analysis pipeline (scripts available upon request). Plug-in runs of at least 20 homozygous SNPs were compiled. Homozygous regions in the patient's genome were compared with regions from parents and those exclusively found in the patient were retained and sorted according to size. Regions overlapping with centromeres were tagged. Regions spanning candidate genes for IBD (*CHUK*, *CYBA*, *CYBB*, *FERMT3*, *FOXP3*, *IKBKB*, *IKBKG*, *IL10*, *IL10RA*, *IL10RB*, *IL1A*, *IL1R1*, *IL2RA*, *IRAK4*, *ITGB2*, *LIG4*, *NCF1*, *NFKB1*, *NFKB2*, *NHEJ1*, *NOD2*, *RAG1*, *RAG2*, *RASGRP1*, *REL*, *RELA*, *RELAB*, *STAT3*, *STXBP2*, *TNFRSF13B*, *WAS*) were examined for presence of a homozygous region in the patient.

Multiplexed whole exome next-generation sequencing in a nuclear trio

Original genomic DNA was isolated from peripheral lymphocytes of the index patient and her parents. Genomic DNA concentration was determined using the Qubit Quant-iT™ method (Invitrogen, Carlsbad, California, USA) and 2000 ng of high quality DNA of the trio was used for barcoded fragment library preparation and multiplexed enrichment for the SOLiD NGS platform using our in-house protocol [32]. In brief, DNA pool was fragmented using the Covaris™ S2 System (Applied Biosystems, Carlsbad, California, USA) to approximately 150 bp short fragments. After fragmentation, fragments were blunt-ended and phosphorylated at the 5′ end using End-It™ DNA End-Repair Kit (EpiCenter, Madison, Wisconsin, USA) and purified with the Agencourt AMPure XP

system (Beckman Coulter Genomics, Danvers, Massachusetts, USA) followed by ligation of double-stranded truncated versions of adaptors complementary to the SOLiD NGS platform. Ligation was performed using the Quick Ligation Kit (New England BioLabs, Ippswich, Massachusetts, USA). After purification with the AMPure system, nick translation on non-phosphorylated and non-ligated 3′-ends, barcoding and amplification in single PCR was performed for each library separately. Intensity of library bands was checked on 2% agarose gel (Lonza FlashGel System). PCR products were purified with AMPure system to remove adaptor dimmers and heterodimmers. Amplified library fragments ranging 175–225 bp were size selected on 4% agarose gel and gel slices were purified using QIAquick Gel Extraction Kit (Qiagen, Hilden, Germany). Libraries of the trio were equimolarly pooled with two other barcoded libraries unrelated to this project (n=5) and enriched in a multiplexed setup for the Agilent SureSelect Human All Exon 50Mb Kit (Agilent Technologies, Santa Clara, California, USA). Enriched library pool fragments were amplified using 12 PCR cycles and elongated to a full-length adaptor sequence required for SOLiD sequencing. All adaptor, primer and barcode sequences are available in a previous publication [32]. SOLiD sequencing was performed according to the SOLiD 4 manual to obtain to produce enough 50 bp reads to obtain sufficient coverage for a single allele in each library.

Variant detection and analysis

Raw sequencing reads were mapped against the human reference genome hg19/GRCh37 using our custom pipeline based on the Burrows-Wheeler Alignment (BWA) algorithm. Single nucleotide variants and small indels (≤7nt) were called by our custom analysis pipeline as described before [33]. The criteria for variant detection were set to enable also *de novo* heterozygous variants: minimal allele support based on 2 seeds of a read, strand balance set off, cut-off for coverage was set to 10 reads, cut-off for non-reference allele (NRA) % was set to 15% and clonality filter that keeps maximally five clonal reads with the same start site and removes reads above this level. All common and rare polymorphisms present in Ensembl62 (based on NCBI dbSNP Build 133 for humans) were tagged as known, variants present in our in-house database (60 tested samples) were considered for sequencing errors or Dutch population specific variants; other variants were considered to be novel and thus fulfill the criteria for ultra-rare disease. For each variant, location in genomic sequence, amino acid change, effect on the protein function, conservation score and prediction programs (Polyphen, Polyphen2, SIFT, Condel) were collected and subsequently used for prioritization for candidate variants. Three inheritance hypotheses were tested: 1) recessive with homozygous variant present in affected child (NRA>75%) and heterozygous in parents (5%<NRA>80%), 2) compound heterozygous where one heterozygous allele inherited from father and second from mother (5%<NRA>80%) and 3) autosomal *de novo* with heterozygous

allele present only in child (5%<NRA>80%) and not inherited from parents (NRA=0). Confirmation of selected candidate mutations was performed by capillary sequencing and primer information is available upon request.

Sanger sequencing

DNA of the index patient and twelve additional IO IBD patients was extracted from peripheral blood cells according to standard procedures. Testing of the coding sequences and exon-intron boundaries of the *ANKZF1* gene was performed by standard Sanger sequencing. Sequencing conditions and primer sequences are available upon request. Segregation analysis for the two patients with two mutated *ANKZF1* alleles was performed to confirm the expected inheritance pattern. Sanger sequencing of cloned cDNA synthesized from RNA isolated from peripheral blood of the patient with compound heterozygous *ANKZF1* V32_Q87del and E152K mutations was used to detect exon splicing consequences.

Antibodies and reagents

In this study, the following antibodies were used: rabbit anti-ANKZF1 (HPA035208, Sigma-Aldrich, St. Louis, Missouri, USA), mouse anti-tubulin (T9026, Sigma-Aldrich), mouse anti-TOM20 (612278, BD Biosciences, San Jose, California, USA), mouse anti-LC3 (0231-100, NanoTools, Teningen, Germany), mouse anti-p62 (sc-28359, Santa Cruz Biotechnology, Dallas, Texas, USA), goat anti-actin (sc-1616, Santa Cruz Biotechnology), goat anti-HA (A00168, GenScript, Piscataway, New Jersey, USA), mouse anti-HA (H3663, Sigma-Aldrich), mouse anti-Flag M2 (F3165, Sigma-Aldrich), rabbit anti-Flag (F7425, Sigma-Aldrich), mouse anti-Flag M2-peroxidase (HRP) (A8592, Sigma-Aldrich), mouse anti-GFP (11814460001, Roche, Basel, Switzerland), rabbit anti-phosphoglycerate kinase 1 (PGK1) (kindly provided by dr. F.M. Reggiori), swine anti-rabbit immunoglobulins/HRP (P0399, Dako, Glostrup, Denmark), rabbit anti-mouse immunoglobulins/HRP (P0161, Dako), donkey anti-mouse IgG IRDye 680 (926-32222, LI-COR, Lincoln, Nebraska, USA), donkey anti-goat IgG IRDye 800CW (926-32214, LI-COR), donkey anti-rabbit IgG IRDye 680RD (926-68073, LI-COR), donkey anti-mouse IgG Cy5 (715-175-150, Jackson ImmunoResearch Laboratories, West Grove, Pennsylvania, USA), goat anti-rabbit IgG Alexa Fluor 568 (A11011, Invitrogen), goat anti-rabbit IgG Alexa Fluor 488 (A11008, Invitrogen), anti-human CD3-PE (555333, BD Pharmingen, San Diego, California, USA), anti-human CD14-PerCP/Cy5.5 (301824, BioLegend, San Diego, California, USA) and anti-human CD19-APC (555415, BD Pharmingen).

H_2O_2 30% was purchased from VWR (Radnor, Pennsylvania, USA), cycloheximide and hydroxychloroquine from Sigma-Aldrich and MG132 from Cayman Chemical (Ann Arbor, Michigan, USA).

Generation of plasmids

pcDNA3-Flag-ANKZF1 was generated by adding restriction sites KpnI and XhoI and a Flag-tag to *ANKZF1* (HsCD00322220, Dana-Farber/Harvard Cancer Center, Boston, Massachusetts, USA) and cloning a KpnI-XhoI fragment into the respective cloning site of pcDNA3 (Invitrogen). Using site-directed mutagenesis the pcDNA3-Flag-ANKZF1-R585Q and pcDNA3-Flag-ANKZF1-E152K mutants were constructed. pcDNA3-HA-VCP was generated by adding restriction sites HINDIII and NOTI and a HA-tag to *VCP* (HsCD00347285, Dana-Farber/Harvard Cancer Center) and cloning a HINDIII-NOTI fragment into the respective cloning site of pcDNA3. pMT2-Flag-FOXP3 was described previously [34]. pRS416-Vms1-GFP was generated by amplifying *Vms1* from genomic yeast DNA by PCR and adding restriction sites XhoI and BamHI to *Vms1*. *Vms1* was cloned into a pRS416 vector already containing a GFP tag at the C' terminus (kindly provided by dr. F.M. Reggiori). pRS416-ANKZF1-GFP was generated by adding restriction sites XhoI and BclI to *ANKZF1* and cloning it into the pRS416 vector already containing a GFP tag at the C' terminus. In both pRS416-Vms1-GFP and pRS416-ANKZF1-GFP the TPI promotor was cloned as a KpnI-XhoI fragment. Using site-directed mutagenesis the pRS416-ANKZF1 R585Q-GFP and pRS416-ANKZF1 E152K-GFP mutants were constructed. pCAGGS-pOTC-GFP (kindly provided by dr. R.C. Muise-Helmericks) has been described previously [35].

Cell culture

PBMCs were isolated from human peripheral blood by density gradient centrifugation using Ficoll-Paque Plus (GE Health Care, Little Chalfont, Great Britain) and cultured in Roswell Park Memorial Institute (RPMI) 1640 Medium with GlutaMAX (Life Technologies, Carlsbad, California, USA) supplemented with 10% HyClone (Thermo Scientific, Waltham, Massachusetts, USA), 100 U/ml penicillin (Gibco, Carlsbad, California, USA), 100 µg/ml streptomycin (Gibco) and 50 µM 2-mercaptoethanol (Sigma-Aldrich) at 37°C and 5% CO_2.

B-lymphocytes were transformed with EBV to enable performing experiments with immortalized B-lymphocytes. To this end PBMCs were cultured in RPMI 1640 Medium with GlutaMAX (Life Technologies) supplemented with 10% heat-inactivated FBS (GE health care), 100 U/ml penicillin (Gibco), 100 µg/ml streptomycin (Gibco) and 50 µM 2-mercaptoethanol (Sigma-Aldrich) at 37°C and 5% CO_2. Transduction was performed by adding 1 ml supernatant containing EBV to 5-10·10^6 PBMCs in 1 ml culturing medium. After one day 10 µg/ml cyclosporin was added. When outgrowth of cells was observed, culturing medium was replaced. After six weeks a fully transformed culture of B-lymphocytes was obtained.

U2OS cells (derived from human osteosarcoma cells) and HEK293FT cells (derived from human embryonal kidney cells) were cultured in DMEM with GlutaMAX and

high glucose (Life Technologies) supplemented with 10% heat-inactivated FBS (GE health care), 100 U/ml penicillin (Gibco) and 100 µg/ml streptomycin (Gibco) at 37°C and 5% CO_2.

Fibroblasts were isolated from a skin biopsy according to a standard procedure used in the hospital. Thereafter these cells were cultured as described for U2OS and HEK293FT cells.

shRNA viral transduction of U2OS cells

A lentiviral construct was used containing shRNA control (SHC002, Sigma-Aldrich) or shRNA targeting *ANKZF1* (TRCN0000150131, Sigma-Aldrich) and a puromycin resistance gene in the pLKO.1 vector. HEK293FT cells were grown in 10 cm dishes. After one day lentivirus was produced by cotransfection of 5 µg pLKO.1 vector containing shRNA, 1.8 µg lentiviral packaging vector pLP/VSVG and 3.25 µg lentiviral packaging vector psPAX2 overnight using 50 µl polyethylenimine (PEI) (Polysciences Inc., Warrington, Pennsylvania, USA). The next day the medium was replaced and the cells were cultured for 24 hours. The supernatant containing virus was collected and filtered through a 0.2 µM filter. Transduction was performed by adding 1 ml of viral supernatant, 1 ml culturing medium and 8 µg/ml polybrene to $0.5 \cdot 10^5$ U2OS cells, which had been cultured overnight. After one day the cells were washed with PBS and new culturing medium was added. Selection was achieved by adding 1 µg/ml puromycin (Sigma-Aldrich).

Quantitative real-time polymerase chain reaction

RNA was isolated from different cell types using the RNeasy Mini kit (Qiagen) according to the manufacturer's protocol. cDNA was synthesized using the iScript cDNA synthesis kit (BIO-Rad, Hercules, California, USA) and amplified using SYBR green supermix (BIO-Rad) in a MyIQ single-color real-time PCR detection system (BIO-Rad) according to the manufacturer's protocol. To quantify the data the comparative Ct method was used. The relative quantity was defined as $2^{-\Delta\Delta Ct}$. *β2-microglobulin*, *GAPDH*, *HPRT1* and *RPL13* were used as housekeeper genes. The average of the Ct values of these genes was used as reference. The primers are listed in Table 1.

Western blotting

Cells were lysed in Laemmli buffer (0.12 mol/L Tris-HCl pH 6.8, 4% SDS, 20% glycerol, 0.05 µg/µl bromphenol blue, 35 mmol/L 2-mercaptoethanol) and incubated at 100°C for 5 minutes. The protein concentration was measured by performing a Lowry protein assay. Equal amounts of proteins were separated by SDS-PAGE, transferred to a polyvinylidene difluoride membrane (Merck Millipore, Billerica, Massachusetts, USA), blocked with 5% milk protein in TBST (0.3% Tween, 10 mM Tris pH 8 and 150 mM NaCl in H_2O) and probed with primary antibodies as indicated in Table 2.

Table 1. qRT-PCR primers

Gene	Forward primer	Reverse primer
ANKZF1	TCCTGTTCAGGCTCAGGGGAGAG	AGGGCAGACAGGAGAGGCTTGTC
β2-microglobulin	ATGAGTATGCCTGCCGTGTGA	GGCATCTTCAAACCTCCATG
GAPDH	AAATCCCATCACCATCTTCCA	CATGGTTCACACCCATGACGAA
HPRT1	TGACACTGGCAAAACAATGCA	GGTCCTTTTCACCAGCAAGCT
RPL13	CTATGACCAATAGGAAGAGCA	GCAGAGTATATGACCAGGTGG

Table 2. Antibodies for Western blot

Antibody	Dilution
Goat anti-actin	1:5000
Rabbit anti-ANKZF1	1:1000
Mouse anti-Flag	1:3000
Mouse anti-Flag HRP	1:10000
Mouse anti-GFP	1:3000
Goat anti-HA	1:2500
Mouse anti-LC3	1:1000
Mouse anti-p62	1:1000
Rabbit anti-PGK1	1:7500
Mouse anti-tubulin	1:10000

The membranes were washed with TBST and incubated with appropriate secondary antibodies. Immunocomplexes were detected using enhanced chemoluminescence (GE Healthcare) or the LI-COR Odyssey.

Immunoprecipitation

U2OS cells were grown in 10 cm dishes for one day and transfected with a mixture of 1 µg HA-VCP, 1 µg Flag-ANKZF1 and 10 µl PEI overnight. The next day the cells were washed with PBS and cultured for 24 hours in medium. The cells were left untreated or treated with H_2O_2, washed twice with cold PBS and lysed in RIPA buffer (20 mM Tris pH 7.4, 150 mM NaCl, 1% NP40, 0.1% SDS, 5 mM EDTA) with 1% HALT protease inhibitor (Thermo Scientific). After a preclear using uncoupled protein G agarose beads (Merck Millipore) 1:500 rabbit anti-Flag antibody (Sigma-Aldrich) was added and immunoprecipitation was performed using uncoupled protein G agarose beads (Merck Millipore). The beads were three times washed in RIPA buffer with 1% HALT protease inhibitor and sample buffer (0.12 mol/L Tris-HCl pH 6.8, 4% SDS, 20% glycerol, 0.05 µg/µl bromphenol blue, 35 mM 2-mercaptoethanol) was added. The samples were incubated at 100°C for 5 minutes and subjected to Western blot.

Confocal imaging - Localization studies

U2OS cells were seeded on poly-L-lysine (Sigma-Aldrich) coated coverslips in a 6-wells plate and untransfected or transfected with a mixture of 0.2 µg Flag-ANKZF1, 0.2 µg HA-VCP, 0.2 µg pOTC-GFP and 3 µl PEI per well. The cells were left untreated or treated with H_2O_2, washed with PBS and fixed with 4% paraformaldehyde (VWR) for 30 minutes at room temperature. After quenching with 50 mM NH_4Cl (Merck, Whitehouse Station, New Jersey, USA) for 10 minutes, the cells were permeabilized in permeabilization buffer (PBS with 0.1% saponin (Sigma-Aldrich), 2% BSA (Sigma-Aldrich), 10% normal donkey serum (Jackson ImmunoResearch Laboratories) and if cells were transfected 10% normal goat serum (Jackson ImmunoResearch Laboratories)) for 10 minutes at room temperature. The cells were incubated with primary antibodies in permeabilization buffer for 60 minutes at room temperature as indicated in Table 3, after which they were three times washed with permeabilization buffer. The cells were incubated with appropriate secondary antibodies in permeabilization buffer for 60 minutes at room temperature, washed three times with permeabilization buffer, washed once with PBS and H_2O and mounted in Prolong Gold with Dapi (Invitrogen). The samples were analyzed with a 63x objective on a Zeiss LSM 700 fluorescence microscope.

Table 3. Antibodies for confocal imaging

Antibody	Dilution
Rabbit anti-ANKZF1	1:400
Rabbit anti-Flag	1:500
Mouse anti-HA	1:500
Mouse anti-Tom20	1:750

Confocal imaging - Proximity ligation assay

PLA detection was performed according to the manufacturer's protocol (Olink Bioscience, Uppsala, Sweden). In short, U2OS cells grown on poly-L-lysine coated coverslips in a 6-wells plate were transfected with a mixture of 0.2 µg Flag-ANKZF1, 0.2 µg HA-VCP and 2 µl PEI per well. The cells were left untreated or treated with H_2O_2, washed with PBS, fixed with 4% paraformaldehyde for 30 minutes at room temperature, quenched with 50 mM NH_4Cl for 10 minutes and permeabilized in permeabilization buffer (PBS with 0.1% saponin, 2% BSA and 10% normal donkey serum) for 10 minutes at room temperature. Cells were incubated with primary antibodies in permeabilization buffer for 60 minutes at room temperature as indicated in Table 3 and three times washed with permeabilization buffer. Cells were incubated with the secondary Duolink In Situ PLA Probe anti-mouse PLUS (Sigma-Aldrich) and Duolink In Situ PLA Probe anti-rabbit MINUS (Sigma-Aldrich) antibodies for 60 minutes at 37°C in dark and three times washed in a buffer containing 10 mM Tris pH 7.5, 150 mM NaCl and 0.05% Tween

before detection of the probes using the Duolink In Situ PLA detection kit (Sigma-Aldrich). Cells were analyzed with a 63x objective on a Zeiss LSM 700 fluorescence microscope.

Flow cytometry - Mitochondrial integrity

U2OS cells were seeded in a 24-wells plate and left untreated or treated with H_2O_2. The cells were once washed with PBS, detached from the surface of the well using trypsin (Gibco), collected in a 96-wells plate and washed again with PBS. The cells were stained with 10 µg/ml rhodamine-123 (Invitrogen) in DMEM for 30 minutes at 37°C, washed three times with PBS and analyzed using the FACS Canto II (BD Biosciences).

Flow cytometry – Apoptosis

200000 PBMCs or EBV transformed B-lymphocytes were seeded in a 96-wells plate. The cells were left untreated or treated with H_2O_2 and washed once with PBS. The cells were stained with 1:40 Annexin V FITC (Immunotools, Friesoythe, Germany) in 1x Annexin V binding buffer (BD Pharmingen) in dark for 15 minutes at room temperature. PBMCs were also stained with 1:100 anti-human CD3-PE (BD Pharmingen) and 1:100 anti-human CD19-APC (BD Pharmingen) to distinguish different types of mononuclear cells. The cells were once washed with 1x Annexin V binding buffer, after which PBMCs were stained with 1:1000 Sytox Blue (Invitrogen) and EBV transformed B-lymphocytes with 1:50 propidium iodide (Sigma-Aldrich). All samples were analyzed using the FACS Canto II (BD Biosciences).

Metabolic characterization

Per well of a poly-L-lysine coated 24-wells Seahorse culture plate 50000 U2OS cells or 160000 fibroblasts were seeded. After one day the cells were left untreated or treated with H_2O_2 and regular medium was replaced by XF medium, consisting of RPMI 1640 Medium (Life Technologies) supplemented with 10 mM glucose (Merck), 2 mM L-glutamin (Gibco) and 1 mM sodium pyruvate (Gibco). OCR and ECAR were measured at baseline and after treatment of the cells with 10 µM oligomycin (Seahorse Biosciences, Massachusetts, USA), 1 µM FCCP (Seahorse Biosciences) and 100 µM rotenone (Seahorse Biosciences) using the XF-24 Extracellular Flux Analyzer (Seahorse Biosciences).

Yeast assays - Yeast strains, growth media and transformation

Saccharomyces cerevisiae strain BY4742 was used as WT strain. A BY4742 Δ*Vms1* yeast strain was commercially available. The yeast strains were grown in rich medium containing 1% yeast extract, 2% peptone and 2% glucose. Empty vector pRS416 was transformed into the BY4742 yeast strain and empty vector pRS416, Vms1-GFP,

ANKZF1-GFP WT, ANKZF1-GFP R585Q or ANKZF1-GFP E152K in the BY4742 Δ*Vms1* yeast strain according to a standard procedure [36]. The transformed yeast strains were grown in SMD (0.67% yeast nitrogen base, 2% glucose and amino acids and vitamins as needed) lacking uracil.

Yeast assays - Trichloroacetic Acid (TCA) protein precipitation

Yeast strains were grown overnight in SMD lacking uracil at 30°C. 2 OD600 was collected and after centrifugation incubated with 500 µl icecold 10% TCA for 30 minutes on ice. The yeast were spinned, cold acetone was added to the pellet and the pellet was resuspended by sonification. After incubation at 20°C for 20 minutes the yeast were spinned and the pellet was dried. Glass beads, sample buffer and 5 µl 0.5 M ammoniumacetate were added and the samples were subjected to Western blot.

Yeast assays - Growth assay

Yeast strains were grown overnight in SMD lacking uracil at 30°C. Serial five-fold dilutions of 0.4 OD600 were spotted on SMD plates lacking uracil without H_2O_2 or with 3 mM H_2O_2. The plates were incubated at 30°C for 2 days.

Statistics

Statistical analysis was performed using the unpaired student's t-test with Welch's correction assuming a Gaussian distribution (Prism GraphPad Software). A p-value ≤0.05 was considered statistically significant.

Study approval

The study was approved by the Institutional Review Boards of the University Medical Center Utrecht and the Hospital for Sick Children Toronto. All participants provided written informed consent for the collection of samples and subsequent analysis.

Acknowledgments

We would like to thank the members of the laboratory of Edwin Cuppen for technical support on genetic studies and the members of the laboratory of Paul Coffer for helpful discussions.

References

1. Kaser A, Zeissig S, Blumberg RS. Inflammatory bowel disease. *Annu Rev Immunol* 2010;28:573–621
2. Khor B, Gardet A, Xavier RJ. Genetics and pathogenesis of inflammatory bowel disease. *Nature* 2011;474:307–317
3. Xavier RJ, Podolsky DK. Unravelling the pathogenesis of inflammatory bowel disease. *Nature* 2007; 448:427–434
4. Levine A, Griffiths A, Markowitz J, Wilson DC, Turner D, Russell RK, Fell J, Ruemmele FM, Walters T, Sherlock M, Dubinsky M, Hyams JS. Pediatric modification of the Montreal classification for inflammatory bowel disease: the Paris classification. *Inflamm Bowel Dis* 2011;17:1314–1321
5. Heyman MB, Kirschner BS, Gold BD, Ferry G, Baldassano R, Cohen SA, Winter HS, Fain P, King C, Smith T, El-Serag HB. Children with early-onset inflammatory bowel disease (IBD): analysis of a pediatric IBD consortium registry. *J Pediatr* 2005;146:35–40
6. Polito JM, Childs B, Mellits ED, Tokayer AZ, Harris ML, Bayless TM. Crohn's disease: influence of age at diagnosis on site and clinical type of disease. *Gastroenterology* 1996;111:580–586
7. Paul T, Birnbaum A, Pal DK, Pittman N, Ceballos C, LeLeiko NS, Benkov K. Distinct phenotype of early childhood inflammatory bowel disease. *J Clin Gastroenterol* 2006;40:583–586
8. Gilissen C, Hoischen A, Brunner HG, Veltman JA. Unlocking Mendelian disease using exome sequencing. *Genome Biol* 2011;12:228
9. Ng SB, Nickerson DA, Bamshad MJ, Shendure J. Massively parallel sequencing and rare disease. *Hum Mol Genet* 2010;19:R119-124
10. Ng SB, Buckingham KJ, Lee C, Bigham AW, Tabor HK, Dent KM, Huff CD, Shannon PT, Jabs EW, Nickerson DA, Shendure J, Bamshad MJ. Exome sequencing identifies the cause of a mendelian disorder. *Nat Genet* 2010;42:30–35
11. Glocker E-O, Kotlarz D, Boztug K, Gertz EM, Schäffer AA, Noyan F, Perro M, Diestelhorst J, Allroth A, Murugan D, Hätscher N, Pfeifer D, Sykora K-W, Sauer M, Kreipe H, Lacher M, Nustede R, Woellner C, Baumann U, Salzer U, Koletzko S, Shah N, Segal AW, Sauerbrey A, Buderus S, Snapper SB, Grimbacher B, Klein C. Inflammatory bowel disease and mutations affecting the interleukin-10 receptor. *N Engl J Med* 2009;361:2033–2045
12. Glocker E-O, Frede N, Perro M, Sebire N, Elawad M, Shah N, Grimbacher B. Infant colitis--it's in the genes. *Lancet* 2010;376:1272
13. Worthey EA, Mayer AN, Syverson GD, Helbling D, Bonacci BB, Decker B, Serpe JM, Dasu T, Tschannen MR, Veith RL, Basehore MJ, Broeckel U, Tomita-Mitchell A, Arca MJ, Casper JT, Margolis DA, Bick DP, Hessner MJ, Routes JM, Verbsky JW, Jacob HJ, Dimmock DP. Making a definitive diagnosis: successful clinical application of whole exome sequencing in a child with intractable inflammatory bowel disease. *Genet Med* 2011;13:255–262
14. Blaydon DC, Biancheri P, Di W-L, Plagnol V, Cabral RM, Brooke MA, van Heel DA, Ruschendorf F, Toynbee M, Walne A, O'Toole EA, Martin JE, Lindley K, Vulliamy T, Abrams DJ, MacDonald TT, Harper JI, Kelsell DP. Inflammatory skin and bowel disease linked to ADAM17 deletion. *N Engl J Med* 2011;365:1502–1508
15. Avitzur Y, Guo C, Mastropaolo LA, Bahrami E, Chen H, Zhao Z, Elkadri A, Dhillon S, Murchie R, Fattouh R, Huynh H, Walker JL, Wales PW, Cutz E, Kakuta Y, Dudley J, Kammermeier J, Powrie F,

Shah N, Walz C, Nathrath M, Kotlarz D, Puchaka J, Krieger JR, Racek T, Kirchner T, Walters TD, Brumell JH, Griffiths AM, Rezaei N, Rashtian P, Najafi M, Monajemzadeh M, Pelsue S, McGovern DPB, Uhlig HH, Schadt E, Klein C, Snapper SB, Muise AM. Mutations in tetratricopeptide repeat domain 7A result in a severe form of very early onset inflammatory bowel disease. *Gastroenterology* 2014;146:1028–1039

16. Heo J-M, Livnat-Levanon N, Taylor EB, Jones KT, Dephoure N, Ring J, Xie J, Brodsky JL, Madeo F, Gygi SP, Ashrafi K, Glickman MH, Rutter J. A stress-responsive system for mitochondrial protein degradation. *Mol Cell* 2010;40:465–480
17. van Loosdregt J, Fleskens V, Fu J, Brenkman AB, Bekker CPJ, Pals CEGM, Meerding J, Berkers CR, Barbi J, Gröne A, Sijts AJAM, Maurice MM, Kalkhoven E, Prakken BJ, Ovaa H, Pan F, Zaiss DMW, Coffer PJ. Stabilization of the transcription factor Foxp3 by the deubiquitinase USP7 increases Treg-cell-suppressive capacity. *Immunity* 2013;39:259–271
18. Parsons MJ, Green DR. Mitochondria in cell death. *Essays Biochem* 2010;47:99–114
19. Youle RJ, van der Bliek AM. Mitochondrial fission, fusion, and stress. *Science* 2012;337:1062–1065
20. Dipple KM, McCabe ER. Phenotypes of patients with 'simple' Mendelian disorders are complex traits: thresholds, modifiers, and systems dynamics. *Am J Hum Genet* 2000;66:1729–1735
21. Nadeau JH. Modifier genes in mice and humans. *Nat Rev Genet* 2001;2:165–174
22. Romeo G, McKusick VA. Phenotypic diversity, allelic series and modifier genes. *Nat Genet* 1994;7: 451–453
23. Adolph T-E, Niederreiter L, Blumberg RS, Kaser A. Endoplasmic reticulum stress and inflammation. *Dig Dis* 2012;30:341–346
24. Kaser A, Lee A-H, Franke A, Glickman JN, Zeissig S, Tilg H, Nieuwenhuis EES, Higgins DE, Schreiber S, Glimcher LH, Blumberg RS. XBP1 links ER stress to intestinal inflammation and confers genetic risk for human inflammatory bowel disease. *Cell* 2008;134:743–756
25. Kaser A, Martínez-Naves E, Blumberg RS. Endoplasmic reticulum stress: implications for inflammatory bowel disease pathogenesis. *Curr Opin Gastroenterol* 2010;26:318–326
26. Ron D, Walter P. Signal integration in the endoplasmic reticulum unfolded protein response. *Nat Rev Mol Cell Biol* 2007;8:519–529
27. Restivo NL, Srivastava MD, Schafer IA, Hoppel CL. Mitochondrial dysfunction in a patient with crohn disease: possible role in pathogenesis. *J Pediatr Gastroenterol Nutr* 2004;38:534–538
28. Santhanam S, Rajamanickam S, Motamarry A, Ramakrishna BS, Amirtharaj JG, Ramachandran A, Pulimood A, Venkatraman A. Mitochondrial electron transport chain complex dysfunction in the colonic mucosa in ulcerative colitis. *Inflamm Bowel Dis* 2012;18:2158–2168
29. Sifroni KG, Damiani CR, Stoffel C, Cardoso MR, Ferreira GK, Jeremias IC, Rezin GT, Scaini G, Schuck PF, Dal-Pizzol F, Streck EL. Mitochondrial respiratory chain in the colonic mucosal of patients with ulcerative colitis. *Mol Cell Biochem* 2010;342:111–115
30. Beltrán B, Nos P, Dasí F, Iborra M, Bastida G, Martínez M, O'Connor J-E, Sáez G, Moret I, Ponce J. Mitochondrial dysfunction, persistent oxidative damage, and catalase inhibition in immune cells of naïve and treated Crohn's disease. *Inflamm Bowel Dis* 2010;16:76–86
31. Nazli A, Yang P-C, Jury J, Howe K, Watson JL, Söderholm JD, Sherman PM, Perdue MH, McKay DM. Epithelia under metabolic stress perceive commensal bacteria as a threat. *Am J Pathol* 2004; 164:947–957

32. Harakalova M, Mokry M, Hrdlickova B, Renkens I, Duran K, van Roekel H, Lansu N, van Roosmalen M, de Bruijn E, Nijman IJ, Kloosterman WP, Cuppen E. Multiplexed array-based and in-solution genomic enrichment for flexible and cost-effective targeted next-generation sequencing. *Nat Protoc* 2011;6:1870–1886
33. Nijman IJ, Mokry M, van Boxtel R, Toonen P, de Bruijn E, Cuppen E. Mutation discovery by targeted genomic enrichment of multiplexed barcoded samples. *Nat Methods* 2010;7:913–915
34. van Loosdregt J, Vercoulen Y, Guichelaar T, Gent YYJ, Beekman JM, van Beekum O, Brenkman AB, Hijnen D-J, Mutis T, Kalkhoven E, Prakken BJ, Coffer PJ. Regulation of Treg functionality by acetylation-mediated Foxp3 protein stabilization. *Blood* 2010;115:965–974
35. Yano M, Kanazawa M, Terada K, Namchai C, Yamaizumi M, Hanson B, Hoogenraad N, Mori M. Visualization of mitochondrial protein import in cultured mammalian cells with green fluorescent protein and effects of overexpression of the human import receptor Tom20. *J Biol Chem* 1997;272: 8459–8465
36. Gietz RD, Schiestl RH. High-efficiency yeast transformation using the LiAc/SS carrier DNA/PEG method. *Nat Protoc* 2007;2:31–34

Chapter 3

Loss of syntaxin 3 causes variant microvillus inclusion disease

Désirée Y. van Haaften-Visser*, Caroline L. Wiegerinck*, Andreas R. Janecke*, Kerstin Schneeberger*, Georg F. Vogel*, Johanna C. Escher, Rüdiger Adam, Cornelia E. Thöni, Kristian Pfaller, Alexander J. Jordan, Cleo-Aron Weis, Isaac J. Nijman, Glen R. Monroe, Peter M. van Hasselt, Ernest Cutz, Judith Klumperman, Hans Clevers, Edward E.S. Nieuwenhuis, Roderick H.J. Houwen, Gijs van Haaften, Michael W. Hess#, Lukas A. Huber#, Janneke M. Stapelbroek#, Thomas Müller#, Sabine Middendorp#

*# These authors contributed equally

Gastroenterology 2014;147:65–68

Abstract

Microvillus inclusion disease (MVID) is a disorder of intestinal epithelial differentiation characterized by life-threatening intractable diarrhea. MVID can be diagnosed based on loss of microvilli, microvillus inclusions, and accumulation of subapical vesicles. Most patients with MVID have mutations in *myosin Vb* that cause defects in recycling of apical vesicles. Whole exome sequencing of DNA from patients with variant MVID showed homozygous truncating mutations in *syntaxin 3* (*STX3*). STX3 is an apical receptor involved in membrane fusion of apical vesicles in enterocytes. Patient-derived organoid cultures and overexpression of truncated STX3 in Caco-2 cells recapitulated most characteristics of variant MVID. We conclude that loss of STX3 function causes variant MVID.

Microvillus inclusion disease (MVID) represents a form of congenital diarrhea. Patients typically present with persistent diarrhea within a few days, weeks, or months after birth, resulting in severe dehydration and metabolic acidosis. Current treatment comprises life-long total parenteral nutrition (TPN) and eventual small-bowel and/or liver transplantation [1]. The pathologic hallmarks of MVID are variable loss of brush-border microvilli, microvillus inclusions, and numerous subapical vesicles (secretory granules) in villus enterocytes [2]. In parallel, variant cases of MVID are described with milder clinical phenotypes permitting partial or complete weaning from TPN [3,4].

Mutations in *myosin Vb* (*MYO5B*) have been found to cause classic MVID and our mutation detection rate exceeded 90% in more than 60 MVID patients [5,6] (and unpublished data). MYO5B is a motor protein that facilitates protein trafficking and recycling in polarized cells by Rab11-dependent mechanisms. *MYO5B* mutations result in mislocalization of apical proteins and disrupted enterocyte polarization, leading to MVID [5,7]. Interestingly, *MYO5B* mutations were absent in 2 referrals classified as variant MVID on the basis of clinical presentation.

Patient 1 was a 1-year-old Dutch girl born as the third child of a niece–uncle marriage, who developed watery diarrhea and severe metabolic acidosis from the second day of life. Currently, she receives daily intravenous sodium bicarbonate supplementation and is TPN-dependent but tolerates minimal enteral feeding for varying periods.

Patient 2 was an 18-month-old boy from Pakistan, the first child of a first-cousin marriage, who presented with frequent watery stools in the second week of life and several episodes of severe acidosis. The frequency of loose stools decreased after the early introduction of hydrolysate formula. Pulmonary infections occur frequently and he persistently suffers from mild acidosis, renal tubulopathy, and episodic vomiting. Despite increasing tolerance of enteral nutrition, he still requires partial parenteral nutrition and daily sodium bicarbonate supplementation for adequate growth.

Light and electron microscopy on duodenal and rectal biopsy specimens from both patients showed the histologic characteristics of MVID (**Figure 1A–D and Supplementary Figure 1**): accumulation of periodic acid–Schiff–positive subapical vesicles, intracellular microvillus inclusions, and variable loss of brush border. In contrast to classic MVID, we observed multiple microvilli at the basolateral membranes.

After the exclusion of *MYO5B* mutations by Sanger sequencing, we performed whole exome sequencing—independently for patients 1 and 2—for identifying the causal gene. One single gene, *syntaxin 3* (*STX3*), harbored supposedly disease-causing mutations in both patients. We identified a homozygous nonsense mutation (c.739C>T, p.Arg247*, Ensembl COSM193004) in exon 9 and a homozygous frame-shifting 2-bp insertion (c.372_373dup, p.Arg125Leufs*7) in exon 6 of *STX3* in patients 1 and 2, respectively (**Supplementary Figure 2A and B**). Both mutations were confirmed by

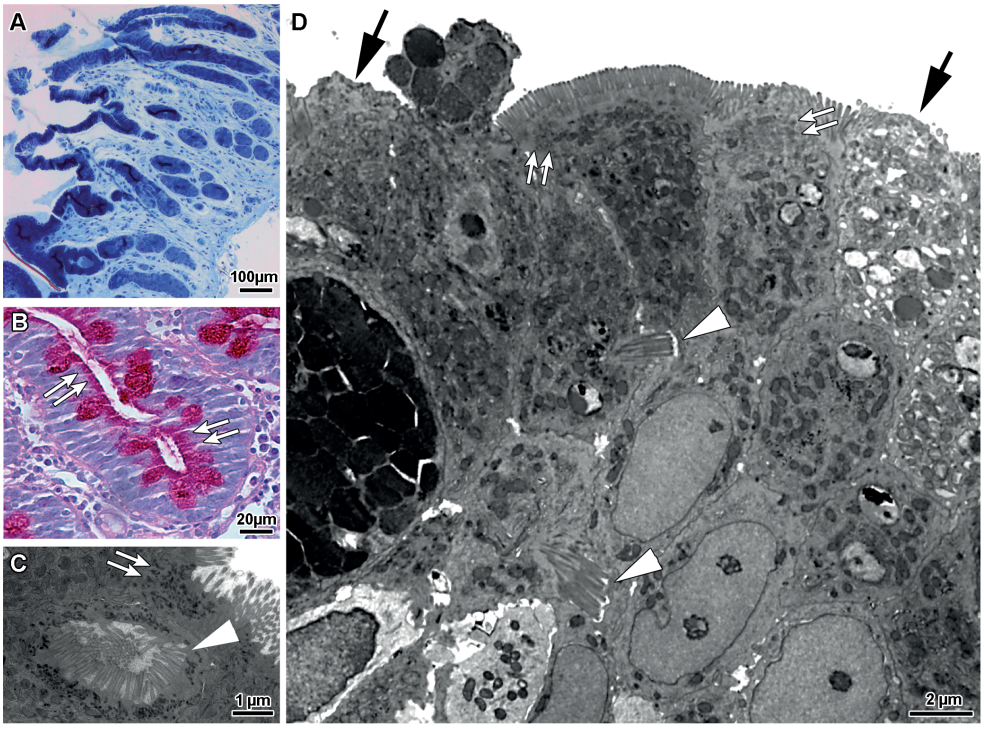

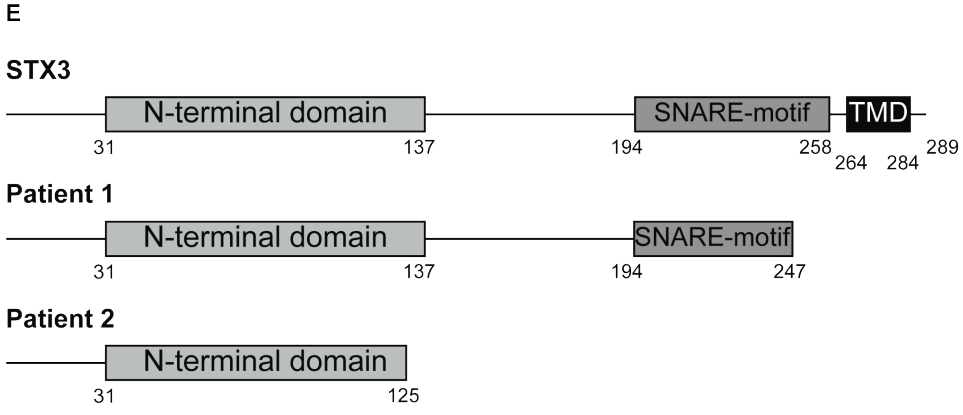

Figure 1. Histology of duodenal biopsy specimens from patients with variant MVID. (A) Toluidine blue staining shows mild focal villus atrophy. **(B)** Subapical accumulation of periodic acid–Schiff–positive vesicles in crypt epithelium (double arrows). **(C)** Secretory granules (double arrows) and microvillus inclusions (arrowhead). **(D)** Transmission electron microscopy shows basolateral microvilli (arrowheads), subapical vesicles (double arrows), atrophic brush border (arrows), and local cell shedding. **(E)** STX3 protein is predicted to be truncated in patient 1 (premature stop at Arg247) and patient 2 (2-bp insertion at Arg125 and premature stop after Arg130). TMD, transmembrane domain.

Sanger sequencing, co-segregated with the disease in the families, and were predicted to cause cellular STX3 protein depletion and truncation (**Figure 1E**), which was supported by Western blotting (**Supplementary Figure 2C**). Sanger sequencing of five additional MYO5B-negative MVID samples did not show *STX3* mutations.

Stable expression of truncated versions of STX3, corresponding to the patients' mutations, recapitulated all histologic hallmarks of MVID in Caco-2 cell cultures (**Figure 2 and Supplementary Figure 3A–E**), including a statistically significant increase of both microvillus inclusions and basolateral microvilli (**Supplementary Table 1**).

Disruption of cell polarity was reflected further by the formation of intercellular lumina within the cell multilayer (**Figure 2 and Supplementary Figure 3C and D**). Confocal laser-scanning microscopy showed mislocalization of STX3 (**Supplementary Figure 3F**), and Western blotting confirmed a reduction of endogenous STX3 levels

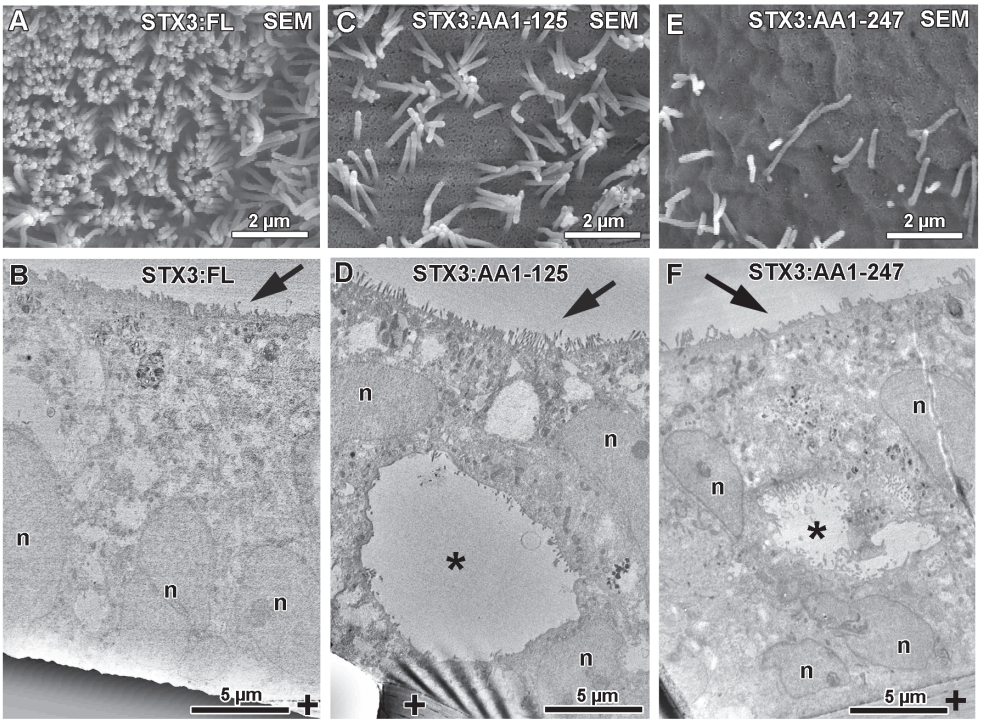

Figure 2. Scanning electron microscopy (SEM) and transmission electron microscopy of Caco-2 cells overexpressing full-length or truncated STX3 (STX3:FL, and STX3:AA1-125 or STX3:AA1-247). (A-B) Polarized monolayer with intact brush border (arrow). **(C-D)** Impaired brush border. Note wide intercellular lumen (asterisk) with scarce microvilli within the cell multilayer. **(E-F)** Cell multilayer with highly eroded brush border and intercellular lumen. n, nuclei; +, cell culture filter membrane.

by overexpression of truncated— but not full-length—STX3 protein (**Supplementary Figure 4**).

Together, these data suggest a dominant-negative effect of truncated STX3, disturbing epithelial polarity.

In addition, we used a recently established 3-dimensional culture of intestinal stem cells (organoids) [8]. Differentiated organoids from duodenal biopsy specimens of MVID patient 1 were devoid of syntaxin 3 staining and recapitulated most morphologic characteristics of the disease (**Supplementary Figure 5**).

The maintenance of epithelial cell function requires the establishment and continuous renewal of differentiated apical and basolateral plasma membrane domains with distinct lipid and protein compositions. STX3, an apically targeted N-ethylmaleimide-sensitive factor attachment protein receptor (SNARE) establishes and maintains polarity, which is necessary for protein trafficking, vesicle fusion, and exocytosis in intestinal, liver, kidney, and gastric parietal cells [9–11]. Target-SNAREs assemble into complexes with vesicle SNAREs, attached to recycling or biosynthetic vesicles [12]. In enterocytes, the apical SNARE complex including STX3 facilitates fusion of the target membrane and vesicles that have been trafficked into close apposition by the Rab11-regulated effector protein MYO5B [11].

Here, we have identified *STX3* mutations in 2 patients with variant MVID, in whom *MYO5B* mutations had been excluded. We were able to mimic the human MVID phenotype by overexpression of truncated STX3 in vitro, indicating loss of STX3 causes variant MVID. Consistent with our findings, it was reported that disruption of STX3 function or ablation of its apical targeting signal impairs delivery of apical markers in vitro, emphasizing syntaxin 3 is likely to act as a key regulatory SNARE in intestinal epithelium [10,13].

Disturbed delivery of apical constituents is a common defect in both classic and variant MVID. In classic MVID, MYO5B deficiency disrupts trafficking between apical recycling endosomes and the apical membrane [14]. In variant MVID, a traffic arrest of apically destined vesicles results from STX3 loss-of-function owing to defective apical docking and exocytosis. Both classic and variant MVID enterocytes display characteristic microvillus inclusions, which might arise from the fusion of apical transport or recycling vesicles under conditions of reduced delivery to the apical plasma membrane. The appearance of microvilli at the basolateral membrane in variant MVID might result from the binding of vesicles to the basolateral syntaxin 4 protein, which is highly homologous to STX3 [13].

Interestingly, patients with mutations in the STX3 binding protein *STXBP2/Munc18-2*, causing familial hemophagocytic lymphohistiocytosis type 5, who have persistent

chronic diarrhea after hematopoietic stem cell transplantation, also showed microvillus atrophy and histologic findings reminiscent of MVID [15].

In conclusion, these data provide a conceptual advance in MVID research because the newly identified causal gene *STX3* will improve the diagnosis, prognosis, genetic counseling, and prenatal screening for MVID.

Acknowledgments

The authors thank members of the Clevers lab (Hubrecht Institute); The Cell Microscopy Center (University Medical Center Utrecht); B. Witting, K. Gutleben, C. Herrmann (Innsbruck), and Y. Meng Heng (Toronto) for technical assistance; and K. Biermann (Pathology, Erasmus MC) for biopsy specimens of patient 1.

References

1. Ruemmele FM, Schmitz J, Goulet O. Microvillous inclusion disease (microvillous atrophy). *Orphanet J Rare Dis* 2006;1:22
2. Sherman PM, Mitchell DJ, Cutz E. Neonatal enteropathies: defining the causes of protracted diarrhea of infancy. *J Pediatr Gastroenterol Nutr* 2004;38:16–26
3. Croft NM, Howatson AG, Ling SC, Nairn L, Evans TJ, Weaver LT. Microvillous inclusion disease: an evolving condition. *J Pediatr Gastroenterol Nutr* 2000;31:185–189
4. Iancu TC, Mahajnah M, Manov I, Shaoul R. Microvillous Inclusion Disease: Ultrastructural Variability. *Ultrastruct Pathol* 2007;31:173–188
5. Müller T, Hess MW, Schiefermeier N, Pfaller K, Ebner HL, Heinz-Erian P, Ponstingl H, Partsch J, Röllinghoff B, Köhler H, Berger T, Lenhartz H, Schlenck B, Houwen RJ, Taylor CJ, Zoller H, Lechner S, Goulet O, Utermann G, Ruemmele FM, Huber LA, Janecke AR. MYO5B mutations cause microvillus inclusion disease and disrupt epithelial cell polarity. *Nat Genet* 2008;40:1163–1165
6. Ruemmele FM, Müller T, Schiefermeier N, Ebner HL, Lechner S, Pfaller K, Thöni CE, Goulet O, Lacaille F, Schmitz J, Colomb V, Sauvat F, Revillon Y, Canioni D, Brousse N, de Saint-Basile G, Lefebvre J, Heinz-Erian P, Enninger A, Utermann G, Hess MW, Janecke AR, Huber LA. Loss-of-function of MYO5B is the main cause of microvillus inclusion disease: 15 novel mutations and a CaCo-2 RNAi cell model. *Hum Mutat* 2010;31:544–551
7. Szperl AM, Golachowska MR, Bruinenberg M, Prekeris R, Thunnissen A-MWH, Karrenbeld A, Dijkstra G, Hoekstra D, Mercer D, Ksiazyk J, Wijmenga C, Wapenaar MC, Rings EHHM, van IJzendoorn SCD. Functional characterization of mutations in the myosin Vb gene associated with microvillus inclusion disease. *J Pediatr Gastroenterol Nutr* 2011;52:307–313
8. Sato T, Vries RG, Snippert HJ, van de Wetering M, Barker N, Stange DE, van Es JH, Abo A, Kujala P, Peters PJ, Clevers H. Single Lgr5 stem cells build crypt–villus structures in vitro without a mesenchymal niche. *Nature* 2009;459:262–265
9. Delgrossi MH, Breuza L, Mirre C, Chavrier P, Le Bivic A. Human syntaxin 3 is localized apically in human intestinal cells. *J Cell Sci* 1997;110 (Pt 1:2207–2214
10. Sharma N, Low SH, Misra S, Pallavi B, Weimbs T. Apical targeting of syntaxin 3 is essential for epithelial cell polarity. *J Cell Biol* 2006;173:937–948
11. Carmosino M, Valenti G, Caplan M, Svelto M. Polarized traffic towards the cell surface: how to find the route. *Biol Cell* 2010;102:75–91
12. Jahn R, Scheller RH. SNAREs--engines for membrane fusion. *Nat Rev Mol Cell Biol* 2006;7:631–643
13. Beest MBA t., Chapin SJ, Avrahami D, Mostov KE. The Role of Syntaxins in the Specificity of Vesicle Targeting in Polarized Epithelial Cells. *Mol Biol Cell* 2005;16:5784–5792
14. Thoeni CE, Vogel GF, Tancevski I, Geley S, Lechner S, Pfaller K, Hess MW, Müller T, Janecke AR, Avitzur Y, Muise A, Cutz E, Huber LA. Microvillus inclusion disease: loss of Myosin vb disrupts intracellular traffic and cell polarity. *Traffic* 2014;15:22–42
15. Stepensky P, Bartram J, Barth TF, Lehmberg K, Walther P, Amann K, Philips AD, Beringer O, Zur Stadt U, Schulz A, Amrolia P, Weintraub M, Debatin K-M, Hoenig M, Posovszky C. Persistent defective membrane trafficking in epithelial cells of patients with familial hemophagocytic lymphohistiocytosis type 5 due to *STXBP2/MUNC18-2* mutations. *Pediatr Blood Cancer* 2013;60:1215–1222

Supplementary Materials and Methods

Human Material

All participants provided written informed consent to participate in this study according to a protocol reviewed and approved by our institutional review boards. Duodenal organoids from 3 healthy controls and patient 1 were generated from duodenal biopsy specimens obtained during duodenoscopy for diagnostic purposes. Whole blood was collected for genetic analysis. The healthy control group included patients susceptible for celiac disease or inflammatory bowel disease with normal pathology.

Whole Exome Sequencing

Genomic DNA was isolated from whole-blood samples using standard manual or robotic procedures. Exome sequencing on patient 1 and her parents was performed as reported previously [1], with the exception that the Agilent (Santa Clara, CA) SureSelect Human All Exon 50Mb Kit V4 was used for enrichment, and sequencing was performed according to the manufacturer's protocol on the Solid5500 (Life technologies, Carlsbad, CA) sequencing platform. We obtained an average coverage of 59-, 63-, and 59-fold for the mother, father, and patient, respectively. Alignment and variant annotation was performed as reported previously [1]. Filtering of rare variants (allele frequency, <0.1; seen <10 times in our in-house database consisting of exome data from 150 individuals and never seen in the homozygous state in our in-house database) with a predicted effect at the protein level for a recessive inheritance model left us with 2 variants, of which the nonsense variant in STX3 was the strongest candidate based on the literature.

The exome of patient 2 was enriched from genomic DNA using Roche-Nimblegen's SeqCap EZ Exome v2 (35-Mb capture region) Exome Enrichment Kit and sequenced using the Illumina HiSeq2000 to a median coverage of 74× according to the manufacturer's protocol, producing approximately 10 gigabases of paired-end 101-bp sequence reads by analysis with CASAVA v1.8 (Illumina, Inc). Sequencing reads were aligned to the human genome (hg19) with Burrows–Wheeler transformation. Polymerase chain reaction duplicates were removed with PICARD (available: http://picard.sourceforge.net) and single-nucleotide substitutions (SNPs), and small indels were identified with the samtools mpileup software and quality-filtered with the Genome Analysis Toolkit (Dice Holdings, New York, NY). All variants were submitted to SeattleSeq (available: http://snp.gs.washington.edu/SeattleSeqAnnotation/) for annotation, categorization into synonymous and nonsynonymous SNPs or indels, and for filtering using the data from the Single Nucleotide Polymorphism database (dbSNP137), the 1000 Genomes Project, the National Heart, Lung, and Blood Institute Exome Sequencing Project Exome Variant Server. The identified mutation was absent from an in-house database of 70 sequenced individuals. Where applicable, variants were classified by predicted

protein effects with Polymorphism Phenotyping v2 (PolyPhen 2) and Scale-invariant feature transform (SIFT).

A spreadsheet-based comparison of all nonconservative and rare homozygous exomic variants of patients 1 and 2 showed a single gene, *STX3*, which harbored supposedly deleterious mutations in both patients.

Sanger Sequencing

The *STX3* mutations from patients 1 and 2 and their parents were verified using Sanger sequencing. Exons 9 and 6 of *STX3* were polymerase chain reaction–amplified in total genomic DNA isolated from peripheral blood lymphocytes of patients 1 and 2 and their parents, respectively, using intronic primers (all sequences available on request). Purified with the Exonuclease I–shrimp alkaline phosphatase enzymes (USB, Cleveland, OH), polymerase chain reaction products were sequenced bidirectionally using the BigDye Terminator v3.1 Cycle Sequencing Kit (Applied Biosystems, Foster City, CA). Fragments were separated electrophoretically on an ABI3730xl DNA Analyzer (Applied Biosystems) and analyzed with JSI SeqPilot software (Kippenheim, Germany). Codon numbering was based on the published online amino acid and messenger RNA sequences of *STX3* (available: http://www.ncbi.nlm.nih.gov.proxy.library.uu.nl/) using the first methionine as an initiation codon.

Organoid Culture

Crypts were isolated from duodenal biopsy specimens of patient 1 and 3 healthy controls and cultured as described previously [2]. The organoids were maintained in expansion medium (containing epidermal growth factor, noggin, R-spondin1, WNT3A, nicotinamide, SB202190, and A83-01) and passaged weekly for 5–10 weeks. To induce differentiation, organoids were cultured in differentiation medium (which is expansion medium without SB202190, nicotinamide, and WNT3A) for 5 days.

Plasmids

Human full-length and truncated *STX3* complementary DNA was polymerase chain reaction–amplified from Caco-2 complementary DNA and ligated into a pENTR4-mCitrine vector using EcoRI and XbaI restriction sites, c-terminally, and in frame with the mCitrine fluorescent protein. The fusion constructs were cloned into the lentiviral expression vector pCCL-EF1a-BlastiR-DEST using the Gateway multicloning technology (Life technologies).

Cell Culture

Caco-2 cells (American Type Culture Collection, Manassas, VA) were grown under standard conditions in Dulbecco's modified Eagle medium containing high glucose, 10%

heat-inactivated fetal bovine serum, 100 U/mL penicillin, 100 µg/mL streptomycin, and 1 mM sodium pyruvate. For lentiviral transduction of Caco-2 cells, Hek293LTV cells were transfected using Lipofectamine LTX (Invitrogen) with the lentiviral expression plasmids together with the vesicular stomatitis virus–G plasmid and the lentiviral gag-pol packaging vector PAX2. Forty-eight and 72 hours after transfection, the viral particle containing supernatant was harvested and directly used for Caco-2 cell infection. Six days after infection, Caco-2 cells were selected with 10 µg/mL BlasticidinS (Invitrogen). For biochemical and microscopical analyses, untreated and genetically modified Caco-2 cells were grown for 14 days on 24-mm Costar Transwell polycarbonate filters (Corning, NY). Three biological replicates from 2 independent experiments were analyzed.

Western Blotting

Western blotting after 10% sodium dodecyl sulfate–polyacrylamide gel electrophoresis and transfer onto polyvinylidene difluoride membranes (GE Healthcare, Little Chalfont, United Kingdom) of Caco-2 lysates was performed as previously described [3]. Incubation with primary antibodies was performed overnight at 4°C. Blots were developed using a chemiluminescence detection system (Santa Cruz). Mouse monoclonal anti-tubulin (1:5000; Sigma Aldrich, Cambridge, United Kingdom), mouse monoclonal anti-enhanced green fluorescent protein (1:1000; Roche, Penzberg, Germany), and rabbit monoclonal anti–syntaxin 3 (1:1000; Abcam ab133750) were used. Secondary horseradish-peroxidase–conjugated anti-rabbit and anti-mouse antibodies (Sigma Aldrich) were used at a dilution of 1:5000.

Organoids were lysed in Laemmli buffer (0.12 mol/L Tris-HCl, pH 6.8, 4% sodium dodecyl sulfate, 20% glycerol, 0.05 µg/µL bromphenol blue, and 35 mmol/L β-mercaptoethanol) and incubated at 100°C for 5 minutes. Detection of syntaxin 3 and tubulin was performed using the Odyssey system (LI-COR, Lincoln, NE) by incubating the blots with donkey anti-rabbit IgG IRDye 680RD (926-68073; LI-COR) and donkey anti-mouse IgG IRDye 680 (926-32222; LI-COR).

Histology

Paraffin slides were generated from biopsy material and organoids. Tissues were fixed in 4% formalin overnight and 4% neutral buffered formalin for 45 minutes at room temperature, respectively. Sections (3-µm thick) were subjected to periodic acid–Schiff staining according to standard techniques. Semithin resin sections (see later) were stained with 1% toluidine blue to illustrate gross morphology of the intestinal mucosa.

Immunofluorescence and Immunohistochemistry

Duodenal biopsy specimens were embedded in Tissue-Tek optimum cutting temperature Compound and frozen at -80°C. Sections were fixed for 20 minutes in 4% PFA in phosphate-buffered saline without calcium and magnesium, and permeabilized for 5 minutes with 0.3% Triton X-100 (Sigma Aldrich). After washing with phosphate-buffered saline, slides were blocked for 1 hour at room temperature with 5% bovine serum albumin and 15% goat serum in phosphate-buffered saline. Incubation with primary antibodies was performed overnight at 4°C with rabbit monoclonal anti–syntaxin 3 (Abcam) or mouse monoclonal anti-CD10 (ImmunoTools, Germany). Alexa568 goat anti-rabbit, Alexa568 goat anti-mouse and Alexa488 phalloidin (Life technologies) were used for fluorescence and actin cytoskeleton labeling, respectively.

Caco-2 cells grown for 14 days on filters were fixed with 4% buffered paraformaldehyde solution and processed essentially as previously described [4]. Briefly, fixed Caco-2 cells were permeabilized with 0.3% Triton X-100 (Sigma-Aldrich) for 30 minutes and subsequently blocked with phosphate-buffered saline containing 15% goat serum for 1 hour at room temperature. Mouse monoclonal anti-CD26/dipeptidylpeptidase IV (HBB3/775/42, obtained from the Developmental Studies Hybridoma Bank, created by the National Institute of Child Health and Human Development of the National Institutes of Health, and maintained at the Department of Biology, University of Iowa, Iowa City, IA) and rabbit monoclonal anti–syntaxin 3 (Abcam) primary antibody were incubated overnight at 4°C and labeled with secondary antibody Alexa568 goat anti-mouse and anti-rabbit (Invitrogen), respectively. Actin filaments were stained with phalloidin-Alexa568 (1:500; Invitrogen) in blocking solution for 1 hour at room temperature.

Both biopsy material and Caco-2 cells were incubated with Hoechst 33342 (1:10,000; Thermo Scientific, Waltham, MA) to stain nuclei and mounted in Mowiol (Sigma-Aldrich). Epifluorescence images were recorded with an Axio Imager M1 (Carl Zeiss; Oberkochen, Germany) fluorescent microscope equipped with a charge-coupled device camera (SPOT Xplorer; Visitron Systems, Puchheim, Germany) and analyzed with ImageJ, version 1.49a software (National Institutes of Health, Bethesda, MD). Confocal image stacks were recorded with a Leica SP5 confocal fluorescence microscope (Leica Microsystems), deconvolved using Huygens Professional Deconvolution and AnalysisSoftware (Scientific Volume Imaging, Hilversum, The Netherlands), exported using Imaris 3D rendering (Bitplane AG, Zürich, Switzerland), and afterward adjusted for brightness, contrast, and pixel size in GNU Image Manipulation Program version 2.8.10 (GIMP) open source software.

Organoids were cultured for 5 days in expansion medium and fixed in 4% buffered paraformaldehyde solution for 30 minutes at room temperature. Immunofluorescent labeling was performed as described [5]. Primary monoclonal antibodies used were

rabbit anti-human syntaxin 3 (clone EPR8543, 1:100; Abcam) and rat anti-human α6-integrin (clone GoH3, 1:200; BD Pharmingen). Secondary antibodies used were Alexa488-conjugated goat anti-rabbit (Life Technologies) and Dylight649-conjugated goat anti-rat (Biolegend). F-actin was stained with phalloidin-Tetramethylrhodamine (TRITC) (Sigma-Aldrich). Confocal image stacks were recorded with a LSM 710 confocal fluorescent microscope (Carl Zeiss) and analyzed with Volocity software version 6.3 (Perkin Elmer).

Transmission Electron Microscopy

Intestinal biopsy specimens, organoids, and Caco-2 cell cultures were processed according to standard procedures [4]. Briefly, biopsy specimens and Caco-2 cells were fixed with 4% buffered paraformaldehyde solution overnight at room temperature and organoids in 0.1 mol/L PHEM buffer (60 mmol/L 1,4-piperazinediethanesulfonic acid, 25 mmol/L HEPES, 2 mmol/L MgCl2, 10 mmol/L ethylene glycol-bis(β-aminoethyl ether)-N,N,N′,N′-tetraacetic acid, pH 6.9) for 3.5 hours at room temperature and then stored in 1% paraformaldehyde in 0.1 mol/L PHEM buffer at 4°C. Before embedding, the specimens were postfixed with 1% OsO4 (optionally followed by 1.5% $K_3Fe[CN]_6$, and subsequently 0.5% uranyl acetate). Samples then were dehydrated and embedded into Epon epoxy resin (Polysciences GmbH, Eppelheim, Germany). Ultrathin sections of 60 nm were contrasted with uranyl acetate and lead citrate.

Scanning Electron Microscopy

Caco-2 cell cultures were processed according to standard procedures [6].

Morphometry and Statistics

The frequency of microvillus inclusions and sites of basolateral microvilli in Caco-2 cells, stably expressing mCitrine-STX3:FL, mCitrine-STX3:AA1-125, and mCitrine-STX3:AA1-247, was estimated by quantitative epifluorescence microscopy and transmission electron microscopy of thin sections cut perpendicularly to the cell culture surface (3 samples from 2 independent experiments, 460–650 cells per condition). The significance of differences between mCitrine-STX3:FL controls and the truncating mutations was tested using 2-sided (2-tailed) P values using the Fisher exact test. Epifluorescence microscopy was used to count the number of ring- and dot-like structures, positive either for actin or the apical marker CD26/dipeptidylpeptidase IV as compared with the cell number; thus, these structures comprised intracellular microvillus inclusions, as well as sites of basolateral microvilli. Transmission electron microscopy was used to further distinguish intracellular microvillus inclusions from sites of basolateral microvilli (**Supplementary Table 1**).

Supplementary References

1. Harakalova M, van Harssel JJT, Terhal PA, van Lieshout S, Duran K, Renkens I, Amor DJ, Wilson LC, Kirk EP, Turner CLS, Shears D, Garcia-Minaur S, Lees MM, Ross A, Venselaar H, Vriend G, Takanari H, Rook MB, van der Heyden MAG, Asselbergs FW, Breur HM, Swinkels ME, Scurr IJ, Smithson SF, Knoers N V, van der Smagt JJ, Nijman IJ, Kloosterman WP, van Haelst MM, van Haaften G, Cuppen E. Dominant missense mutations in ABCC9 cause Cantú syndrome. *Nat Genet* 2012;44:793–796
2. Dekkers JF, Wiegerinck CL, de Jonge HR, Bronsveld I, Janssens HM, de Winter-de Groot KM, Brandsma AM, de Jong NWM, Bijvelds MJC, Scholte BJ, Nieuwenhuis EES, van den Brink S, Clevers H, van der Ent CK, Middendorp S, Beekman JM. A functional CFTR assay using primary cystic fibrosis intestinal organoids. *Nat Med* 2013;19:939–945
3. Fialka I, Pasquali C, Lottspeich F, Ahorn H, Huber LA. Subcellular fractionation of polarized epithelial cells and identification of organelle-specific proteins by two-dimensional gel electrophoresis. *Electrophoresis* 1997;18:2582–2590
4. Thoeni CE, Vogel GF, Tancevski I, Geley S, Lechner S, Pfaller K, Hess MW, Müller T, Janecke AR, Avitzur Y, Muise A, Cutz E, Huber LA. Microvillus inclusion disease: loss of Myosin vb disrupts intracellular traffic and cell polarity. *Traffic* 2014;15:22–42
5. Chaki M, Airik R, Ghosh AK, Giles RH, Chen R, Slaats GG, Wang H, Hurd TW, Zhou W, Cluckey A, Gee HY, Ramaswami G, Hong C-J, Hamilton BA, Cervenka I, Ganji RS, Bryja V, Arts HH, van Reeuwijk J, Oud MM, Letteboer SJF, Roepman R, Husson H, Ibraghimov-Beskrovnaya O, Yasunaga T, Walz G, Eley L, Sayer JA, Schermer B, Liebau MC, Benzing T, Le Corre S, Drummond I, Janssen S, Allen SJ, Natarajan S, O'Toole JF, Attanasio M, Saunier S, Antignac C, Koenekoop RK, Ren H, Lopez I, Nayir A, Stoetzel C, Dollfus H, Massoudi R, Gleeson JG, Andreoli SP, Doherty DG, Lindstrad A, Golzio C, Katsanis N, Pape L, Abboud EB, Al-Rajhi AA, Lewis RA, Omran H, Lee EY-HP, Wang S, Sekiguchi JM, Saunders R, Johnson CA, Garner E, Vanselow K, Andersen JS, Shlomai J, Nurnberg G, Nurnberg P, Levy S, Smogorzewska A, Otto EA, Hildebrandt F. Exome capture reveals ZNF423 and CEP164 mutations, linking renal ciliopathies to DNA damage response signaling. *Cell* 2012;150:533–548
6. Ruemmele FM, Müller T, Schiefermeier N, Ebner HL, Lechner S, Pfaller K, Thöni CE, Goulet O, Lacaille F, Schmitz J, Colomb V, Sauvat F, Revillon Y, Canioni D, Brousse N, de Saint-Basile G, Lefebvre J, Heinz-Erian P, Enninger A, Utermann G, Hess MW, Janecke AR, Huber LA. Loss-of-function of MYO5B is the main cause of microvillus inclusion disease: 15 novel mutations and a CaCo-2 RNAi cell model. *Hum Mutat* 2010;31:544–551

Supplementary Table

Supplementary Table 1. Summary of the statistical analyses of Caco-2 cells with full-length or truncated STX3 expression

	DPPIV/CD26 -rings/dots	Actin-rings/dots		*P* value	Intracellular microvillus inclusions		*P* value	Sites of basolateral microvilli		*P* value
STX3-FL	Mean, 0.4%	Mean, 0.2%	~ 500 cells		Mean, 0.0%	~ 460 cells		Mean, 1.5%	~ 460 cells	
STX3-AA1-125	Mean, 11.2%	Mean, 10.8%	~ 500 cells	<.0001	Mean, 1.7%	~ 650 cells	<.0038	Mean, 9.8%	~ 650 cells	<.0001
STX3-AA1-247	Mean, 8.4%	Mean, 10.2%	~ 500 cells	<.0001	Mean, 1.8%	~ 500 cells	<.0039	Mean, 12.5%	~ 500 cells	<.0001
	Fluorescence microscopy	Fluorescence microscopy			TEM			TEM		

TEM, transmission electron microscopy

Supplementary Figures

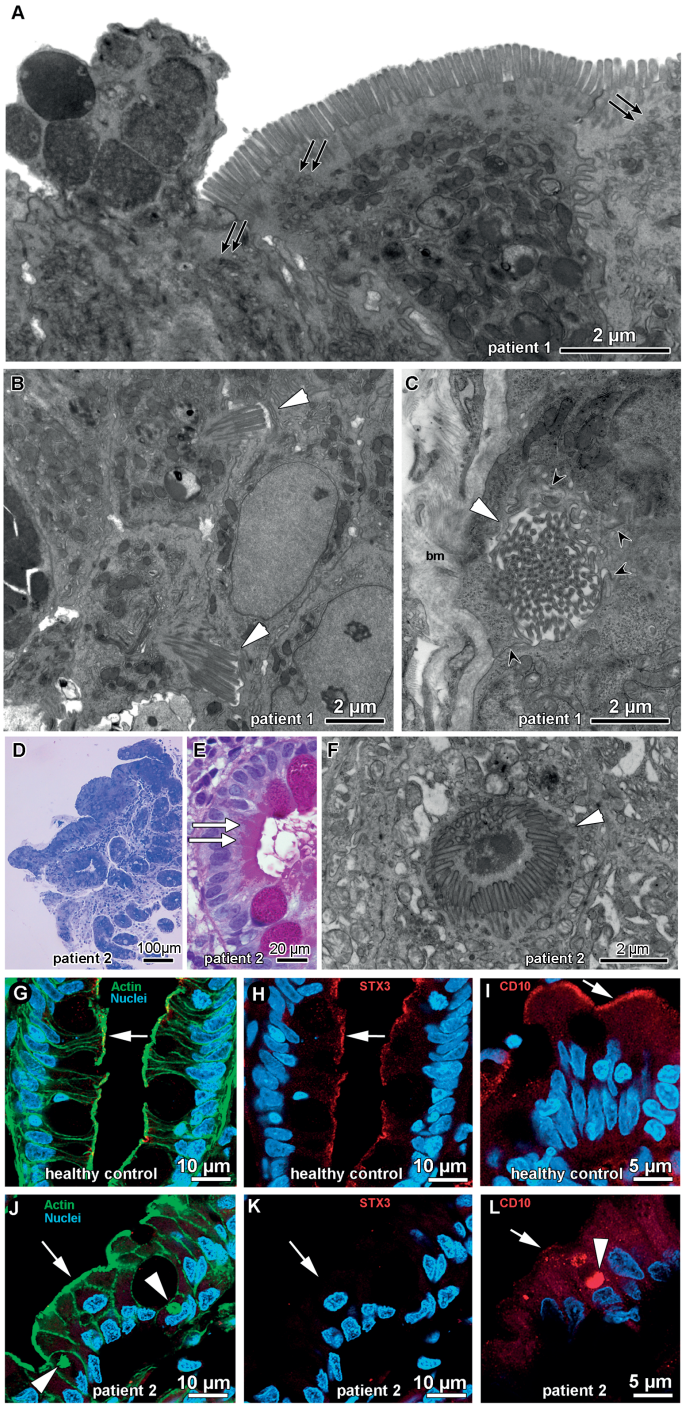

Supplementary Figure 1. (A–C) Ultrastructural details from MVID patient 1 (as described in Figure 1D). (A) Subapical vesicle accumulations, representing secretory granules (double arrows). (B) Basolateral microvilli (arrowheads). (C) Basolateral microvilli (arrowhead) (black arrowheads show cell junctions). bm, basement membrane. **(D–F)** Histology and transmission electron microscopy of duodenal biopsy specimens from patient 2 with variant MVID. (D) Toluidine blue staining shows mild focal villus atrophy. (E) Subapical accumulation of periodic acid–Schiff–positive vesicles in crypt epithelium (double arrows). (F) Microvillus inclusion (arrowhead). **(G–L)** Fluorescence microscopy showing villus epithelium of duodenal biopsy specimens from (G–I) healthy control and (J–L) MVID patient 2. Controls display proper distribution of (G) actin, (H) STX3, and (I) the apical marker CD10. Biopsy samples from patient 2 show (J) dot- and ring-like actin-rich inclusions (arrowheads), and (K) absence of STX3-staining and (L) cytoplasmic mislocalization of CD10. The apical plasma membrane is marked by arrows, microvillus inclusions are highlighted by arrowheads, and nuclei are counterstained with Hoechst dye.

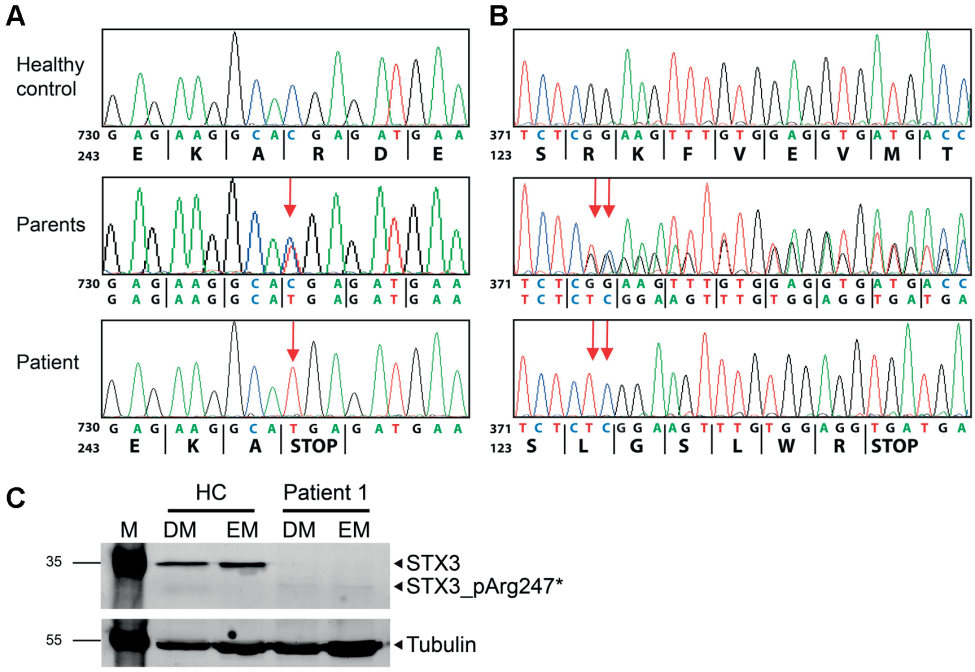

Supplementary Figure 2. Sanger sequencing of STX3 in peripheral blood of healthy controls, parents, and patients. (A) Patient 1: c.739C>T mutation leads to a premature stop at Arg247. **(B)** Patient 2: 2-bp insertion (c.372_373dup) leads to frameshift and premature stop after Arg130. **(C)** Western blot for STX3 on organoids from healthy control and patient 1 cultured in expansion medium (EM) or differentiation medium (DM). Representative of 2 samples from patient 1 and 2 controls. HC, healthy control; M, marker.

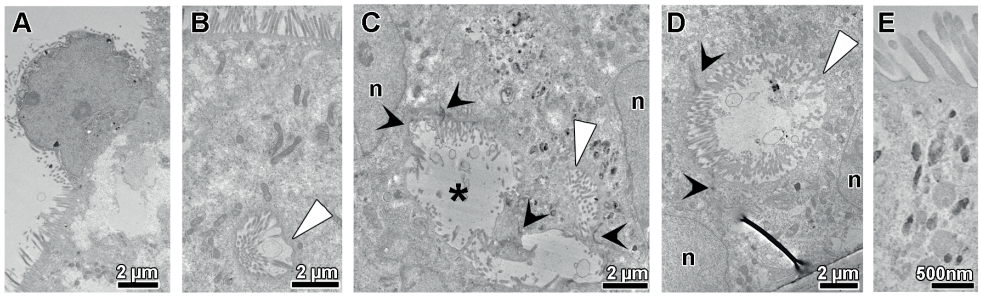
A
2 µm
B
2 µm
C
n
n
*
2 µm
D
n
n
2 µm
E
500nm

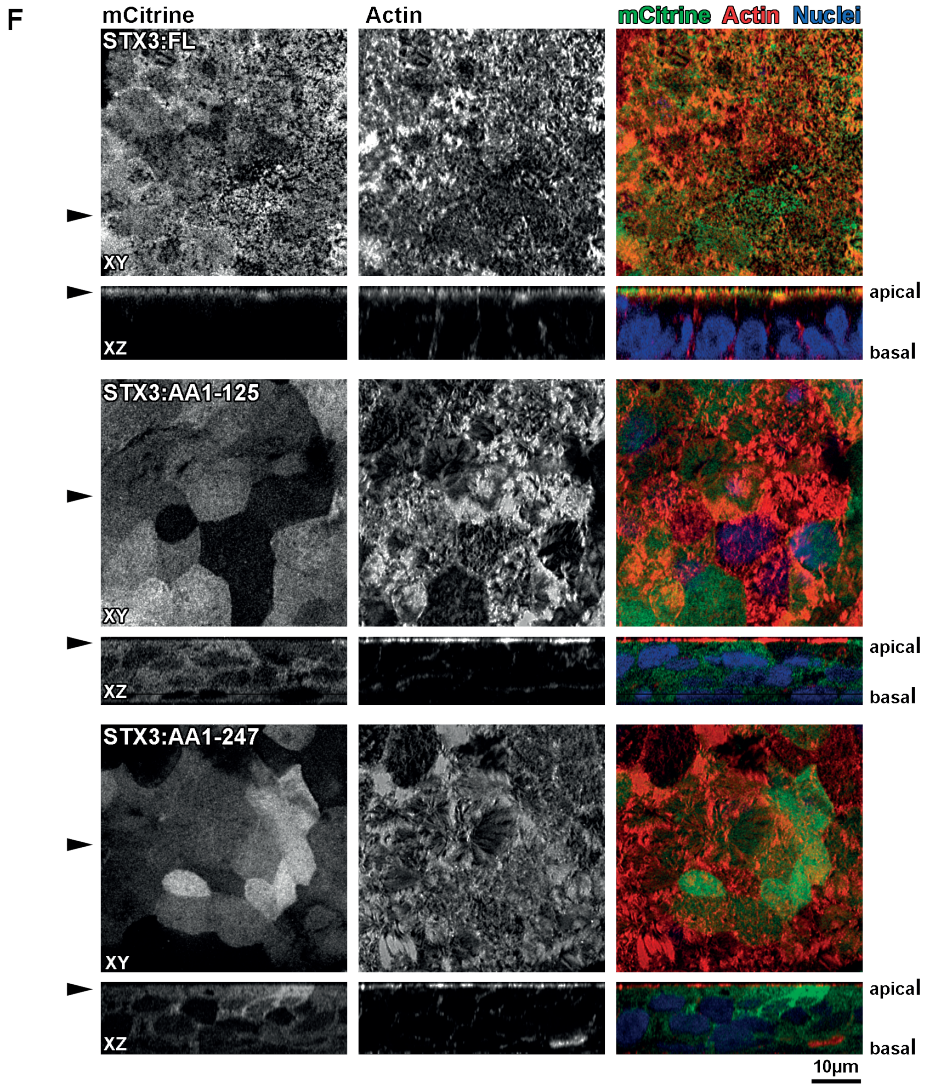
F
mCitrine
Actin
mCitrine Actin Nuclei
STX3:FL
XY
XZ
apical
basal
STX3:AA1-125
XY
XZ
apical
basal
STX3:AA1-247
XY
XZ
apical
basal
10µm

Supplementary Figure 3. (A–E) Transmission electron microscopy of Caco-2 cells stably expressing truncated STX3 (STX3:AA1-247). Cytologic details of STX3:AA1-247. (A) Denuded, shedding cell. (B) Cytoplasmic microvillus inclusion (arrowhead). (C) Pleomorphic intercellular lumen (asterisk) and associated basolateral microvilli (white arrowhead) (black arrowheads show cell junctions). (D) Basolateral microvilli (white arrowhead) (black arrowheads show cell junctions). (E) Subapical vesicles, resembling secretory granules. **(F)** Confocal fluorescence microscopy of Caco-2 cells, stably expressing mCitrine-STX3:FL (upper), mCitrine-STX3:AA1-125 (middle), and mCitrine-STX3:AA1-247 (lower) fusion proteins in xy and xz projections. Fluorescent signal of mCitrine (left), filamentous actin (middle), and merged channels including nuclear counterstaining (right). STX3:FL and endogenous STX3 localize strictly apically, whereas STX3:AA1-125 and STX3:AA1-247 are found throughout the cytoplasm. Expression of the truncated forms of STX3 results in multilayered growth of Caco-2 cells. Arrowheads on the left side indicate the optical section planes of xy and xz, respectively. Note the reduced apical actin signal in mCitrine-STX3:AA1-247.

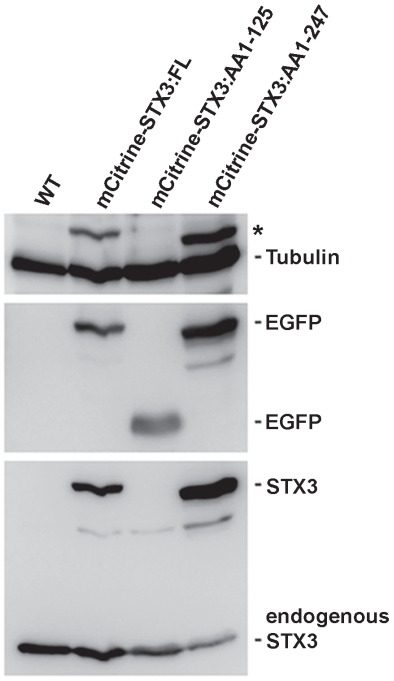

Supplementary Figure 4. Western blot illustrating the overexpression of mCitrine-STX3FL, mCitrineSTX3:AA1-125, and mCitrineSTX3:AA1-247 in Caco-2 cells, compared with untransduced cells (WT). EGFP shows the overexpression via detection of the mCitrine tag. Rabbit anti-STX3 antibody confirms overexpression of the STX3-mCitrine fusion construct (upper STX3 band) as well as endogenous STX3. Endogenous STX3 levels clearly decrease upon overexpression of STX3:AA1-25 and 1-247. Rabbit anti-STX3 antibody does not detect the short STX3:AA1-125. Tubulin was used as loading control (asterisk, unspecific band).

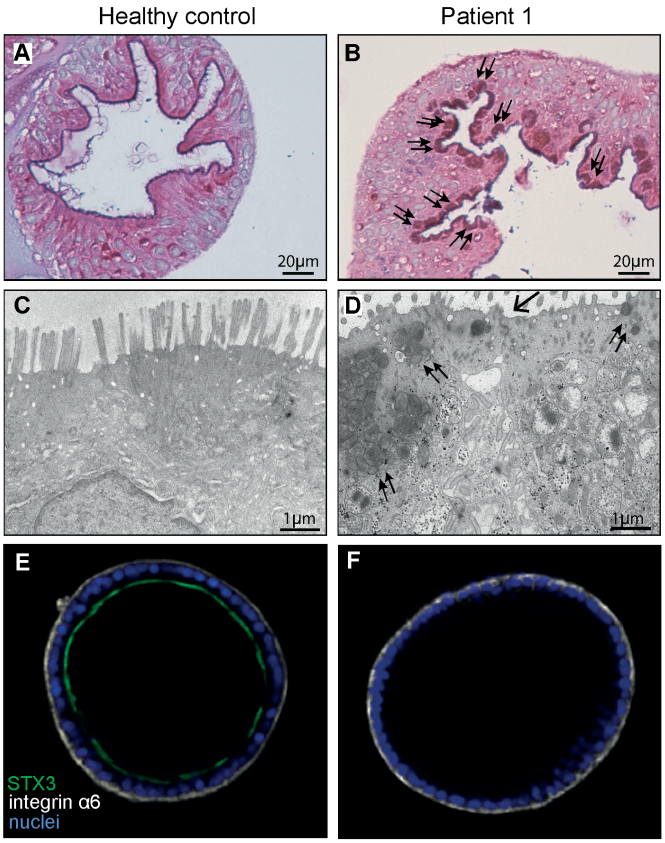

Supplementary Figure 5. Organoids derived from duodenal biopsy specimens from (A, C, and E) healthy control and (B, D, and F) patient 1 were incubated in differentiation medium for 5 days before harvesting. **(A)** Periodic acid–Schiff staining of apical brush border in the control sample, and **(B)** subapically accumulating material (double arrows) in the patient sample. Normal brush-border microvilli in **(C)** control sample contrast with partial loss of microvilli (arrow) and subapical accumulation of vesicles (double arrows) in **(D)** patient sample. **(E and F)** Confocal immunofluorescence microscopy shows the localization of STX3 (green) and integrin α6 (basolateral marker; white) in organoids from (E) healthy control and loss of STX3 in (F) patient 1.

Chapter 4

Loss of function of DGAT1 is associated with fat intolerance

Désirée Y. van Haaften – Visser*, Jorik M. van Rijn*, Freddy T.M. Kokke, Klaske D. Lichtenbelt, Maarten P.G. Massink, Karen J. Duran, Peter J.G. Nikkels, Edward E.S. Nieuwenhuis, Paul J. Coffer, Roderick H.J. Houwen, Gijs van Haaften, Sabine Middendorp

* These authors contributed equally

Manuscript in preparation

Abstract

Congenital diarrheal disorders (CDD) are rare disorders of the gastrointestinal system that result in, often fatal, malnutrition in the first weeks of life. Recently, a unique protein-losing enteropathy (PLE) phenotype was associated with mutations in the *DGAT1* gene, causing severe diarrhea and hypoalbuminemia in four unrelated families. *DGAT1* encodes diacylglycerol O-acyltransferase 1, which is responsible for the production of triacylglycerol.

Here, we identified a previously unknown *DGAT1* mutation in two brothers with vomiting and failure to thrive due to fat intolerance. Whole exome sequencing revealed a novel homozygous *DGAT1* c.629_631delCCT mutation, which leads to ubiquitin-mediated proteasomal degradation of enterocytic DGAT1. By generating monolayers from patient-derived duodenal organoid cultures, we have developed a functional assay to assess DGAT1 function in vitro. We show that upon stimulation of enterocytes with oleic acid, *DGAT1* mutant patients show an increased accumulation of lipid droplets compared to controls.

Our findings show that DGAT1 deficiency is not only a cause of congenital diarrhea with PLE, but is also linked to fat intolerance. These data indicate that newly identified *DGAT1* mutant patients can potentially be treated with a fat-free diet to resolve diarrhea and/or vomiting.

Introduction

Congenital diarrheal disorders (CDD) are a group of rare inherited intestinal disorders that are characterized by persistent life-threatening intractable diarrhea and nutrient malabsorption. CDDs are classified based upon their aberrations in absorption and transport of nutrients and electrolytes, enterocyte differentiation and polarization, enteroendocrine cell differentiation or dysregulation of the intestinal immune response [1]. One form of CDD is protein losing enteropathy (PLE). Patients with homozygous mutations in *DGAT1* (OMIM #: 604900) have been described to present with both congenital diarrhea and symptoms of protein losing enteropathy [2–4].

DGAT1 is, together with DGAT2, responsible for the conversion of diacylglycerol (DAG) and fatty acyl CoA to triacylglycerol (TAG) in humans [5,6]. Triacylglycerol is the main energy substrate stored in human adipose tissue and is essential for milk production in the mammary gland and for VLDL-mediated transport of lipids to peripheral tissues [7,8]. In the human small intestine only *DGAT1* is highly expressed, whereas *DGAT2* is mainly expressed in the liver [3,9]. The active domain of DGAT1 is located in the lumen of the endoplasmic reticulum. In the enterocyte, TAG is stored in lipid droplets or packaged into chylomicrons for secretion into the lymphatic system [5,10,11].

Disruption of any step of TAG absorption can result in fat malabsorption. Clinical manifestations of fat malabsorption are vomiting, steatorrhea, abdominal distension and failure to thrive. Furthermore, deficiencies of triacylglycerol and lipid soluble vitamins can lead to severe complications, including ophthalmological and neurological abnormalities [12–16]. Diseases causing fat malabsorption highly interfere with the quality of life, since life-long dietary changes and lipid-soluble vitamin suppletion are the only current treatment [12–16].

Here, we performed whole exome sequencing in two brothers with fat intolerance and identified a previously unknown homozygous deletion of three nucleotides in exon 7 of *DGAT1*, leading to loss of a serine residue in DGAT1 protein. By using patient-specific organoids, we show that this mutation causes a complete loss of protein in intestinal epithelial cells, most likely due to an increased ubiquitin-mediated proteasomal degradation of DGAT1. We determined that upon stimulation with oleic acid patient cells favoured storage of fatty acids in lipid droplets.

In conclusion, we show that DGAT1 dysfunction is not only associated with congenital diarrhea and protein losing enteropathy, but also with fat intolerance, indicating that a fat-free diet might be the first line of therapy for *DGAT1* mutant patients.

Results

Homozygous *DGAT1* mutation in two brothers with fat intolerance

The oldest brother presented at the age of one month with vomiting and failure to thrive. Physical examination showed a dystrophic boy without further abnormalities. A scintigraphy was performed, which showed esophageal hypomotility and delayed gastric emptying. Extensive additional research, including endoscopy, imaging, metabolic research and genetic research, did not reveal a diagnosis. Initially the patient was treated with total parenteral feeding (TPN), which reversed the symptoms. By experiment, a fat restricted diet was introduced, which enabled enteral feeding again. Incidental ingestion of low amounts of fat causes abdominal pain and vomiting within roughly one hour after ingestion. The boy receives monthly infusions of Intralipid® and Omegaven® and suppletion of lipid-soluble vitamins, leading to normal plasma levels of lipid-soluble vitamins and fatty acids, except for decreased levels of behenic acid, lignoceric acid and linoleic acid. Neuropsychological evaluation due to the fat restricted diet showed an average cognition, delayed velocity and attention deficit. In addition, he was diagnosed with Gilles de la Tourette Syndrome, which is treated with dexamphetamine.

The youngest brother presented with vomiting in the first days of life, which was reversed after immediate introduction of a fat restricted diet. Like his brother, he is supplemented with lipid-soluble vitamins and monthly infusions of Intralipid® and Omegaven®, leading to normal plasma levels of lipid-soluble vitamins and fatty acids, except for decreased levels of lignoceric acid and linoleic acid. He was also diagnosed with Gilles de la Tourette Syndrome, which is treated with dexamphetamine.

When the brothers were 10 and 7 years old, respectively, they presented in our academic center for a second opinion. Both patients underwent a gastro duodenoscopy, which showed no macroscopic or microscopic abnormalities (**Supplementary Figure 1A and 1B**). Since the symptoms initiated very early in life and two siblings were affected, a hereditary cause was expected, although the parents were not known to be consanguineous. To identify potential genetic defects, whole exome sequencing was performed. The largest homozygous region shared between the two siblings was a region of 9 Mb on chromosome 8. In this region we identified four rare variants with a predicted effect at the protein level. These variants were c.958G>A (p.Glu320Lys) in *SLC45A4* (NM_001080431.1), c.618_623delCCACCA (p.His206_His208delinsHis) in *MAFA* (NM_201589.3), c.4486C>T (p.Arg1496Cys) in *PLEC* (NM_201380.2) and c.629_631delCCT (p.Ser210_Tyr211delinsTyr) in *DGAT1* (NM_012079.5). Inspection of homozygous variants outside the largest homozygous region did not yield additional candidate variants of interest. The mutation in *DGAT1* was the most interesting for follow-up because of the known role of DGAT1 in lipid metabolism. Sanger sequencing confirmed the homozygous state of this *DGAT1* mutation in the two

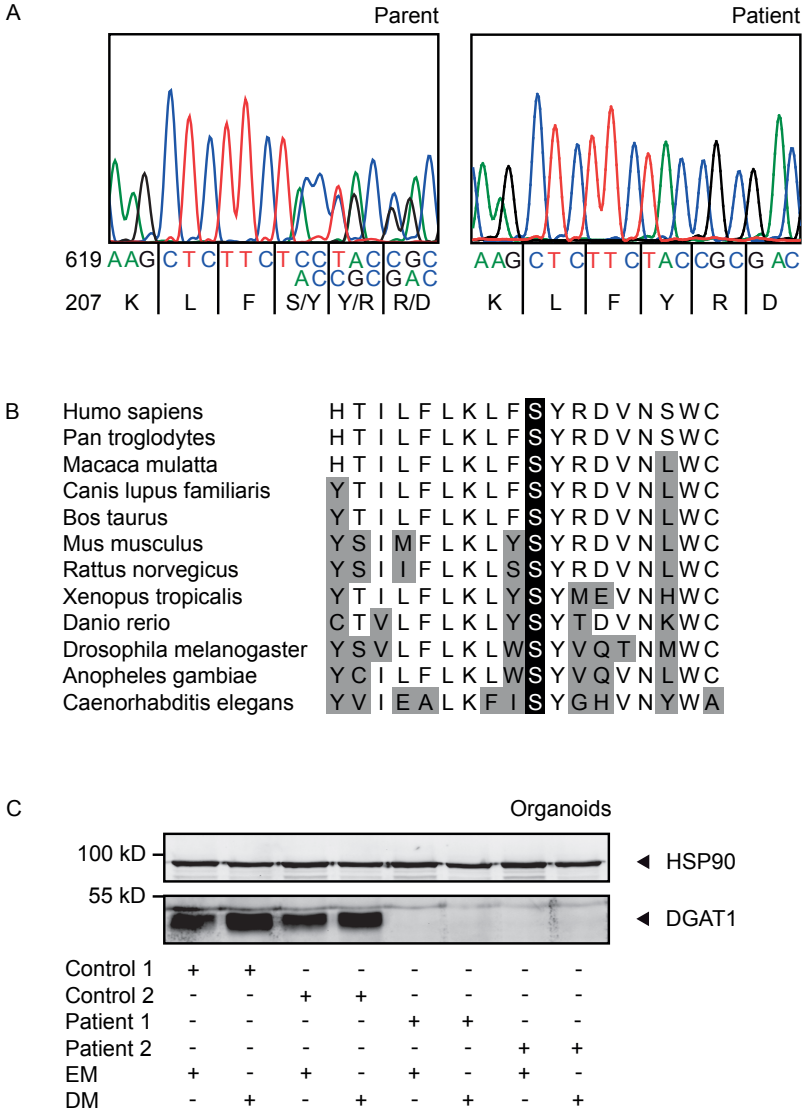

Figure 1. Homozygous *DGAT1* c.629_631delCCT mutation in two brothers with fat intolerance.
(A) Sanger sequencing of *DGAT1* in peripheral blood derived genomic DNA from patients with fat intolerance and their parents. The sequence of only one parent and one patient is depicted. **(B)** Alignment of amino acids 201 till 218 of human DGAT1 among indicated species. Serine deleted in DGAT1 c.629_631delCCT is marked in black. Amino acids different from human sequence are indicated in grey. **(C)** DGAT1 protein expression in undifferentiated (EM) and differentiated (DM) organoids from two healthy controls and two patients with homozygous *DGAT1* c.629_631delCCT mutation. Protein expression was determined by Western blot analysis using anti-DGAT1 and anti-HSP90 antibodies. Results are representative of three independent experiments. EM, expansion medium; DM, differentiation medium.

siblings and heterozygosity in both parents (**Figure 1A**). The novel c.629_631delCCT mutation in *DGAT1* is a deletion of three nucleotides in exon 7, leading to an in-frame deletion of a single serine at amino acid position 210. This uncharged amino acid with a polar side chain is highly conserved among several species (**Figure 1B**).

Taken together, we identified a novel *DGAT1* mutation in two brothers diagnosed with fat intolerance.

DGAT1 c.629_631delCCT results in increased proteasomal degradation of DGAT1

To study the consequences of the *DGAT1* c.629_631delCCT mutation, organoids were generated from duodenal biopsies obtained from the two brothers and compared to duodenal organoids derived from two healthy controls. Organoids were maintained in expansion medium (EM) and sequentially differentiated in differentiation medium (DM) to determine DGAT1 mRNA and protein expression (**Supplementary Figure 2A**). We confirmed proper expansion and differentiation of the healthy and mutant organoid cultures by determining mRNA levels of *LGR5* and *SI* as markers of intestinal stem cells and differentiated enterocytes, respectively (**Supplementary Figure 2B**). The *DGAT1* mRNA expression was similar in control and patient organoids and was induced upon differentiation (**Supplementary Figure 2B**). Despite normal mRNA expression, DGAT1 protein expression was completely absent in organoids derived from the patients compared to organoids derived from controls, when cultured in either EM or DM (**Figure 1C**).

To confirm that the *DGAT1* c.629_631delCCT mutation specifically leads to reduced DGAT1 protein levels without affecting mRNA levels, Caco-2 cells were stably transfected with Flag-DGAT1 wild-type (WT) or Flag-DGAT1 c.629_631delCCT. Indeed, *DGAT1* mRNA expression was similar in both cell lines (**Supplementary Figure 3A**), but the DGAT1 protein expression was almost absent when DGAT1 was mutated (**Figure 2**). Incubation with the proteasome inhibitor MG132 shows that the

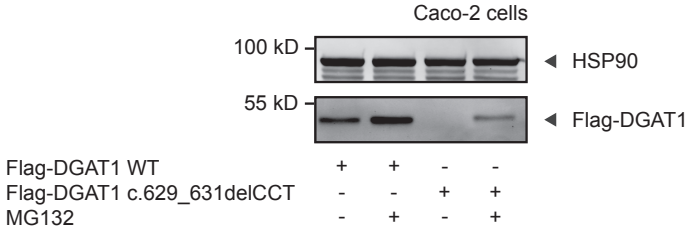

Figure 2. DGAT1 c.629_631delCCT results in increased proteasomal degradation of DGAT1.
Caco-2 cells were stably transfected with indicated constructs and left untreated or treated with 2 μM MG132 for 16 hours. Protein expression was determined by Western blot analysis using anti-Flag and anti-HSP90 antibodies. Results are representative of three independent experiments.

loss of protein in Caco-2 cells is at least partially due to proteasomal degradation of the mutant DGAT1 (**Figure 2**).

To further investigate the increased proteasomal degradation of DGAT1 c.629_631delCCT, we determined the level of ubiquitination of the mutant protein. Therefore, Caco-2 cells were co-transfected with His-ubiquitin and Flag-DGAT1 WT or Flag-DGAT1 c.629_631delCCT and treated with MG132. A ubiquitin pulldown assay showed that ubiquitination of Flag-DGAT1 c.629_631delCCT was increased compared to ubiquitination of Flag-DGAT1 WT (**Supplementary Figure 3B**).

Taken together, these data show that DGAT1 c.629_631delCCT results in increased ubiquitination of DGAT1 leading to increased proteasomal degradation and loss of DGAT1 protein in an Caco-2 based overexpression model.

DGAT1 c.629_631delCCT mutation results in accumulation of lipid droplets

When free fatty acids (FFA) are taken up by the enterocyte, they can be processed in three different ways. First they can be used in the FA oxidation pathway to produce energy. Alternatively, they can be used to generate DAG which can either be processed into TAG or phospholipids. Generated DAG or TAG will be stored in lipid droplets. We hypothesized that in absence of DGAT1, enterocytes will generate DAG which will be processed into phosholipids or stored in lipid droplets. To analyse lipid droplet formation, we performed an LD540 staining in organoids that were incubated with oleic acid for 48 hours. We observed an increased accumulation of lipid droplets in *DGAT1* mutant organoids compared to healthy controls (**Figure 3**). These data are in contrast with the recent data described in *DGAT1* mutant fibroblasts, where it was found that patient fibroblasts accumulated less lipid droplets when incubated with oleic acid for 2 hours [2]. This discrepancy may be caused by the difference in metabolic pathways in fibroblasts or because of the different time window.

These data indicate that *DGAT1* c.629_631delCCT results in an increased accumulation of lipid droplets in the enterocyte upon FFA stimulation.

Discussion

In this paper we identified a homozygous *DGAT1* c.629_631delCCT mutation in two brothers with fat intolerance. This mutation leads to an increased ubiquitin-mediated proteasomal degradation of DGAT1 in a Caco-2 cell model. The *DGAT1* c.629_631delCCT mutation causes a deletion of a highly conserved serine, which potentially leads to protein misfolding and subsequent ubiquitination and proteasomal degradation. Our patients are currently thriving on a fat-free diet with periodical supplementation of essential fatty acids and fat-soluble vitamins.

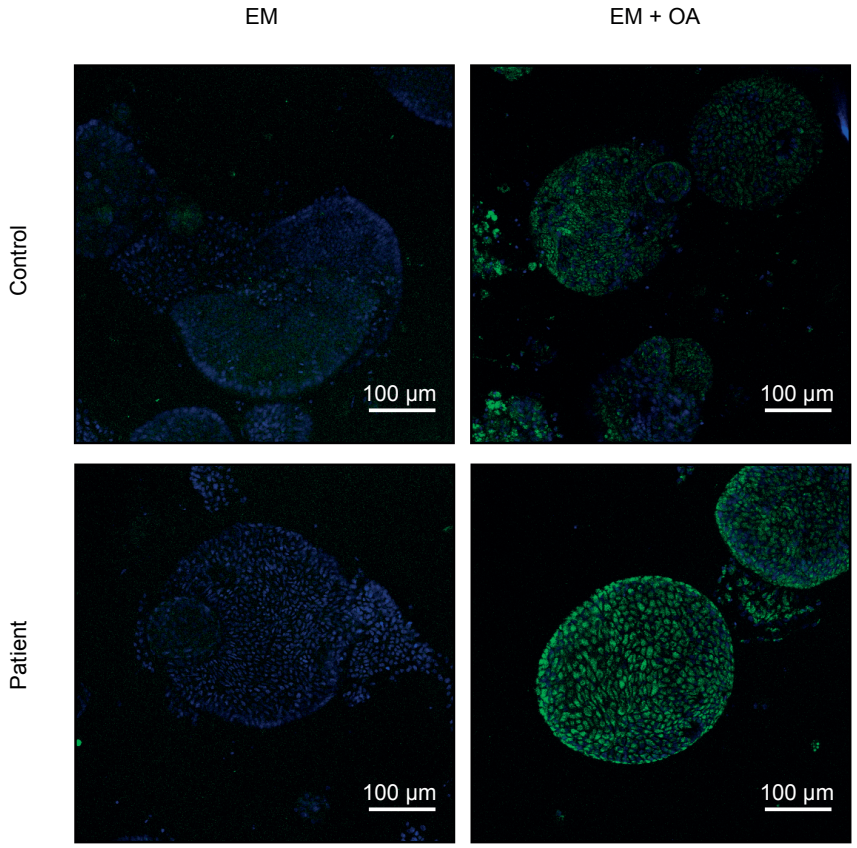

Figure 3. *DGAT1* c.629_631delCCT mutation results in increased lipid droplet accumulation. Immunofluorescent images of LD540 staining of organoids from healthy control and *DGAT1* mutant patients after control (EM) and oleic acid (OA) treatment for 17 hours. Intracellular lipid droplets stain green, nuclei are counterstained with DAPI (blue). Representative images of three healthy controls and two patients.

Although DGAT1 dysfunction has not been described in patients with fat intolerance before, *DGAT1* mutations have previously been associated with congenital diarrhea and protein-losing enteropathy [2–4]. Haas et al. described two siblings from the Ashkenazi Jewish population with severe congenital diarrhea, hypoalbumenia and hypertriglyceridemia due to a homozygous *DGAT1* splice site mutation resulting in skipping of exon 8 and a complete loss of DGAT1 protein activity [3]. In Stephen et al. a homozygous missense variant in exon 10 of *DGAT1* (p.L295P, located in the highly conserved MBOAT domain) was described in two patients from Arab-Muslim descent with a similar clinical syndrome. This mutation was associated with reduced amounts of DGAT1 protein in patient-derived fibroblasts. Interestingly, these patients all currently follow a regular or dairy-free diet [4]. Most recently, Gluchowski et al. described a missense mutation in exon

3 that resulted in partial loss of function of DGAT1 and a less severe clinical phenotype in twins of South Asian descent, who are currently following a low-fat diet [2]. It is unclear yet how these different *DGAT1* mutations, which result in a partial to complete loss of protein, are causing such different phenotypes. Future studies using genetically modified organoids that contain the various genetic mutations that were described in other patients, may shed light on the potential different response to fatty acids.

For further therapy development, we will test the effect of clinically available proteasome inhibitors, such as bortezomib [17], since we show that MG132 was able to rescue some protein degradation in our mutant Caco-2 model. Further studies are necessary to investigate if this approach will restore some protein function and lead to improved lipid metabolism in enterocytes upon incubation with oleic acid.

Our findings expand the differential diagnosis of vomiting in neonates. Clinicians should maintain a high suspicion for DGAT1 deficiency in cases of unexplained vomiting, especially when associated with failure to thrive and fat intolerance, and could consider a fat-free diet with supplementation of essential fatty acids and fat-soluble vitamins as a first line of therapy when this gene is found mutated. In conclusion, the findings described in this paper show that *DGAT1* mutations not only cause congenital diarrhea and protein-losing enteropathy, but are also linked to fat intolerance.

Materials and Methods

Study approval

The study was approved by the Institutional Review Board of the University Medical Center Utrecht. All participants provided written informed consent for the collection of samples and subsequent analysis.

Whole exome sequencing, data analysis and Sanger sequencing

Whole exome sequencing and data analysis were performed on one of the affected siblings as described previously [18]. A variant was defined as rare, when the allele frequency in the ExAC database was lower than 0.01. Confirmation of selected candidate mutations was performed by capillary sequencing.

Organoid culture

Duodenal biopsies were obtained from two healthy controls and two patients during duodenoscopy for diagnostic purposes. Crypts were isolated and organoids were generated as described previously [19]. The healthy controls were patients suspected of celiac disease or inflammatory bowel disease with normal pathology. The organoids were maintained in matrigel (BD Biosciences, San Jose, USA) with EM as described

previously supplemented with 100 µg/ml primocin (InvivoGen, San Diego, USA) and cultured at 37°C and 5% CO_2 [19]. Medium was refreshed every two or three days and organoids were split 1:2 every week by mechanical disruption or trypsinisation. To induce differentiation, organoids were cultured in DM (which is EM lacking WNT3A, nicotinamide and SB202190) for five days, as described previously [19].

Caco-2 cell culture

The human colorectal adenocarcinoma Caco-2 cell line was cultured in DMEM with GlutaMAX and high glucose (Life Technologies, Carlsbad, USA) supplemented with 10% heat-inactivated Fetal Bovine Serum (FBS) (GE health care, Little Chalfont, Great Britain), 100 U/ml penicillin (Gibco), 100 µg/ml streptomycin (Gibco) and 1 mM sodiumpyruvate (Gibco) at 37°C and 5% CO_2.

Generation of plasmids

pcDNA3-Flag-DGAT1 wild-type (WT) was generated by adding restriction sites Kpn1 and EcoR1 and a Flag-tag to DGAT1 (HsCD00044349, Dana-Farber/Harvard Cancer Center, Boston, USA) and cloning a Kpn1-EcoR1 fragment into the respective cloning site of pcDNA3 (Invitrogen, Carlsbad, USA). Using site-directed mutagenesis the pcDNA3-Flag-DGAT1 c.629_631delCCT mutant was constructed. His-ubiquitin was kindly provided by prof. dr. B.M. Burgering [20].

Generation of stably transfected Caco-2 cells

Caco-2 cells were grown in 10 cm dishes. The cells were transfected with a mixture of 3 µg pcDNA3, Flag-DGAT1 WT or Flag-DGAT1 c.629_631delCCT and 9 µl GenJet™ Reagent (SL100489-CACO, SignaGen Laboratories, Rockville, USA). The next day the medium was refreshed and after 48 hours post-transfection 900 µg/ml G418 (ant-gn-5, InvivoGen) was added. Stably transfected cell lines were obtained after one week.

Quantitative real-time polymerase chain reaction

RNA was isolated from organoids grown in either EM or DM for five days using TRIzol® LS Reagent (Invitrogen) according to the manufacturer's protocol. From Caco-2 cells RNA was isolated using the RNeasy Mini kit (Qiagen, Hilden, Germany) according to the manufacturer's protocol. cDNA was synthesized using the iScript cDNA synthesis kit (BIO-Rad, Hercules, USA) and amplified using SYBR green supermix (BIO-Rad) in a Light Cycler96® (Roche, Basel, Switzerland) according to the manufacturer's protocol. The comparative Ct method was used to quantify the data. The relative quantity was defined as $2^{-\Delta\Delta Ct}$. In organoids and Caco-2 cells *HP1* and *HPRT1* were used as housekeeper genes respectively. *Sucrase-isomaltase (SI)* and *LGR5* were used to determine the differentiation status of organoids. The sequences of the primers were: *DGAT1-*

forward (FW): cgacgtgggagccgc, *DGAT1*-reverse (RV): gctcaagatcagcatcacca, *HP1*-FW: cccacgtcccaagatggat, *HP1*-RV: ctgatgcaccactcttctggaa, *SI*-FW: ggacactggcttggagacaac, *SI*-RV: tccagcgggtacagagatgat, *LGR5*-FW: gaatcccctgcccagtctc, *LGR5*-RV: attgaaggcttcgcaaattct, *HPRT1*-FW: tgacactggcaaaacaatgca, *HPRT1*-RV: ggtccttttcaccagcaagct.

Western blotting

Caco-2 cells or organoids were lysed in Laemmli buffer (0.12 mol/L Tris-HCl pH 6.8, 4% SDS, 20% glycerol, 0.05 µg/µl bromphenol blue, 35 mmol/L β-mercaptoethanol) and incubated at 100°C for 5 minutes. The protein concentration was measured by performing a Lowry protein assay. Equal amounts of proteins were separated by SDS-PAGE, transferred to a polyvinylidene difluoride membrane (Merck Millipore, Billerica, USA), blocked with 5% milk protein in TBST (0.3% Tween, 10 mM Tris-HCl pH8 and 150 mM NaCl in H_2O) and probed with primary antibodies. The membranes were washed with TBST and incubated with appropriate secondary antibodies. Immunocomplexes were detected using the LI-COR Odyssey.

The primary antibodies used were mouse anti-Flag M2 (1:3000; F3165, Sigma-Aldrich), rabbit anti-DGAT1 (1:1000; ab181180, Abcam) and rabbit anti-HSP90 (1:10000; kindly provided by prof. dr. L.J. Braakman). The secondary antibodies used were donkey anti-mouse IgG IRDye 680 (1:10000; 926-32222, LI-COR, Lincoln, USA) and donkey anti-rabbit IgG IRDye 680RD (1:10000; 926-68073, LI-COR). Caco-2 cells transfected with Flag-DGAT1 c.629_631delCCT were left untreated or treated with 2 µM MG132 (Cayman Chemicals, Ann Arbor, USA) for 16 hours.

Ubiquitin pulldown assay

Caco-2 cells were grown in 10 cm dishes and co-transfected with 3 µg pcDNA3, Flag-DGAT1 WT or Flag-DGAT1 c.629_631delCCT and 3 µg His-ubiquitin. Thirty-two hours post-transfection 2 µM MG132 was added and the cells were incubated at 37°C for 16 hours. The cells were once washed with PBS and lysed in lysis buffer pH 8.0 containing 8 M urea (GE Health Care), 7 mM NaH_2PO_4 (Merck, Whitehouse Station, USA), 100 mM Na_2HPO_4 (Merck), 10 mM Tris-HCl pH 8.0 (Roche), 0.2% Triton-X100 (Sigma-Aldrich), 10 mM imidazole (Sigma-Aldrich) and 5 mM N-ethylmaleimide (Sigma-Aldrich). 10 mM β-mercaptoethanol (Sigma-Aldrich) and Ni-NTA agarose beads (Qiagen) were added and the cells were tumbled for two hours at room temperature. The beads were washed twice in buffer pH 8.0, two times in buffer pH 6.3 (12 mM urea, 100 mM NaH_2PO_4, 30 mM Na_2HPO_4, 15 mM Tris-HCl pH 6.3, 0.3% Triton X-100, 30 mM imidazole) and once in wash buffer (100 mM NaCl (Sigma-Aldrich), 20% glycerol (Sigma-Aldrich), 20 mM Tris-HCl pH 8.0, 2 mM dithiothreitol (GE Health Care) and 10 mM imidazole). Sample buffer (0.12 M Tris-HCl pH 6.8, 4% SDS, 20% glycerol, 0.05 µg/µl bromphenol blue and 35 mM β-mercaptoethanol) was

added. The samples were incubated at 100°C for 5 minutes and subjected to Western blot.

Fluorescent imaging of lipid droplets

Organoids were grown in EM for 6 days and incubated with 1 mM oleic acid for 48 hours before fixation in 4% formaldehyde for 30-40 minutes at room temperature. Cells were washed in PBS and stained with 0.05 µg/ml LD540 (kindly provided by B. Spee) in PBS for 1 hour at room temperature in dark. Cells were washed twice in PBS and incubated with DAPI for 10 minutes at room temperature. Cells were washed in PBS and mounted on a coverslip with Fluorsave (Merck Millipore). Imaging of the organoids was performed using a Leica SP8X confocal microscope.

Statistics

Statistical analysis was performed using the unpaired student's t-test with Welch's correction assuming a Gaussian distribution (Prism GraphPad Software). A p-value ≤0.05 was considered statistically significant.

Acknowledgments

We thank Edwin Stigter and Nanda Verhoeven-Duif for help at various stages of the project.

References

1. Overeem AW, Posovszky C, Rings EHMM, Giepmans BNG, van IJzendoorn SCD. The role of enterocyte defects in the pathogenesis of congenital diarrheal disorders. *Dis Model Mech* 2016;9: 1–12
2. Gluchowski NL, Chitraju C, Picoraro JA, Mejhert N, Pinto S, Xin W, Kamin DS, Winter HS, Chung WK, Walther TC, Farese R V. Identification and characterization of a novel DGAT1 missense mutation associated with congenital diarrhea. *J Lipid Res* 2017;58:1230–1237
3. Haas JT, Winter HS, Lim E, Kirby A, Blumenstiel B, DeFelice M, Gabriel S, Jalas C, Branski D, Grueter CA, Toporovski MS, Walther TC, Daly MJ, Farese R V. DGAT1 mutation is linked to a congenital diarrheal disorder. *J Clin Invest* 2012;122:4680–4684
4. Stephen J, Vilboux T, Haberman Y, Pri-Chen H, Pode-Shakked B, Mazaheri S, Marek-Yagel D, Barel O, Di Segni A, Eyal E, Hout-Siloni G, Lahad A, Shalem T, Rechavi G, Malicdan MC V, Weiss B, Gahl WA, Anikster Y. Congenital protein losing enteropathy: an inborn error of lipid metabolism due to DGAT1 mutations. *Eur J Hum Genet* 2016;24:1268–1273
5. Iqbal J, Hussain MM. Intestinal lipid absorption. *Am J Physiol Endocrinol Metab* 2009;296:E1183-1194
6. Yen C-LE, Stone SJ, Koliwad S, Harris C, Farese R V. Thematic review series: glycerolipids. DGAT enzymes and triacylglycerol biosynthesis. *J Lipid Res* 2008;49:2283–2301
7. Coleman RA, Mashek DG. Mammalian triacylglycerol metabolism: synthesis, lipolysis, and signaling. *Chem Rev* 2011;111:6359–6386
8. Yen C-LE, Nelson DW, Yen M-I. Intestinal triacylglycerol synthesis in fat absorption and systemic energy metabolism. *J Lipid Res* 2015;56:489–501
9. Cases S, Stone SJ, Zhou P, Yen E, Tow B, Lardizabal KD, Voelker T, Farese R V. Cloning of DGAT2, a second mammalian diacylglycerol acyltransferase, and related family members. *J Biol Chem* 2001; 276:38870–38876
10. Abumrad NA, Davidson NO. Role of the gut in lipid homeostasis. *Physiol Rev* 2012;92:1061–1085
11. Hussain MM. Intestinal lipid absorption and lipoprotein formation. *Curr Opin Lipidol* 2014;25: 200–206
12. Cefalù AB, Norata GD, Ghiglioni DG, Noto D, Uboldi P, Garlaschelli K, Baragetti A, Spina R, Valenti V, Pederiva C, Riva E, Terracciano L, Zoja A, Grigore L, Averna MR, Catapano AL. Homozygous familial hypobetalipoproteinemia: two novel mutations in the splicing sites of apolipoprotein B gene and review of the literature. *Atherosclerosis* 2015;239:209–217
13. Hooper AJ, Burnett JR. Update on primary hypobetalipoproteinemia. *Curr Atheroscler Rep* 2014; 16:423
14. Lee J, Hegele RA. Abetalipoproteinemia and homozygous hypobetalipoproteinemia: a framework for diagnosis and management. *J Inherit Metab Dis* 2014;37:333–339
15. Peretti N, Sassolas A, Roy CC, Deslandres C, Charcosset M, Castagnetti J, Pugnet-Chardon L, Moulin P, Labarge S, Bouthillier L, Lachaux A, Levy E. Guidelines for the diagnosis and management of chylomicron retention disease based on a review of the literature and the experience of two centers. *Orphanet J Rare Dis* 2010;5:24

16. Zamel R, Khan R, Pollex RL, Hegele RA. Abetalipoproteinemia: two case reports and literature review. *Orphanet J Rare Dis* 2008;3:19
17. Chen D, Frezza M, Schmitt S, Kanwar J, Dou QP. Bortezomib as the first proteasome inhibitor anticancer drug: current status and future perspectives. *Curr Cancer Drug Targets* 2011;11:239–253
18. Massink MPG, Créton MA, Spanevello F, Fennis WMM, Cune MS, Savelberg SMC, Nijman IJ, Maurice MM, van den Boogaard M-JH, van Haaften G. Loss-of-Function Mutations in the WNT Co-receptor LRP6 Cause Autosomal-Dominant Oligodontia. *Am J Hum Genet* 2015;97:621–626
19. Wiegerinck CL, Janecke AR, Schneeberger K, Vogel GF, van Haaften-Visser DY, Escher JC, Adam R, Thöni CE, Pfaller K, Jordan AJ, Weis C-A, Nijman IJ, Monroe GR, van Hasselt PM, Cutz E, Klumperman J, Clevers H, Nieuwenhuis EES, Houwen RHJ, van Haaften G, Hess MW, Huber LA, Stapelbroek JM, Müller T, Middendorp S. Loss of syntaxin 3 causes variant microvillus inclusion disease. *Gastroenterology* 2014;147:65–68.e10
20. van der Horst A, de Vries-Smits AMM, Brenkman AB, van Triest MH, van den Broek N, Colland F, Maurice MM, Burgering BMT. FOXO4 transcriptional activity is regulated by monoubiquitination and USP7/HAUSP. *Nat Cell Biol* 2006;8:1064–1073

Supplementary Figures

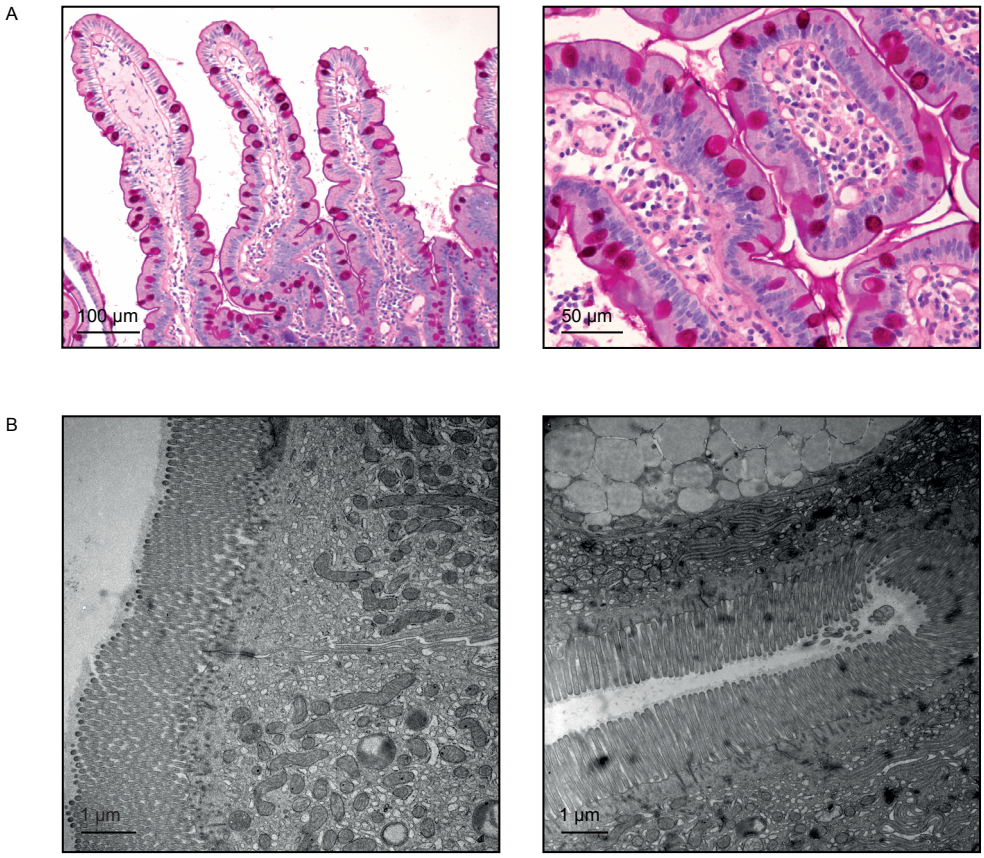

Supplementary Figure 1. *DGAT1* mutant patients show normal intestinal pathology. (A) PAS staining and **(B)** electron microscopy on patient biopsies show no aberrant pathology of the small intestine.

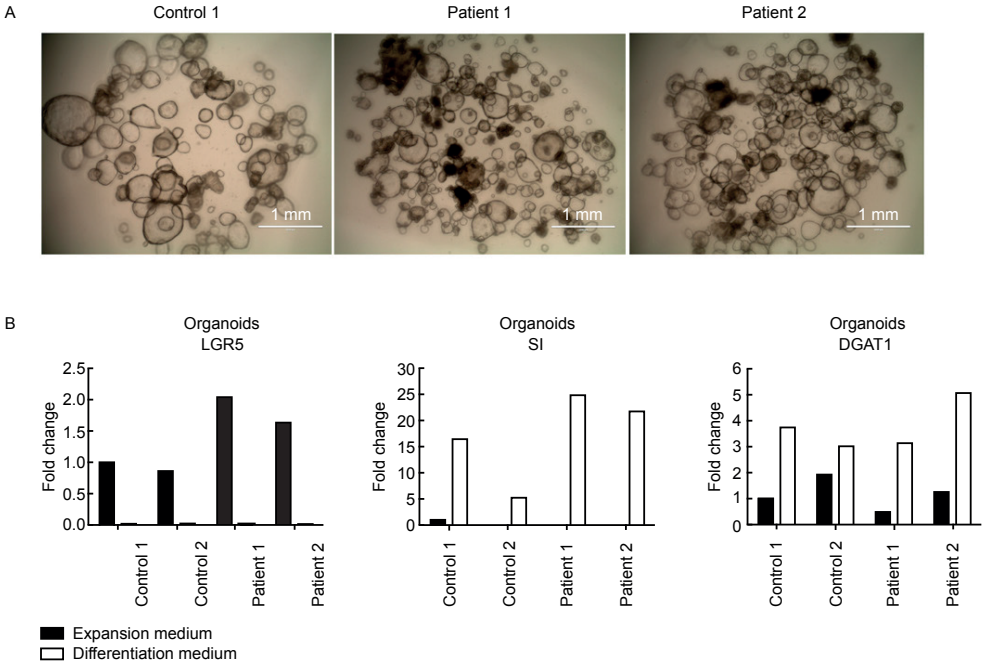

Supplementary Figure 2. Organoids from *DGAT1* mutant patients grow and differentiate normally. (A) Organoids derived from duodenal biopsies of the two patients show similar characteristics as healthy control organoids. **(B)** qRT-PCR analysis of *LGR5*, sucrase isomaltase (*SI*) and *DGAT1* mRNA expression in organoids from two healthy controls and two patients with homozygous *DGAT1* c.629_631delCCT mutation. Results are representative of three independent experiments.

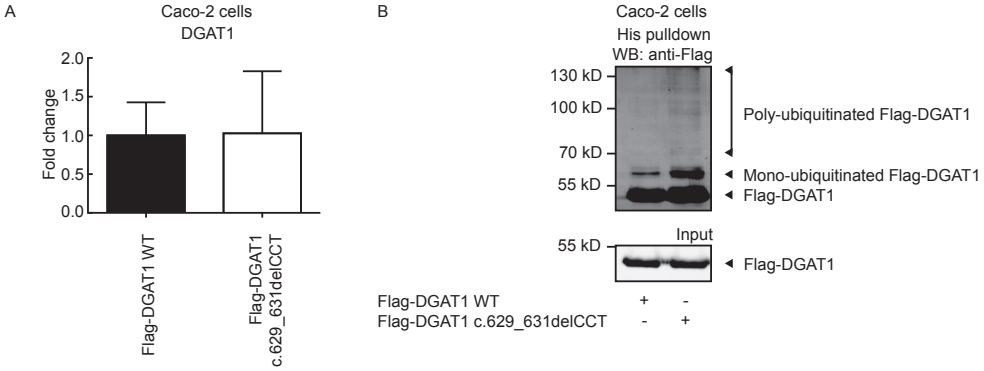

Supplementary Figure 3. DGAT1 c.629_631delCCT protein is degraded by ubiquitination
(A) qRT-PCR analysis of *DGAT1* mRNA expression in Caco-2 cells stably transfected with indicated constructs. Average and standard deviation of three independent experiments are shown. **(B)** Caco-2 cells were transiently transfected with His-ubiquitin and indicated constructs and treated with 2 µM MG132 for 16 hours. Ubiquitination of DGAT1 was determined by a His pulldown and subsequent Western blot analysis using anti-Flag antibodies. Results are representative of three independent experiments.

Chapter 5

Next-generation sequencing as a novel tool in the diagnosis of monogenetic GI disease: congenital diarrhea as an example

Désirée Y. van Haaften – Visser, Caroline L. Wiegerinck,
Charlotte I. de Bie, Johanna C. Escher, Janneke M. Stapelbroek,
Peter M. van Hasselt, Roderick H.J. Houwen, Marielle E. van Gijn

Submitted

Abstract

When a hereditary cause is suspected in a patient with congenital diarrhea currently associated genes are sequentially screened for causative mutations. This approach is now gradually replaced by next-generation sequencing (NGS), a high-throughput technique that allows simultaneous sequencing of multiple genes. We performed NGS in two patients with congenital diarrhea in whom a genetic cause was suspected. In the first patient tricho-hepato-enteric syndrome was diagnosed by analyzing a set of genes known to be associated with congenital diarrhea. In the second patient we sequenced the whole exome and once again analyzed the genes that at that time were known to be associated with congenital diarrhea, which did not reveal a diagnosis. By extending the analysis to the remaining genes of the exome, mutations in an, at that time, new gene for congenital sodium diarrhea were found. These cases illustrate both the value of NGS in the diagnostics of congenital diarrhea and the power of the two-step analysis performed in the second patient. We suggest that NGS, and especially this two-step approach, should be implemented in the diagnostics of congenital diarrhea, and might also be useful in the diagnostic process of other genetically heterogeneous pediatric gastrointestinal and hepatic diseases.

Introduction

Congenital diarrhea is a potentially life-threatening disorder that can have a variety of causes, including abnormal enterocyte differentiation and polarization, aberrant enteroendocrine cell differentiation, a disturbed intestinal immune cell response and compromised digestion, absorption and transport of nutrients and electrolytes [1]. The majority of patients will present with severe diarrhea in the first weeks of life [1]. Causes can be both hereditary and non-hereditary.

In patients with congenital diarrhea, a rapid diagnosis is essential for a timely and effective therapy, to determine prognosis, as well as for genetic counseling. Furthermore, it may facilitate early detection of additional symptoms, which is beneficial for the prognosis. Unfortunately, the diagnostic process can be very time-consuming, especially when a genetic cause is suspected. This is mainly because the genetic techniques currently used are based on sequencing of single genes, which makes it necessary to select the most likely candidate gene(s). This is often difficult due to the large genetic and phenotypic heterogeneity of congenital diarrhea.

The last few years next-generation sequencing (NGS) has become available as a technique to quickly analyze a specific set of genes [2,3] and whole exomes [4]. It is a high-throughput sequencing technique that allows parallel sequencing of a large set of genes, making a priori selection of specific genes unnecessary. Here, we introduce NGS as a novel tool in the diagnosis of congenital diarrhea. We show that NGS can facilitate the diagnostic process of congenital diarrhea by identifying the underlying genetic defect using NGS in two patients with congenital diarrhea. We suggest a two-step approach: first, to analyze all known congenital diarrhea causing genes; when no disease-causing mutation is discovered, the analysis can be extended to the whole exome.

Case 1

We present a girl of Moroccan descent that was born at term from a consanguineous marriage with a weight of 1770 gram (-3 standard deviation (SD)). Because of this dysmaturity she was admitted to the hospital, where it was noted that she produced loose and frequent stool and had poor weight gain despite adequate intake. Although various types of formula feeding, including elemental formula, were tried, only with total parenteral nutrition (TPN) the consistency and frequency of the stools definitively improved and the girl started to gain weight.

At six weeks of age the patient was referred to a university hospital for diagnostics and treatment of the diarrhea. At that time we observed a girl with a weight, height and head circumference of 1850 gram (-6.2 SD), 51 cm (-5.4 SD) and 34.5 cm (-2.2

SD) respectively. She had several mild dysmorphic features, including a high forehead, a posteriorly rotated left ear, hypertelorism, micrognathia and a sandal gap on both sides. Improvement of the diarrhea after cessation of enteral feeding (and introduction of TPN) suggested osmotic diarrhea. However, secretory diarrhea could not be excluded as the patient continued to have some diarrhea on TPN. Laboratory investigations showed normal plasma sodium and potassium levels: 140 mmol/l (hospital reference values: 136-145 mmol/l) and 4.1 mmol/l (3.5-5.1 mmol/l) respectively. Fecal levels of α1-antitrypsin, fat, elastase and reducing substances were determined as markers for enteric protein loss, fat malabsorption, pancreatic insufficiency and carbohydrate malabsorption respectively, and were all normal as well. Metabolic screening in urine and plasma also did not show any abnormalities. At the age of six weeks a gastroduodenoscopy was performed. Histopathologic evaluation of duodenal biopsies showed mild inflammation. With PAS and CD10 stainings an intact brush border without cytoplasmic reactivity was seen. However, electron microscopy demonstrated partial atrophy of microvilli and electron dense inclusions partially resembling microvillous inclusion disease (MVID). Although this raised the suspicion of MVID, no other typical features of MVID were present and with Sanger sequencing no mutations were identified in *MYO5B* and *STX3*, making MVID very unlikely.

Yet, because of the diarrhea being present from birth, the mild dysmorphic features and her parents being consanguineous, a genetic cause of the congenital diarrhea was still very likely. So subsequently a set of congenital diarrhea causing genes was screened for mutations (**Supplementary Table 1**). We identified a homozygous c.3187C>T p.(Arg1063*) mutation in *SKIV2L* (NM_006929.4), introducing a preliminary STOP codon, thereby diagnosing tricho-hepato-enteric (THE) syndrome in this child.

Case 2

Secondly, we present a Syrian boy from a consanguineous marriage that was born after a gestational age of eight months with a birth weight of 1250 gram. During pregnancy polyhydramnios was present and after birth a distended abdomen was noted. Although initially defaecation had to be triggered with a probe, soon after birth his defaecation pattern changed to spontaneous fulminant watery diarrhea two to four times a day.

At the age of thirteen years he came to the Netherlands as a refugee, where he presented in our university hospital with complaints of frequent watery diarrhea, which was recently complicated by occasional blood staining. Physical examination showed a pale boy with a height of 131.2 cm (-3.83 SD) and a weight of 30 kg (weight/height 1.24 SD). No further abnormalities were found, especially no dysmorphic features. The diarrhea persisted after cessation of enteral feeding, suggesting a secretory cause. Laboratory

investigations showed normal plasma and fecal electrolyte levels and pH: plasma sodium 136 mmol/l (136-146 mmol/l), plasma pH 7.38 (7.37-7.45), plasma bicarbonate 22.1 mmol/l (22-28 mmol/l), fecal sodium 114 mmol/l (<160 mmol/l), fecal potassium 17.9 mmol/l (<200 mmol/l), fecal chloride 41.9 mmol/l and fecal pH 7.0. Fecal osmolality was 238 mOsmol/kg and urinary sodium level 66 mmol/l. Fecal levels of calprotectin, fat and elastase were determined, which were all normal: 31 mg/l (0-50 mg/l), <5.2 g/24 hour (0.0-5.0g/24 hour) and 322 µg/g (200-10000 µg/g) respectively. The fecal α1-antitrypsin level was slightly elevated (1.6 mg/g (0.0-1.1 mg/g)). At coloscopy a lymphocytic colitis was found, for which budesonide was given for six months. No effect on the diarrhea was noted however, although the occasional blood staining disappeared. Apart from the diarrhea, which is perceived as troublesome, he is doing well, with no dietary restrictions and, apart from oral iron suppletion for iron deficiency anemia, without any other supplements.

Because of the persistent diarrhea, the presentation in the first month of life and his parents being consanguineous, a genetic cause of his disorder was suspected. Using NGS the whole exome was sequenced. First, all genes known to be associated with congenital diarrhea were analyzed (**Supplementary Table 1**), but no underlying mutation was discovered. Subsequent analysis of the remaining part of the exome identified a homozygous c.475G>A p.(G159R) mutation in *SLC9A3* (NM_004174.2) diagnosing congenital sodium diarrhea.

Discussion

In this paper we introduce NGS as a novel diagnostic tool in patients with congenital diarrhea. The great value of NGS in these patients is illustrated by the histories of the two patients we describe. These cases illustrate that with NGS, in contrast to sequential sequencing of single genes, a fast diagnosis can be made, thereby shortening the time between presentation and diagnosis, which can be essential for timely initiation of the correct treatment, beneficial for disease prognosis and important for genetic counseling.

The first patient presented with congenital diarrhea and failure to thrive requiring TPN. A homozygous *SKIV2L* mutation was identified by performing NGS and analyzing the genes included in the congenital diarrhea gene panel, diagnosing THE syndrome. This syndrome is a rare autosomal recessive disease, characterized by intractable diarrhea starting at young age, dysmorphic facial features and hair abnormalities. Many patients also suffer from intra-uterine growth restriction, immunodeficiency, liver disease and skin abnormalities. THE syndrome is caused by mutations in *TTC37* or *SKIV2L*, which encode parts of the SKI complex. The human SKI complex has a role in decay of aber-

rant mRNA [5]. The exact mechanism by which the diarrhea is caused when this gene is mutated remains unknown.

The second patient presented with a history of congenital diarrhea not requiring dietary restrictions. Within the whole exome, a specific set of genes known to be associated with congenital diarrhea was analyzed, which did not reveal an underlying gene defect. Then, by analyzing the remaining part of the whole exome, a homozygous *SLC9A3* mutation was identified. *SLC9A3* was only recently described as a congenital sodium diarrhea associated gene, and after our analysis was completed, so this gene was not included yet in the set of congenital diarrhea associated genes we used (**Supplementary Table 1**). Nevertheless, we were able to identify a homozygous mutation in *SLC9A3* as the cause of disease in this patient by subsequently analyzing the whole exome. This case therefore demonstrates the usefulness of the two-step whole exome approach in a diagnostic setting.

Congenital sodium diarrhea is an extremely rare genetic disease characterized by profuse watery diarrhea with a high fecal sodium level [6–8]. Both a classical and syndromic form of congenital sodium diarrhea have been described. The classical form can be caused by mutations in *GUCY2C* and *SLC9A3* [9,10]. *GUCY2C* encodes receptor guanylate cyclase C. Dominant activating mutations in *GUCY2C* lead to a decreased intestinal sodium and water absorption and an increased chloride secretion [9]. *SLC9A3* encodes NHE3, which is a Na^+/H^+ exchanger, that is highly abundant in the intestine [10]. The syndromic form of congenital sodium diarrhea is caused by mutations in *SPINT2*, which encodes SPINT2, a serine-protease inhibitor [11].

Targeted NGS (TNGS), which is NGS using a fixed set of genes, has the potential to quickly pinpoint the gene defect in disorders with extensive genetic heterogeneity. This technique is already widely available in a diagnostic setting and used for several diseases including primary immunodeficiencies, epileptic disorders and cardiomyopathies [2,3,12]. However, when using TNGS only a fixed set of genes is sequenced, making it necessary to adapt the panel and order and validate a new enrichment and sequencing kit whenever a newly described gene has to be added. Indeed novel disease associated genes are discovered continuously, so panels should be updated very regularly [9,10,13]. This drawback can be overcome by sequencing the whole exome at the start of the analysis. Then the set of genes to be analyzed in a specific disorder can be updated instantaneously using bioinformatics, whenever a new disease associated gene has been described. Furthermore, in contrast to TNGS it allows for extension of the analysis to the whole exome, when the initial panel analysis did not result in a diagnosis and a genetic cause of the disease is strongly suspected, as was the case in our second patient. The two-step approach we describe is also preferred over directly analyzing a whole exome, because the latter will result in unsolicited findings and the identification of many sequence variants of unknown clinical significance, which makes interpretation difficult.

Conclusion

The two-step whole exome analysis we describe here for identifying a possible genetic cause of congenital diarrhea has two major advantages. First, it will significantly shorten the diagnostic process as compared to the sequential analysis of each gene that is implemented in this disease. Secondly, it allows for extension of the analysis to genes outside the panel with known congenital diarrhea associated genes. Similarly, the implementation of NGS in the diagnostic process of other genetically heterogeneous pediatric gastrointestinal and hepatic diseases, for example neonatal cholestasis, will be of great value.

References

1. Canani RB, Castaldo G, Bacchetta R, Martín MG, Goulet O. Congenital diarrhoeal disorders: advances in this evolving web of inherited enteropathies. *Nat Rev Gastroenterol Hepatol* 2015;12: 293–302
2. Nijman IJ, van Montfrans JM, Hoogstraat M, Boes ML, van de Corput L, Renner ED, van Zon P, van Lieshout S, Elferink MG, van der Burg M, Vermont CL, van der Zwaag B, Janson E, Cuppen E, Ploos van Amstel JK, van Gijn ME. Targeted next-generation sequencing: a novel diagnostic tool for primary immunodeficiencies. *J Allergy Clin Immunol* 2014;133:529–534
3. de Koning TJ, Jongbloed JDH, Sikkema-Raddatz B, Sinke RJ. Targeted next-generation sequencing panels for monogenetic disorders in clinical diagnostics: the opportunities and challenges. *Expert Rev Mol Diagn* 2015;15:61–70
4. Worthey EA, Mayer AN, Syverson GD, Helbling D, Bonacci BB, Decker B, Serpe JM, Dasu T, Tschannen MR, Veith RL, Basehore MJ, Broeckel U, Tomita-Mitchell A, Arca MJ, Casper JT, Margolis DA, Bick DP, Hessner MJ, Routes JM, Verbsky JW, Jacob HJ, Dimmock DP. Making a definitive diagnosis: successful clinical application of whole exome sequencing in a child with intractable inflammatory bowel disease. *Genet Med* 2011;13:255–262
5. Fabre A, Martinez-Vinson C, Goulet O, Badens C. Syndromic diarrhea/Tricho-hepato-enteric syndrome. *Orphanet J Rare Dis* 2013;8:5
6. Booth IW, Stange G, Murer H, Fenton TR, Milla PJ. Defective jejunal brush-border Na+/H+ exchange: a cause of congenital secretory diarrhoea. *Lancet (London, England)* 1985;1:1066–1069
7. Holmberg C, Perheentupa J. Congenital Na+ diarrhea: a new type of secretory diarrhea. *J Pediatr* 1985;106:56–61
8. Müller T, Wijmenga C, Phillips AD, Janecke A, Houwen RH, Fischer H, Ellemunter H, Frühwirth M, Offner F, Hofer S, Müller W, Booth IW, Heinz-Erian P. Congenital sodium diarrhea is an autosomal recessive disorder of sodium/proton exchange but unrelated to known candidate genes. *Gastroenterology* 2000;119:1506–1513
9. Müller T, Rasool I, Heinz-Erian P, Mildenberger E, Hülstrunk C, Müller A, Michaud L, Koot BGP, Ballauff A, Vodopiutz J, Rosipal S, Petersen B-S, Franke A, Fuchs I, Witt H, Zoller H, Janecke AR, Visweswariah SS. Congenital secretory diarrhoea caused by activating germline mutations in GUCY2C. *Gut* 2015
10. Janecke AR, Heinz-Erian P, Yin J, Petersen B-S, Franke A, Lechner S, Fuchs I, Melancon S, Uhlig HH, Travis S, Marinier E, Perisic V, Ristic N, Gerner P, Booth IW, Wedenoja S, Baumgartner N, Vodopiutz J, Frechette-Duval M-C, De Lafollie J, Persad R, Warner N, Tse CM, Sud K, Zachos NC, Sarker R, Zhu X, Muise AM, Zimmer K-P, Witt H, Zoller H, Donowitz M, Müller T. Reduced sodium/proton exchanger NHE3 activity causes congenital sodium diarrhea. *Hum Mol Genet* 2015; 24:6614–6623
11. Heinz-Erian P, Müller T, Krabichler B, Schranz M, Becker C, Rüschendorf F, Nürnberg P, Rossier B, Vujic M, Booth IW, Holmberg C, Wijmenga C, Grigelioniene G, Kneepkens CMF, Rosipal S, Mistrik M, Kappler M, Michaud L, Dóczy L-C, Siu VM, Krantz M, Zoller H, Utermann G, Janecke AR. Mutations in SPINT2 cause a syndromic form of congenital sodium diarrhea. *Am J Hum Genet* 2009;84:188–196

12. Lemke JR, Riesch E, Scheurenbrand T, Schubach M, Wilhelm C, Steiner I, Hansen J, Courage C, Gallati S, Bürki S, Strozzi S, Simonetti BG, Grunt S, Steinlin M, Alber M, Wolff M, Klopstock T, Prott EC, Lorenz R, Spaich C, Rona S, Lakshminarasimhan M, Kröll J, Dorn T, Krämer G, Synofzik M, Becker F, Weber YG, Lerche H, Böhm D, Biskup S. Targeted next generation sequencing as a diagnostic tool in epileptic disorders. *Epilepsia* 2012;53:1387–1398
13. Wiegerinck CL, Janecke AR, Schneeberger K, Vogel GF, van Haaften-Visser DY, Escher JC, Adam R, Thöni CE, Pfaller K, Jordan AJ, Weis C-A, Nijman IJ, Monroe GR, van Hasselt PM, Cutz E, Klumperman J, Clevers H, Nieuwenhuis EES, Houwen RHJ, van Haaften G, Hess MW, Huber LA, Stapelbroek JM, Müller T, Middendorp S. Loss of syntaxin 3 causes variant microvillus inclusion disease. *Gastroenterology* 2014;147:65–68

Supplementary Table

Supplementary Table 1. Genes included in NGS gene panel congenital diarrhea

Disease	Gene	OMIM
Abetalipoproteinemia	*MTTP*	157147
Acrodermatitis enteropathica	*SLC39A4*	607059
Autoimmune polyglandular syndrome 1	*AIRE*	607358
Chylomicron retention disease	*SAR1B*	607690
Congenital chloride diarrhea	*SLC26A3*	126650
Congenital disorder of glycosylation type 1B	*MPI*	154550
Congenital lactase deficiency	*LCT*	603202
Congenital short bowel syndrome	*CLMP*	611693
	FLNA	300017
Congenital sodium diarrhea	*GUCY2C*	601330
	SPINT2	605124
Congenital sucrase-isomaltase deficiency	*SI*	609845
Congenital tufting enteropathy	*EPCAM*	185535
	SPINT2	605124
DGAT1 deficiency	*DGAT1*	604900
Enteric anendocrinosis	*NEUROG3*	604882
Enterokinase deficiency	*TMPRSS15*	606635
Fanconi-Bickel syndrome	*SLC2A2*	138160
Glucose-galactose malabsorption	*SLC5A1*	182380
Hereditary pancreatitis	*CFTR*	602421
	PRSS1	276000
	SPINK1	167790
Hypobetalipoproteinemia	*ANGPTL3*	604774
	APOB	107730
	NPC1L1	608010
	PCSK9	607786
IL12-receptor deficiency	*IL12RB1*	601604
Infantile-onset inflammatory bowel disease	*ADAM17*	603639
	IL10	124092
	IL10RA	146933
	IL10RB	123889
	IL21	605384
	NCF4	601488
	TTC7A	609332
	XIAP	300079

Supplementary Table 1. (*continued*)

Disease	Gene	OMIM
IPEX syndrome	*FOXP3*	300292
IPEX-like syndrome	*IL2RA*	147730
	STAT1	600555
	STAT5B	604260
Johanson-Blizzard syndrome	*UBR1*	605981
Lysinuric protein intolerance	*SLC7A7*	603593
Microvillus inclusion disease	*MYO5B*	606540
	STX3	600876
Pancreatic lipase deficiency	*PNLIP*	246600
Primary bile acid malabsorption	*SLC10A2*	601295
Proprotein convertase 1 deficiency	*PCSK1*	162150
Severe combined immunodeficiency	*ADA*	608958
	CD3D	186790
	CD3E	186830
	DCLRE1C	605988
	IL2RG	308380
	IL7R	146661
	JAK3	600173
	NHEJ1	611290
	PNP	164050
	PTPRC	151460
	RAG1	179615
	RAG2	179616
	ZAP70	176947
Shwachman-Diamond syndrome	*SBDS*	607444
Transcobalamin II deficiency	*TCN2*	613441
Tricho-hepato-enteric syndrome	*SKIV2L*	600478
	TTC37	614589
Trypsinogen deficiency	*PRSS1*	276000

Chapter 6

General discussion

Congenital diarrhea is associated with a high morbidity and sometimes mortality, even in the current era. Treatment options include nutritional interventions, immunosuppressive medication, total parenteral nutrition and small bowel transplantation, all of which can severely interfere with quality of life. In addition, the drawback of current therapies is that they generally do not cure the disease, but at best ameliorate symptoms. A prerequisite for improving therapy is a better understanding of the pathophysiology of these diseases. This thesis therefore aimed to identify and study gene defects underlying infantile-onset inflammatory bowel disease, microvillus inclusion disease and severe congenital fat intolerance. Furthermore, the implementation of next-generation sequencing (NGS) in the diagnostics of congenital diarrhea and its potential for identifying genes not yet implicated in this disorder was described.

Infantile-onset inflammatory bowel disease

In **Chapter 2** a novel pathogenic pathway underlying infantile-onset inflammatory bowel disease (IO IBD) was identified by identifying an association between *ANKZF1* mutations and IO IBD. Four IO IBD patients were found to have mutations in *ANKZF1*, of which two with two mutated alleles and two with one mutated allele. Although previously the function of ANKZF1 in mammals was completely unknown, **Chapter 2** identifies ANKZF1 as having an essential role in the mitochondrial response to cellular stress. Deficiency of ANKZF1 was found to be associated with a decreased mitochondrial integrity and respiration under conditions of cellular stress, and *ANKZF1* mutations identified in the two IO IBD patients with two mutated alleles result in a similar deregulated stress response (**Figure 1**).

Although mitochondrial pathology has been observed in IBD patients previously [1–5], this was the first time mitochondrial stress has been linked to the IBD pathogenesis. However, the exact mechanism by which mitochondrial stress causes IBD in these patients is still unknown. The first question that needs to be answered is whether primarily the immune cells or the intestinal epithelial cells are affected in a patient with ANKZF1 dysfunction, as *ANKZF1* is expressed in both celltypes.

While ANKZF1 appears to be broadly expressed, one possibility is that ANKZF1 mutations primarily affect B-lymphocytes and/or T-lymphocytes, causing lymphopenia and immune dysfunction. Since lymphocytes are rapidly dividing cells, which require properly functioning mitochondria to provide energy homeostasis, they may be more susceptible to a breakdown in mitochondrial function. The dysfunction and deficiency of both T-lymphocytes and B-lymphocytes in the IO IBD patient with a homozygous *ANKZF1 R585Q* mutation support this hypothesis. However, the IO IBD patient with compound heterozygous *ANKZF1* mutations did not have lymphopenia, although this

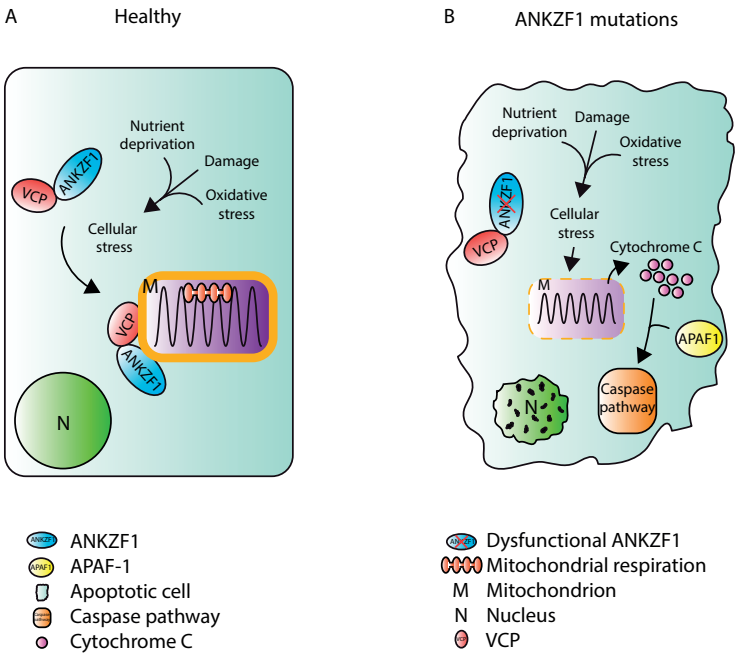

Figure 1. ANKZF1 dysfunction causes mitochondrial dysfunction and apoptosis. ANKZF1 interacts with VCP. Upon cellular stress this complex translocates to the mitochondria (**A**). ANKZF1 dysfunction results in a decreased mitochondrial integrity and mitochondrial respiration. This mitochondrial dysfunction leads to apoptosis, potentially through cytochrome c release and subsequent activation of the caspase pathway (**B**).

does not exclude dysfunction of lymphocytes. Indeed an underlying immune deficiency can manifest itself as IBD and several disease-causing mutations in immune related genes that result in a disturbed T- and/or B-lymphocyte development or function have been identified. These diseases include several types of common variable immune deficiency (CVID), Wiskott Aldrich Syndrome and agammaglobulinemia [6,7]. The exact mechanism by which immune deficiency causes IBD in these disorders is mostly unknown. However, it is hypothesized that altered regulatory pathways or chronic infections with pathogenic or opportunistic bacteria may play a role [6]. Interestingly *LRBA* mutations, which are associated with CVID type 8, result in an increased level of apoptosis in B-lymphocytes [8]. Indeed, apoptosis of immune cells has been described to be associated with autoimmunity, which might be the pathogenic mechanism underlying IBD in these patients [9].

Alternatively, the primary problem in patients with IO IBD due to *ANKZF1* mutations is located in the intestinal epithelial cells. An example of an IO IBD associated gene defect that primarily affects intestinal epithelial cells and is also associated with apoptosis

is mutated *Xbp1*. *Xbp1* encodes XBP1, which is an essential protein in the unfolded protein response [10]. *Xbp1* mutations result in enteritis by both apoptosis of Paneth cells and hyperinflammation of the intestinal epithelial cells [10]. Paneth cells are highly secretory cells, that secrete both antimicrobial peptides and inflammatory mediators in the intestinal lumen [11]. Our results show that mitochondrial stress in patients with dysfunctional ANKZF1 is also associated with increased apoptosis. A possible mechanism of the observed IO IBD is that this also induces inflammation by a decreased antimicrobial response or hyperinflammation. However, further research is essential to study this hypothesis.

Answering the question whether the main problem in a patient with ANKZF1 dysfunction resides in the immune cells or in the epithelial cells has direct consequences for therapy. When only the immune cells are dysfunctional, a hematopoietic stem cell transplantation could be a potential treatment for these children, which is not the case when dysfunction of epithelial cells is the main problem. In the latter case patients may benefit from enterocyte transplantation or gene therapy, when available. Nevertheless, although the exact pathogenesis has not yet been clarified, identification of an association between *ANKZF1* mutations and IO IBD is important for IO IBD patients. By including sequencing of *ANKZF1* in the diagnostic process of IO IBD it can be determined whether this gene is mutated in a specific patient. As such a final diagnosis has important consequences for genetic counseling and will clarify prognosis when a larger cohort will be described.

Microvillus inclusion disease

Chapter 3 describes the identification of *STX3* mutations as novel cause of microvillus inclusion disease (MVID) in two MVID patients without *MYO5B* mutations. *STX3* encodes syntaxin 3, which is a target N-ethylmaleimide-sensitive factor attachment protein receptor (t-SNARE) located on the apical plasma membrane of several cell types including enterocytes [12,13]. Syntaxin 3 binds to specific SNARE proteins on vesicles (v-SNAREs) resulting in docking of these vesicles to the apical plasma membrane and fusion with this membrane [12,14]. Dysfunctional syntaxin 3 leads to mislocalization of apical cargo and subsequently to a disturbed cell polarity [12,15,16] (**Figure 2**).

The involvement of both syntaxin 3 and myosin Vb in the transport of vesicles to the apical plasma membrane strongly indicates that disruption of this pathway is the most important pathogenic mechanism for MVID in humans. When apical cargo cannot be delivered to the apical cell membrane anymore, the polarity of the enterocyte will be disturbed, leading to villus atrophy, accumulation of subapical vesicles and intracellular

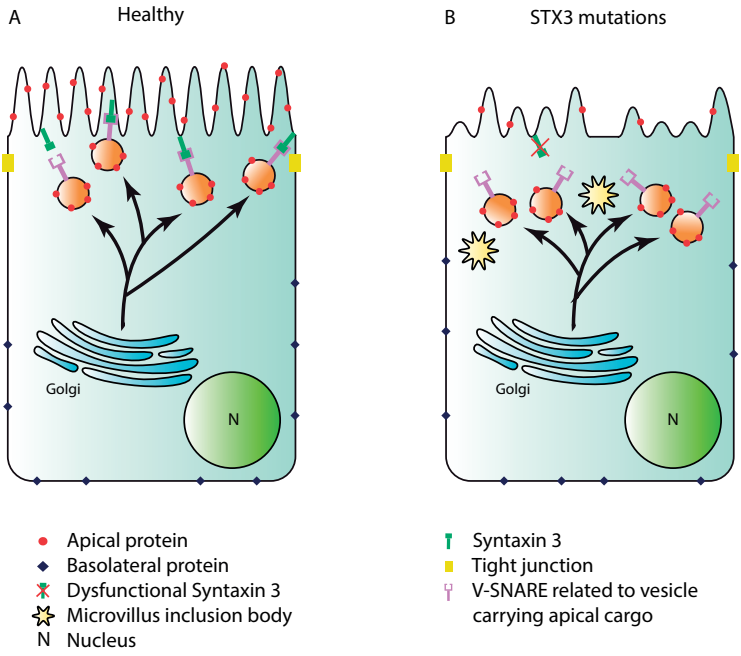

Figure 2. Syntaxin 3 dysfunction disrupts apical cargo exocytosis. Syntaxin 3 is a t-SNARE located on the apical plasma membrane of enterocytes. Binding of syntaxin 3 to specific v-SNAREs on vesicles leads to docking of these vesicles to the apical membrane and fusion of the vesicles with this membrane (**A**). Syntaxin 3 dysfunction decreases apical cargo exocytosis leading to disturbance of the cell polarity and subsequently MVID characterized by partial microvillus atrophy, microvillus inclusions and subapical accumulation of vesicles (**B**).

microvillus inclusions [16–18]. Possibly MVID can also be caused by mutations in genes encoding other essential proteins in apical cargo exocytosis, including *Slp4a*, *Vamp7*, *Munc18-2* and *Rab11* [15]. However, mutations in these genes have not been identified in MVID patients yet.

Although it is too early to define the phenotype of STX3-related MVID because of the small number and young age of MVID patients with *STX3* mutations, it is interesting that both cases described in **Chapter 3** tolerate small amounts of enteral feeding. This raises the question whether *STX3* mutations are associated with a relatively mild phenotype. In this respect it could be hypothesized that the function of syntaxin 3 can be partially adopted by another t-SNARE.

It is known that *STX3* is not only expressed in enterocytes, but also in for example the retina, lens and brain. In brain syntaxin 3 has a role in membrane expansion by docking intracellular vesicles with the plasma membrane. In the retinal photoreceptor cells syntaxin 3 is involved in the biogenesis and renewal of the rod outer segment membranes [19]. The function of syntaxin 3 in the lens has not been described yet.

Recently, non-synonymous *STX3* mutations have been identified in a Tunisian family with autosomal recessively inherited congenital cataract and intellectual disability. These patients did not suffer from diarrhea [19]. It is still unknown why these patients did not develop MVID. Possibly this non-synonymous mutation causes a milder phenotype than the truncating *STX3* mutations identified in the two MVID patients. However, this hypothesis would not explain the lack of congenital cataract and intellectual disability in the two STX3-related MVID patients. Possibly STX3-related MVID patients will develop cataract and intellectual disability at an older age.

Sequencing of *STX3* has already been implemented in the diagnostic process of MVID, both as individual test together with sequencing of *MYO5B* when the clinical diagnosis MVID has been made, and as part of an NGS gene panel when a patient presents with congenital diarrhea and the underlying disease is still unknown. Apart from enabling genetic counseling, knowledge of the underlying gene defect might make it possible to give a prognosis, at least when a larger cohort of patients with STX-related MVID with a longer follow-up has been described.

Developing a therapy for patients with *MYO5B* or *STX3* mutations will be challenging, especially as the *MYO5B* and *STX3* mutations identified so far are very heterogeneous, and include both missense mutations and premature stop codons (**Table 1**) [16,20,21]. However, promising novel therapies including gene therapy, enterocyte transplantation and drugs that restore protein folding or stop codon read-through may be a successful treatment option for MVID patients in the future.

Table 1. MVID-associated mutations [16,20,21]

Gene	Effect	Mutation
MYO5B	Affects actin interaction	p.Cys514Arg, p.Leu528Phe, p.Arg531Trp, p.Pro619Leu
MYO5B	Affects nucleotide binding	p.Gly168Arg, p.Arg219His
MYO5B	Affects allosteric motor rearrangement	p.Val108Gly, p.Gly316Arg, p.Arg401His, p.Cys454insKFC, p.Asn456Ser, p.Arg656Cys
MYO5B	Protein misfolding	p.Ala143Glu, p.Gly435Arg, p.Pro660Leu
MYO5B	Premature terminated protein	p.Trp14Ter,p.Gln149Ter, p.Ser186Ter, p.Ser289Ter, p.Gln341Ter, p.Arg363Ter, p.Ser370ArgfsTer27, p.Trp375Ter, p.Phe450leufsTer30, p.Arg749Ter, p.Tyr755GlyfsTer9, p.Gly777AsnfsTer6, p.Gln891Ter, p.Arg1016Ter, p.Gln1456Ter, p.Asp1586Ter, p.Gln1614Ter, p.Arg1795Ter
MYO5B	Unclassified	p.Met1?, exon2-12del, p.Ile408Phe, p.Arg410His, p.Leu1055dup, p.Leu1343Pro, p.Leu1556Arg, c.4460-1G>C
STX3	Premature terminated protein	p.Arg125LeufsTer7, p.Arg247Ter

Fat intolerance

In **Chapter 4** a homozygous c.629_631delCCT mutation in *DGAT1* was identified as underlying gene defect in two brothers with severe congenital fat intolerance. *DGAT1* encodes diacylglycerol O-acyltransferase 1 (DGAT1), which is responsible for the conversion of diacylglycerol to triacylglycerol [22–24]. The identified *DGAT1* mutation in these patients was associated with an increased ubiquitin-mediated protein degradation and accumulation of lipid droplets (**Figure 3**).

Presumably DGAT1 deficiency due to increased ubiquitin-mediated protein degradation strongly decreases the ability of the enterocyte to convert diacylglycerol to triacylglycerol. Possibly this results in accumulation of diacylglycerol and subsequently storage

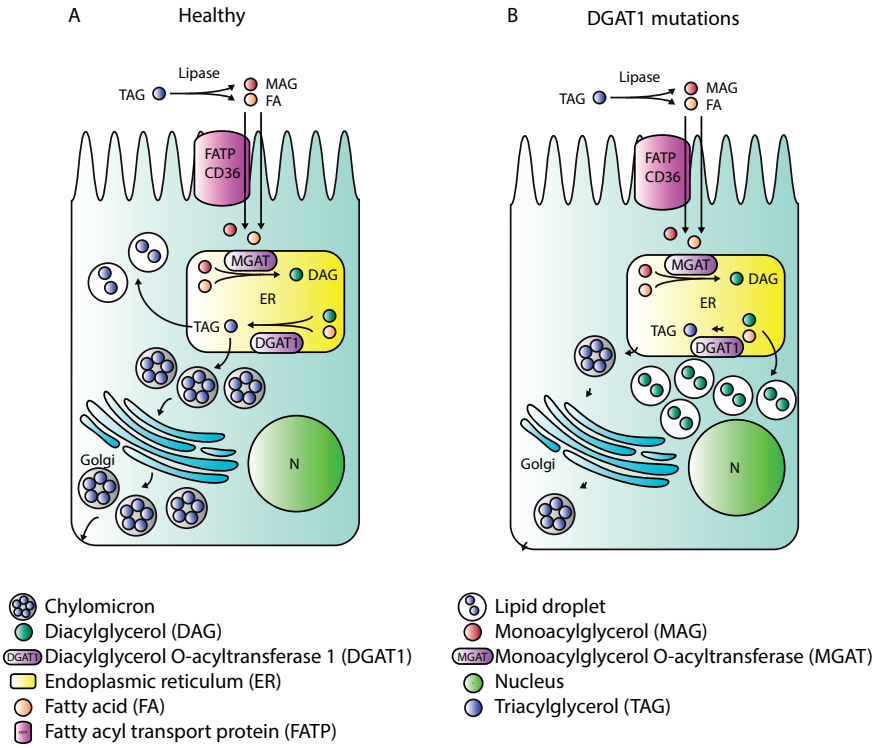

Figure 3. DGAT1 enzymatic deficiency causes fat intolerance. In the intestinal lumen triacylglycerol is hydrolysed to monoacylglycerol and fatty acids. In the endoplasmic reticulum of the enterocyte monoacylglycerol and fatty acids are converted to diacylglycerol by MGAT, which is subsequently converted to triacylglycerol by DGAT1. Triacylglycerol is either stored in lipid droplets or packaged into chylomicrons and secreted in the lymphatic system (**A**). DGAT1 deficiency inhibits the conversion of diacylglycerol to triacylglycerol, presumably leading to accumulation of diacylglycerol in cytosolic lipid droplets and fat intolerance (**B**).

of diacylglycerol in lipid droplets, which could be an explanation for the observed increased amount of lipid droplets in patient enterocytes. This inability of the enterocyte to handle diet lipids might explain the observed fat intolerance.

Recently, four families have been described in which *DGAT1* mutations lead to an autosomal recessively inherited enteropathy [25–27]. Interestingly, these patients all presented with congenital diarrhea, protein-losing enteropathy, failure to thrive and hyperlipidemia [25–27], which differs strongly from the presentation of the two brothers described in this thesis. The protein-losing enteropathy and associated diarrhea might however be a symptom of fat intolerance, since in several patients a fat restricted diet resulted in complete recovery of symptoms [25,26]. It could be argued that mutations leading to an (almost) complete deficiency of DGAT1 are associated with a more severe phenotype. However, both *DGAT1* mutations causing a complete lack of DGAT1 [27] and mutations leading to reduced levels with some remaining DGAT1 activity [25,26] lead to a protein-losing enteropathy and congenital diarrhea, while the homozygous *DGAT1* mutation described in this thesis results in almost complete lack of DGAT1 and is primarily associated with vomiting after fat ingestion. The differences in phenotype might be explained by interindividual variation in compensatory pathways to process diacylglycerol. Maybe accumulation of diacylglycerol due to DGAT1 deficiency or dysfunction leads to increased expression of DGAT2 in enterocytes or increased processing of diacylglycerol in the phospholipid pathway. Another explanation is that modifier genes play a role.

DGAT1-associated enteropathy is a good example of the importance that a genetic diagnosis might have for timely initiating a proper therapy. Both previously described patients with *DGAT1* mutations and the two brothers described in this thesis recovered with a fat restricted diet [25,26]. This suggests that, until curative therapies are available, patients with diarrhea, enteric protein-losing or fat intolerance due to *DGAT1* mutations should be immediately treated with a fat restricted diet, regular Intralipid infusions and supplementation of fat-soluble vitamins. In the meanwhile novel therapies can be developed. Since the *DGAT1* c.629_631delCCT mutation leads to increased proteasomal degradation, compounds that increase protein availability at the apical plasma membrane such as those currently being evaluated for restoration of CFTR folding and function [28–34], may also be beneficial for these patients. Further research will show whether these compounds indeed are a promising novel therapy for (specific) patients with DGAT1 deficiency.

Next-generation sequencing as tool in the diagnostics of genetically heterogeneous diseases

Chapter 2, 3 and 4 show the value of whole exome sequencing (WES) in identifying novel disease-associated genes, thereby increasing our understanding of the pathogenesis of the diseases described, both in general and in individual patients. Even when only one or two patients are available, WES is able to rapidly identify the underlying gene defect [35–37].

Despite the success of WES, it is important to keep the drawbacks of this genetic technique in mind. First, although the coverage is improving, the coverage does not reach 100% yet. The current coverage of whole exome sequencing ranges from 90 to 97%. This means that potential disease-causing mutations may be missed [35,37,38]. Secondly, some mutations are difficult to detect with WES, including copy number variants and expanded nucleotide repeats [35,37]. Furthermore, the filtering process of WES is challenging. When the filtering process is too stringent, potential disease-causing mutations may be excluded. However, less stringent regimens can cause a higher amount of false-positive variants [36–38]. Regardless of the filtering process, it is essential to address the potential pathogenicity of any mutation identified, especially when the mutation is located in a gene that has not been linked to the disease of interest before, for example by *in-silico* investigating the consequences at the protein level, by sequencing the candidate gene in additional patients with the disease of interest and by performing functional experiments. Lastly, WES is associated with ethical issues, since not only variants will be detected that potentially cause the disease under investigation, but also variants in genes that are known to be associated with non-related diseases. Therefore informed consent is essential [35,37–39]. Despite the drawbacks of WES, the great advantages of this technique have justified its current widespread use.

Next to its role in the identification of novel disease-associated genes, NGS is also becoming increasingly important in the diagnostics of genetically heterogeneous diseases. For example NGS has been implemented in the diagnostics of cardiomyopathies, epileptic disorders and primary immunodeficiencies, with excellent results in terms of both diagnostic yield, sensitivity and specificity [37,40–42]. In **Chapter 5** the successful implementation of NGS in the diagnostic process of congenital diarrhea has been described. This chapter also describes the further development of the diagnostic use of this genetic technique. Where previously a fixed, predetermined panel of genes was sequenced, this chapter shows the advantages of initially sequencing the whole exome (WES), and subsequently performing the analysis in two steps. First, all known disease-associated genes are analyzed. When no underlying gene defect is identified, the analysis is extended to the whole exome. This novel approach allows continuous addition of

novel disease-associated genes to a gene panel, and also enables extension of the analysis to the whole exome when analysis of the genes included in the gene panel does not reveal a genetic diagnosis.

Future implications

In the next few years further improvement of the WES technique will give a better coverage of genes, while algorithms for filtering results will become more efficient too. This will have a great impact on the diagnostics and ultimately also on the therapy of hereditary diseases.

Diagnostics of hereditary diseases

The ongoing identification of disease-causing mutations will provide a genetic diagnosis in patients in whom no underlying gene defect had been found so far. A genetic diagnosis is not only essential for patients to understand and accept their disease, it is also important to timely initiate the right therapy. Furthermore, it enables phenotyping, mediated by the development of databases with patient information, including the underlying genetic defect, disease onset and disease course. This phenotyping will have a great impact on the possibility to determine the prognosis in patients with a similar gene defect. Also clinicians will be able to screen patients for additional symptoms that are associated with a specific gene defect, which will lead to earlier treatment of these symptoms or even prevention, which is favourable for the prognosis. The identification of the disease-causing mutation in a patient also enables genetic counseling and prenatal screening. Even population-wide preconceptual genetic screening is now within the bounds of possibility.

Therapy of hereditary diseases

The identification of novel disease-causing mutations and disease-associated genes will also have important consequences for the therapy of genetic diseases. Currently several novel molecular therapies are being developed. Important examples include proteostasis regulators, which already have been implemented in the therapy of a subset of cystic fibrosis patients [43,44], and gene therapy using the CRISPR/Cas technology [45,46]. Furthermore, enterocyte transplantation is a promising novel therapy currently under investigation. To determine whether these therapies can be successful in specific diseases and even individual patients, it is essential to know the disease-causing mutation and the mechanism by which protein deficiency or dysfunction leads to the development of the disease under investigation. WES facilitates this process, which greatly enlarges the potential scope of these therapies.

Concluding remarks

This thesis aimed to further understand the pathogenesis of some pediatric intestinal diseases with the ultimate goal to improve the therapy of these disorders. By using WES novel gene defects have been identified underlying infantile-onset inflammatory bowel disease, microvillus inclusion disease and congenital fat intolerance. These discoveries have been of great value in increasing the knowledge of the pathogenesis of these diseases. At the moment we are in the middle of a revolution in medicine. Novel therapies, including proteostasis regulators, gene therapy and enterocyte transplantation, are being developed, which will highly improve the therapeutic possibilities in genetic diseases. NGS has been shown to be indispensable in this process by identifying novel disease-causing mutations and disease-associated genes and thereby enlarging the potential scope of the newly developed therapies. The implementation of genetics in patient care continues to improve the prospects for patients.

References

1. Restivo NL, Srivastava MD, Schafer IA, Hoppel CL. Mitochondrial dysfunction in a patient with crohn disease: possible role in pathogenesis. *J Pediatr Gastroenterol Nutr* 2004;38:534–538
2. Santhanam S, Rajamanickam S, Motamarry A, Ramakrishna BS, Amirtharaj JG, Ramachandran A, Pulimood A, Venkatraman A. Mitochondrial electron transport chain complex dysfunction in the colonic mucosa in ulcerative colitis. *Inflamm Bowel Dis* 2012;18:2158–2168
3. Sifroni KG, Damiani CR, Stoffel C, Cardoso MR, Ferreira GK, Jeremias IC, Rezin GT, Scaini G, Schuck PF, Dal-Pizzol F, Streck EL. Mitochondrial respiratory chain in the colonic mucosal of patients with ulcerative colitis. *Mol Cell Biochem* 2010;342:111–115
4. Beltrán B, Nos P, Dasí F, Iborra M, Bastida G, Martínez M, O'Connor J-E, Sáez G, Moret I, Ponce J. Mitochondrial dysfunction, persistent oxidative damage, and catalase inhibition in immune cells of naïve and treated Crohn's disease. *Inflamm Bowel Dis* 2010;16:76–86
5. Nazli A, Yang P-C, Jury J, Howe K, Watson JL, Söderholm JD, Sherman PM, Perdue MH, McKay DM. Epithelia under metabolic stress perceive commensal bacteria as a threat. *Am J Pathol* 2004; 164:947–957
6. Kelsen JR, Baldassano RN, Artis D, Sonnenberg GF. Maintaining intestinal health: the genetics and immunology of very early onset inflammatory bowel disease. *Cell Mol Gastroenterol Hepatol* 2015;1: 462–476
7. Uhlig HH. Monogenic diseases associated with intestinal inflammation: implications for the understanding of inflammatory bowel disease. *Gut* 2013;62:1795–1805
8. Lopez-Herrera G, Tampella G, Pan-Hammarström Q, Herholz P, Trujillo-Vargas CM, Phadwal K, Simon AK, Moutschen M, Etzioni A, Mory A, Srugo I, Melamed D, Hultenby K, Liu C, Baronio M, Vitali M, Philippet P, Dideberg V, Aghamohammadi A, Rezaei N, Enright V, Du L, Salzer U, Eibel H, Pfeifer D, Veelken H, Stauss H, Lougaris V, Plebani A, Gertz EM, Schäffer AA, Hammarström L, Grimbacher B. Deleterious mutations in LRBA are associated with a syndrome of immune deficiency and autoimmunity. *Am J Hum Genet* 2012;90:986–1001
9. Massaad MJ, Zhou J, Tsuchimoto D, Chou J, Jabara H, Janssen E, Glauzy S, Olson BG, Morbach H, Ohsumi TK, Schmitz K, Kyriacos M, Kane J, Torisu K, Nakabeppu Y, Notarangelo LD, Chouery E, Megarbane A, Kang PB, Al-Idrissi E, Aldhekri H, Meffre E, Mizui M, Tsokos GC, Manis JP, Al-Herz W, Wallace SS, Geha RS. Deficiency of base excision repair enzyme NEIL3 drives increased predisposition to autoimmunity. *J Clin Invest* 2016;126:4219–4236
10. Kaser A, Lee A-H, Franke A, Glickman JN, Zeissig S, Tilg H, Nieuwenhuis EES, Higgins DE, Schreiber S, Glimcher LH, Blumberg RS. XBP1 links ER stress to intestinal inflammation and confers genetic risk for human inflammatory bowel disease. *Cell* 2008;134:743–756
11. Kaser A, Martínez-Naves E, Blumberg RS. Endoplasmic reticulum stress: implications for inflammatory bowel disease pathogenesis. *Curr Opin Gastroenterol* 2010;26:318–326
12. Sharma N, Low SH, Misra S, Pallavi B, Weimbs T. Apical targeting of syntaxin 3 is essential for epithelial cell polarity. *J Cell Biol* 2006;173:937–948
13. Delgrossi MH, Breuza L, Mirre C, Chavrier P, Le Bivic A. Human syntaxin 3 is localized apically in human intestinal cells. *J Cell Sci* 1997;110:2207–2214

14. Jahn R, Scheller RH. SNAREs--engines for membrane fusion. *Nat Rev Mol Cell Biol* 2006;7: 631–643
15. Vogel GF, Klee KMC, Janecke AR, Müller T, Hess MW, Huber LA. Cargo-selective apical exocytosis in epithelial cells is conducted by Myo5B, Slp4a, Vamp7, and Syntaxin 3. *J Cell Biol* 2015;211: 587–604
16. Wiegerinck CL, Janecke AR, Schneeberger K, Vogel GF, van Haaften-Visser DY, Escher JC, Adam R, Thöni CE, Pfaller K, Jordan AJ, Weis C-A, Nijman IJ, Monroe GR, van Hasselt PM, Cutz E, Klumperman J, Clevers H, Nieuwenhuis EES, Houwen RHJ, van Haaften G, Hess MW, Huber LA, Stapelbroek JM, Müller T, Middendorp S. Loss of syntaxin 3 causes variant microvillus inclusion disease. *Gastroenterology* 2014;147:65–68
17. Müller T, Hess MW, Schiefermeier N, Pfaller K, Ebner HL, Heinz-Erian P, Ponstingl H, Partsch J, Röllinghoff B, Köhler H, Berger T, Lenhartz H, Schlenck B, Houwen RJ, Taylor CJ, Zoller H, Lechner S, Goulet O, Utermann G, Ruemmele FM, Huber LA, Janecke AR. MYO5B mutations cause microvillus inclusion disease and disrupt epithelial cell polarity. *Nat Genet* 2008;40:1163–1165
18. Vogel GF, Hess MW, Pfaller K, Huber LA, Janecke AR, Müller T. Towards understanding microvillus inclusion disease. *Mol Cell Pediatr* 2016;3:3
19. Chograni M, Alkuraya FS, Ourteni I, Maazoul F, Lariani I, Chaabouni HB. Autosomal recessive congenital cataract, intellectual disability phenotype linked to STX3 in a consanguineous Tunisian family. *Clin Genet* 2015;88:283–287
20. van der Velde KJ, Dhekne HS, Swertz MA, Sirigu S, Ropars V, Vinke PC, Rengaw T, van den Akker PC, Rings EHHM, Houdusse A, van IJzendoorn SCD. An overview and online registry of microvillus inclusion disease patients and their MYO5B mutations. *Hum Mutat* 2013;34:1597–1605
21. Perry A, Bensallah H, Martinez-Vinson C, Berrebi D, Arbeille B, Salomon J, Goulet O, Marinier E, Drunat S, Samson-Bouma M-E, Gérard B, Hugot J-P. Microvillous atrophy: atypical presentations. *J Pediatr Gastroenterol Nutr* 2014;59:779–785
22. Iqbal J, Hussain MM. Intestinal lipid absorption. *Am J Physiol Endocrinol Metab* 2009;296:E1183-1194
23. Yen C-LE, Stone SJ, Koliwad S, Harris C, Farese R V. Thematic review series: glycerolipids. DGAT enzymes and triacylglycerol biosynthesis. *J Lipid Res* 2008;49:2283–2301
24. Hiramine Y, Tanabe T. Characterization of acyl-coenzyme A:diacylglycerol acyltransferase (DGAT) enzyme of human small intestine. *J Physiol Biochem* 2011;67:259–264
25. Gluchowski NL, Chitraju C, Picoraro JA, Mejhert N, Pinto S, Xin W, Kamin DS, Winter HS, Chung WK, Walther TC, Farese R V. Identification and characterization of a novel DGAT1 missense mutation associated with congenital diarrhea. *J Lipid Res* 2017;58:1230–1237
26. Stephen J, Vilboux T, Haberman Y, Pri-Chen H, Pode-Shakked B, Mazaheri S, Marek-Yagel D, Barel O, Di Segni A, Eyal E, Hout-Siloni G, Lahad A, Shalem T, Rechavi G, Malicdan MC V, Weiss B, Gahl WA, Anikster Y. Congenital protein losing enteropathy: an inborn error of lipid metabolism due to DGAT1 mutations. *Eur J Hum Genet* 2016;24:1268–1273
27. Haas JT, Winter HS, Lim E, Kirby A, Blumenstiel B, DeFelice M, Gabriel S, Jalas C, Branski D, Grueter CA, Toporovski MS, Walther TC, Daly MJ, Farese R V. DGAT1 mutation is linked to a congenital diarrheal disorder. *J Clin Invest* 2012;122:4680–4684

28. Pedemonte N, Lukacs GL, Du K, Caci E, Zegarra-Moran O, Galietta LJ V, Verkman AS. Small-molecule correctors of defective DeltaF508-CFTR cellular processing identified by high-throughput screening. *J Clin Invest* 2005;115:2564–2571
29. Van Goor F, Straley KS, Cao D, González J, Hadida S, Hazlewood A, Joubran J, Knapp T, Makings LR, Miller M, Neuberger T, Olson E, Panchenko V, Rader J, Singh A, Stack JH, Tung R, Grootenhuis PDJ, Negulescu P. Rescue of DeltaF508-CFTR trafficking and gating in human cystic fibrosis airway primary cultures by small molecules. *Am J Physiol Lung Cell Mol Physiol* 2006;290: L1117-1130
30. Loo TW, Bartlett MC, Wang Y, Clarke DM. The chemical chaperone CFcor-325 repairs folding defects in the transmembrane domains of CFTR-processing mutants. *Biochem J* 2006;395:537–542
31. Hirth BH, Qiao S, Cuff LM, Cochran BM, Pregel MJ, Gregory JS, Sneddon SF, Kane JL. Discovery of 1,2,3,4-tetrahydroisoquinoline-3-carboxylic acid diamides that increase CFTR mediated chloride transport. *Bioorg Med Chem Lett* 2005;15:2087–2091
32. Robert R, Carlile GW, Pavel C, Liu N, Anjos SM, Liao J, Luo Y, Zhang D, Thomas DY, Hanrahan JW. Structural analog of sildenafil identified as a novel corrector of the F508del-CFTR trafficking defect. *Mol Pharmacol* 2008;73:478–489
33. Macia E, Ehrlich M, Massol R, Boucrot E, Brunner C, Kirchhausen T. Dynasore, a cell-permeable inhibitor of dynamin. *Dev Cell* 2006;10:839–850
34. Yoo CL, Yu GJ, Yang B, Robins LI, Verkman AS, Kurth MJ. 4'-Methyl-4,5'-bithiazole-based correctors of defective delta F508-CFTR cellular processing. *Bioorg Med Chem Lett* 2008;18:2610–2614
35. Singleton AB. Exome sequencing: a transformative technology. *Lancet Neurol* 2011;10:942–946
36. Rabbani B, Mahdieh N, Hosomichi K, Nakaoka H, Inoue I. Next-generation sequencing: impact of exome sequencing in characterizing Mendelian disorders. *J Hum Genet* 2012;57:621–632
37. de Koning TJ, Jongbloed JDH, Sikkema-Raddatz B, Sinke RJ. Targeted next-generation sequencing panels for monogenetic disorders in clinical diagnostics: the opportunities and challenges. *Expert Rev Mol Diagn* 2015;15:61–70
38. Fuchs SA, Harakalova M, van Haaften G, van Hasselt PM, Cuppen E, Houwen RHJ. Application of exome sequencing in the search for genetic causes of rare disorders of copper metabolism. *Metallomics* 2012;4:606–613
39. Green RC, Berg JS, Grody WW, Kalia SS, Korf BR, Martin CL, McGuire AL, Nussbaum RL, O'Daniel JM, Ormond KE, Rehm HL, Watson MS, Williams MS, Biesecker LG. ACMG recommendations for reporting of incidental findings in clinical exome and genome sequencing. *Genet Med* 2013;15:565–574
40. Nijman IJ, van Montfrans JM, Hoogstraat M, Boes ML, van de Corput L, Renner ED, van Zon P, van Lieshout S, Elferink MG, van der Burg M, Vermont CL, van der Zwaag B, Janson E, Cuppen E, Ploos van Amstel JK, van Gijn ME. Targeted next-generation sequencing: a novel diagnostic tool for primary immunodeficiencies. *J Allergy Clin Immunol* 2014;133:529–534
41. Lemke JR, Riesch E, Scheurenbrand T, Schubach M, Wilhelm C, Steiner I, Hansen J, Courage C, Gallati S, Bürki S, Strozzi S, Simonetti BG, Grunt S, Steinlin M, Alber M, Wolff M, Klopstock T, Prott EC, Lorenz R, Spaich C, Rona S, Lakshminarasimhan M, Kröll J, Dorn T, Krämer G, Synofzik M, Becker F, Weber YG, Lerche H, Böhm D, Biskup S. Targeted next generation sequencing as a diagnostic tool in epileptic disorders. *Epilepsia* 2012;53:1387–1398

42. Kammermeier J, Drury S, James CT, Dziubak R, Ocaka L, Elawad M, Beales P, Lench N, Uhlig HH, Bacchelli C, Shah N. Targeted gene panel sequencing in children with very early onset inflammatory bowel disease--evaluation and prospective analysis. *J Med Genet* 2014;51:748–755
43. Wainwright CE, Elborn JS, Ramsey BW, Marigowda G, Huang X, Cipolli M, Colombo C, Davies JC, De Boeck K, Flume PA, Konstan MW, McColley SA, McCoy K, McKone EF, Munck A, Ratjen F, Rowe SM, Waltz D, Boyle MP. Lumacaftor-Ivacaftor in Patients with Cystic Fibrosis Homozygous for Phe508del CFTR. *N Engl J Med* 2015;373:220–231
44. Boyle MP, Bell SC, Konstan MW, McColley SA, Rowe SM, Rietschel E, Huang X, Waltz D, Patel NR, Rodman D. A CFTR corrector (lumacaftor) and a CFTR potentiator (ivacaftor) for treatment of patients with cystic fibrosis who have a phe508del CFTR mutation: a phase 2 randomised controlled trial. *Lancet Respir Med* 2014;2:527–538
45. Cong L, Ran FA, Cox D, Lin S, Barretto R, Habib N, Hsu PD, Wu X, Jiang W, Marraffini LA, Zhang F. Multiplex genome engineering using CRISPR/Cas systems. *Science* 2013;339:819–823
46. Sander JD, Joung JK. CRISPR-Cas systems for editing, regulating and targeting genomes. *Nat Biotechnol* 2014;32:347–355

Summary

Congenital diseases of the gastrointestinal tract are characterized by significant morbidity and mortality. Treatment of these diseases can be challenging, since current therapies often do not cure the disease and may severely interfere with the quality of life. A better understanding of the pathogenesis of this group of diseases is the first step to improve therapeutic options. In this thesis we have contributed to this goal by studying several rare congenital intestinal diseases, all presenting in the first months of life, namely infantile-onset inflammatory bowel disease, microvillus inclusion disease and severe congenital fat intolerance. We identified and studied the gene defects underlying these diseases.

Chapter 2 describes the discovery of an association between mutations in *ANKZF1* and infantile-onset inflammatory bowel disease (IO IBD). Out of thirteen IO IBD patients investigated two patients were found to have two mutated *ANKZF1* alleles. In two additional patients one mutated *ANKZF1* allele was identified. ANKZF1 was found to be an essential protein in the mitochondrial response to cellular stress, a function that had not been described before. Depletion of ANKZF1 reduced both mitochondrial integrity and mitochondrial respiration under conditions of cellular stress. The *ANKZF1* mutations identified in both IO IBD patients with two mutated *ANKZF1* alleles resulted in dysfunctional ANKZF1 as shown by decreased mitochondrial respiration and an increased level of apoptosis in patient cells after induction of cellular stress by exposure to hydrogen peroxide. Furthermore, mutated ANKZF1 was not able to rescue the phenotype of Vms1 deficient yeast, which is the yeast homologue of ANKZF1, while wild-type ANKZF1 resulted in partial rescue of this phenotype. Although the exact mechanism by which dysfunctional ANKZF1 results in IO IBD is still unknown, these data indicate that deregulation of mitochondrial integrity likely plays a role in the pathogenesis of this disease.

In **Chapter 3** the identification of *STX3* mutations as novel cause of microvillus inclusion disease (MVID) is described. MVID is a severe disorder characterized by the virtual absence of apical microvilli at the small intestinal epithelial cells, resulting in severe malabsorption and intractable diarrhoea. Most often MVID is the result of mutations in *MYO5B*, which encodes myosin Vb, a motor protein responsible for trafficking of transport vesicles to the apical plasma membrane. **Chapter 3** shows that a subgroup of MVID patients carries *STX3* mutations, which encodes syntaxin 3, a target N-ethylmaleimide-sensitive factor attachment protein receptor (t-SNARE) on the apical plasma membrane of several cell types, including enterocytes. By binding to specific SNARE proteins on vesicles (v-SNAREs), syntaxin 3 is responsible for docking of these vesicles to the apical plasma membrane and fusion of the vesicles with this membrane. The *STX3* mutations of the two patients described in this chapter resulted in a deficiency of syntaxin 3 leading to a disturbed polarity of the enterocytes and variable loss of microvilli.

In **Chapter 4** two brothers with severe congenital fat intolerance were found to have mutations in *DGAT1*, which encodes diacylglycerol O-acyltransferase 1 (DGAT1). DGAT1 is responsible for the conversion of diacylglycerol and fatty acyl CoA to triacylglycerol in enterocytes, a reaction essential for intestinal triacylglycerol absorption. Although *DGAT1* mutations have been previously linked to congenital diarrhea, the association with fat intolerance has not been described before. The *DGAT1* mutation identified in the two brothers with fat intolerance leads to an increased ubiquitin-mediated proteasomal degradation of DGAT1, resulting in a deficiency of this protein. Presumably this subsequently leads to fat malabsorption. It is conceivable that the protein level of this mutated DGAT1 can be increased by some compounds that are known to increase the availability of CFTR at the apical plasma membrane as well, making these compounds a potential novel treatment for these patients.

The discoveries of an association between mutations in *ANKZF1*, *STX3* and *DGAT1* and infantile-onset inflammatory bowel disease, microvillus inclusion disease and severe congenital fat intolerance respectively were mediated by whole exome sequencing. Whole exome sequencing is a next-generation sequencing (NGS) method in which the entire coding part of the genome is sequenced. NGS is not only used in the identification of novel disease-associated genes, but can also be used in the diagnostics of genetically heterogeneous diseases. **Chapter 5** describes the successful implementation of NGS in the diagnostic work up of two patients with congenital diarrhea. Furthermore, it shows the development of NGS as diagnostic tool. Previously only a fixed, predetermined panel of genes was sequenced, but in **Chapter 5** a novel approach is introduced, where the whole exome is sequenced and the subsequent analysis is performed in two steps. First, all genes known to be associated with congenital diarrhea are analyzed. When no underlying mutation is identified, analysis is extended to the whole exome. The advantages of this approach are that newly described disease-associated genes can be continuously added to a gene panel. Furthermore, whole-exome analysis may reveal a diagnosis in patients where no disease-causing mutation could be found when just using a panel consisting of genes already known to be associated with congenital diarrhea.

This thesis increases our understanding of the pathogenesis of infantile-onset inflammatory bowel disease, microvillus inclusion disease and severe congenital fat intolerance. Furthermore it illustrates the great value of next-generation sequencing in the diagnostics of genetically heterogeneous diseases. Identifying a genetic defect underlying a disorder is important, since it enables genetic counseling and may clarify prognosis. However, maybe even more important, understanding the pathogenesis of a disease is also the basis of the development of novel therapeutic approaches. Currently many congenital intestinal diseases can not be cured. However, the functional genomics approach detailed in this thesis may contribute to the development of novel therapies in the near future.

Samenvatting

Aangeboren afwijkingen van de tractus digestivus hebben een aanzienlijke morbiditeit en mortaliteit. Het is daarbij vaak moeilijk om deze ziekten te behandelen, omdat de momenteel beschikbare behandelopties vaak beperkt zijn en daarnaast een sterke invloed kunnen hebben op de kwaliteit van leven van de patiënt. Meer kennis over het ontstaan ("de pathogenese") van deze groep aandoeningen kan helpen de behandelmogelijkheden te verbeteren. Dit proefschrift had daarom als doel de kennis over de pathogenese van enkele van deze aandoeningen, namelijk inflammatoire darmziekte op de zuigelingen- en peuterleeftijd, microvillus inclusie ziekte en ernstige congenitale vetintolerantie, te vergroten door het identificeren en bestuderen van gendefecten die deze ziektes kunnen veroorzaken.

Hoofdstuk 2 beschrijft de associatie tussen fouten ("mutaties") in *ANKZF1* en inflammatoire darmziekte op de zuigelingen- en peuterleeftijd ("infantile-onset inflammatory bowel disease", IO IBD). IO IBD is een chronische darmontsteking, die zich presenteert voor de leeftijd van twee jaar. Bij dertien patiënten met IO IBD werd de code van het *ANKZF1* gen bepaald ("gesequenced"). Twee patiënten hadden een mutatie op beide versies ("allelen") van het *ANKZF1* gen en twee patiënten hadden één gemuteerd *ANKZF1* allel. ANKZF1 blijkt een essentieel eiwit te zijn voor de mitochondriële respons op cellulaire stress, een functie die niet eerder beschreven was. Een tekort aan ANKZF1 leidt tot dysfunctie van de mitochondriën, zodra de cel onder stress komt te staan. De *ANKZF1* mutaties die zijn gevonden in beide patiënten met twee gemuteerde *ANKZF1* allelen resulteren in een dysfunctioneel ANKZF1, wat blijkt uit een verminderde mitochondriële functie na inductie van cellulaire stress door blootstelling van de cellen aan waterstofperoxide. Tevens kan gemuteerd ANKZF1 in gist met een deficiëntie van het op ANKZF1 lijkende eiwit Vms1 de ontbrekende functie niet herstellen, terwijl niet-gemuteerd ANKZF1 hier wel toe in staat is, zij het gedeeltelijk. Hoewel het nog onbekend is hoe dysfunctioneel ANKZF1 exact IO IBD veroorzaakt, suggereren deze data dat aantasting van de mitochondriële functie een belangrijke rol speelt in de pathogenese van deze ziekte.

In **Hoofdstuk 3** wordt de identificatie van *STX3* mutaties als nieuwe oorzaak van microvillus inclusie ziekte ("microvillus inclusion disease", MVID) beschreven. MVID is een ernstige aandoening die wordt gekarakteriseerd door het ontbreken van microvilli op de darmcellen ("enterocyten") in de dunne darm, wat leidt tot ernstige malabsorptie en diarree. Meestal wordt MVID veroorzaakt door mutaties in *MYO5B*, wat codeert voor myosin Vb, een motor eiwit dat verantwoordelijk is voor het vervoeren van transportblaasjes naar de plasmamembraan. **Hoofdstuk 3** toont aan dat een subgroep van de MVID patiënten mutaties heeft in *STX3*, wat codeert voor syntaxin 3, een eiwit dat zich bevindt op het plasmamembraan van verschillende celtypes, zoals enterocyten. Syntaxin 3 is verantwoordelijk voor het binden van transportblaasjes aan het plasmamembraan. De *STX3* mutaties van de twee patiënten die in dit hoofdstuk worden beschreven leiden

tot een tekort aan syntaxin 3 en daardoor tot een verstoring van het transport van de blaasjes in de cel en een variabel verlies van microvilli op de enterocyt.

In **Hoofdstuk 4** worden twee broers beschreven met een ernstige aangeboren ("congenitale") vorm van vetintolerantie. Beiden bleken mutaties te hebben in *DGAT1*, wat codeert voor diacylglycerol O-acyltransferase 1 (DGAT1), een enzym dat verantwoordelijk is voor een essentiële stap in het vetmetabolisme in de enterocyt. *DGAT1* mutaties zijn een bekende oorzaak van congenitale diarree. De associatie van *DGAT1* mutaties met vetintolerantie was echter nog niet eerder beschreven. De *DGAT1* mutaties die zijn gevonden bij de twee broers met vetintolerantie leiden tot een verhoogde afbraak van DGAT1 in de cel, wat resulteert in een tekort aan DGAT1. Waarschijnlijk leidt deze DGAT1 deficiëntie tot een verstoring van het vetmetabolisme in de enterocyten met uiteindelijk vetintolerantie als gevolg. De concentratie van DGAT1 kan in deze patiënten mogelijk verhoogd worden door farmaca die sinds enige tijd met succes ingezet worden bij taaislijmziekte ("cystische fibrose"). Weliswaar is er bij cystische fibrose een tekort aan een ander eiwit, namelijk CFTR, maar het principe van deze behandeling, namelijk verbetering van de concentratie van een gemuteerd maar nog wel werkzaam eiwit, zou mogelijk ook gebruikt kunnen worden bij de behandeling van DGAT1 deficiëntie.

De associaties tussen mutaties in *ANKZF1*, *STX3* en *DGAT1* en respectievelijk IO IBD, MVID en ernstige congenitale vetintolerantie zijn aan het licht gekomen met behulp van whole exome sequencing (WES). WES is een vorm van next-generation sequencing (NGS), waarbij het gehele exoom, het deel van het genoom dat de code bevat voor alle eiwitten in het menselijk lichaam, wordt gesequenced. NGS wordt niet alleen gebruikt bij het opsporen van nieuwe ziekte-geassocieerde genen, maar tevens bij de diagnostiek van ziektebeelden met een genetische achtergrond. **Hoofdstuk 5** beschrijft de succesvolle toepassing van NGS bij de diagnostiek van congenitale diarree. Tevens laat dit hoofdstuk de ontwikkeling zien van NGS als diagnostische methode. Tot nu toe werd een vaste, vooraf bepaalde groep van genen gesequenced. **Hoofdstuk 5** beschrijft echter een nieuwe methode, waarbij het gehele exoom wordt gesequenced en vervolgens de analyse in twee stappen plaatsvindt. Allereerst worden alle genen geanalyseerd waarvan bekend is dat ze geassocieerd zijn met congenitale diarree. Wanneer er geen ziekte-veroorzakende mutatie in deze genen wordt gevonden, wordt de analyse uitgebreid naar het volledige exoom. Een voordeel van deze methode is dat ook een ziekte-veroorzakende mutatie gevonden kan worden in een gen waarvan tot dan toe niet bekend was dat het geassocieerd kon zijn met congenitale diarree. Tevens kunnen deze en andere genen waarvan bekend wordt dat ze ziekte-veroorzakend zijn makkelijk toegevoegd worden aan de groep van genen die primair onderzocht gaat worden.

Dit proefschrift vergroot de kennis over de pathogenese van IO IBD, MVID en ernstige congenitale vetmalabsorptie. Daarnaast benadrukt het de grote waarde van NGS bij de diagnostiek van genetische aandoeningen. Het identificeren van het gendefect dat

een aandoening veroorzaakt is belangrijk, niet alleen omdat het erfelijkheidsvoorlichting mogelijk maakt, maar ook omdat dan de prognose vaak duidelijker wordt. Belangrijker nog is dat het de basis vormt voor het ontwikkelen van nieuwe behandelmethoden. Immers, momenteel kunnen vele congenitale aandoeningen van de darm niet genezen worden. Het onderzoek beschreven in dit proefschrift draagt mogelijk bij aan de ontwikkeling van de zo noodzakelijke nieuwe therapieën.

Dankwoord

Toen ik pas net begonnen was met mijn studie geneeskunde, wist ik al dat ik wilde gaan promoveren. Een wens die gedurende de studie alleen maar sterker werd. Nu is het zover. Wat ben ik blij met het onderzoek dat ik heb mogen doen, de kansen die ik heb gekregen en de personen met wie ik heb mogen samenwerken.

Hoewel het aantal patiënten dat betrokken is geweest bij het onderzoek beperkt is, zijn deze patiënten essentieel geweest voor het tot stand komen van dit proefschrift. Dank jullie wel voor jullie belangeloze bijdrage. Ik hoop, dat de wens voor een therapie die jullie ziekte zal genezen in de toekomst realiteit zal worden.

Prof. dr. R.H.J. Houwen, geachte promotor, beste Roderick. Tien jaar geleden liep ik als vierdejaars student geneeskunde voor het eerst jouw kamer binnen. Ik was op zoek naar een interessant onderzoek voor mijn wetenschapsstage. Deze ontmoeting is bepalend geweest voor de rest van mijn loopbaan. Je bemiddelde niet alleen bij een onderwerp voor mijn eerste onderzoek, maar hebt me daarna ook meerdere andere onderzoeksprojecten aangeboden, die ik met veel plezier heb aangenomen, inclusief dit promotietraject. Daarnaast ben jij altijd een belangrijke referent geweest bij mijn sollicitaties voor zowel mijn beide ANIOS plekken als mijn huidige AIOS positie. Ik wil je vanuit de grond van mijn hart bedanken voor het vertrouwen, dat je al die jaren in mij hebt gehad en jouw steun om mijn dromen, zowel klinisch als wetenschappelijk, waar te maken. Jij hebt me leren denken als een onderzoeker en mijn interesse in pediatrische aandoeningen met een genetische oorzaak gewekt. Ik waardeer het heel erg, dat je tijdens onze gesprekken over het onderzoek altijd oog hield voor de langere termijn en dat ik altijd een snelle reactie kon verwachten op mijn emails en nieuwe versies van manuscripten. Ik hoop dat onze samenwerking niet zal eindigen met het afronden van mijn proefschrift. Heel erg bedankt.

Prof. dr. P.J. Coffer, geachte promotor, beste Paul. Ik weet nog goed, hoe ik als arts begon in jouw laboratorium. Veel verder dan een qRT-PCR en western blot reikten mijn kennis op het gebied van basaal onderzoek niet. Dankjewel dat je mij de kans hebt gegeven om, zeker met mijn achtergrond als arts, basaal wetenschappelijk onderzoek te doen en dat je jouw kennis met mij hebt willen delen. Ik heb in de afgelopen jaren heel veel geleerd over het uitvoeren van basaal onderzoek, niet alleen over de verschillende technieken, maar ook over het opbouwen van evidence. Door jou weet ik nu hoe ik basaal wetenschappelijk onderzoek moet opzetten, uitvoeren en beoordelen. Ik waardeer het heel erg, dat je tijdens het bespreken van mijn resultaten altijd bereid was mee te denken over een oplossing als ik tegen problemen aanliep en dat je ook altijd interesse had in hoe het met me ging. Ik hoop dat ik in de toekomst basaal wetenschappelijk onderzoek zal blijven doen.

Geachte leden van de leescommissie: prof. dr. J. Klumperman, prof. dr. V.V.A.M. Knoers, prof. dr. N.M. Wulffraat, prof. dr. J.C. Escher en prof. dr. E.E.S. Nieuwenhuis. Ik wil jullie hartelijk bedanken voor het kritisch beoordelen van mijn proefschrift.

Prof. dr. M.M. Maurice en prof. dr. E.E.S. Nieuwenhuis, beste Madelon en Edward. Dank jullie wel, dat jullie samen mijn PhD-voortgangscommissie wilden vormen. De jaarlijkse gesprekken zijn heel relevant geweest voor de voortgang van het onderzoek. Edward, naast de PhD-voortgangsgesprekken hebben wij ook enkele malen gesproken over belangrijke keuzes ten aanzien van mijn verdere loopbaan. Ik kan me nog heel goed het gesprek herinneren, waarin we mijn sollicitatie voor de opleiding tot kinderarts bespraken. Dit gesprek heeft er mede toe geleid, dat ik nu AIOS kindergeneeskunde ben. Dankjewel voor je adviezen en vertrouwen en dat het altijd mogelijk is een afspraak te maken. Ik waardeer dit heel erg.

Beste Sabine Middendorp, onze samenwerking begon met het STX3 project, maar is verder gegaan met het DGAT1 project. Jij hebt mij niet alleen de vele mogelijkheden van organoids laten zien, maar je hebt mij ook geleerd hoe belangrijk organoids zijn in een paper om het benodigde bewijs te leveren. Dankjewel dat ik met deze techniek mocht werken en dat ik altijd bij je terecht kon om mijn resultaten en de vervolgexperimenten te bespreken. Ik kijk ernaar uit om het DGAT1 project af te maken.

Aan de onderzoeken beschreven in dit proefschrift hebben heel veel personen meegewerkt. Stuk voor stuk hebben zij een hele belangrijke bijdrage geleverd, waar ik hen heel dankbaar voor ben. Een aantal personen wil ik in het bijzonder bedanken. Beste Joris van Montfrans, mijn promotieonderzoek is enkele jaren geleden begonnen met één patiënt met infantile-onset inflammatory bowel disease. Jouw inzet voor het afnemen van bloed voor het onderzoek is essentieel geweest voor het kunnen uitvoeren van de experimenten voor het ANKZF1 paper. Heel erg bedankt voor je betrokkenheid en dat je altijd bereid was mee te denken over mogelijke pathofysiologische mechanismes. Dear Magdalena Harakalova, thank you so much for your genetic work for the ANKZF1 paper. I appreciate it very much that you were always willing to answer my questions about genetics. Dear Enric Mocholi, thank you for performing the experiments for the revision of the ANKZF1 paper. These results were essential for getting this paper published. Beste Ester Rieter, heel erg bedankt voor al je hulp met de gistexperimenten voor het ANKZF1 paper. Het was erg leuk om ook hier ervaring mee op te doen! Dear Aleixo Muise, it was an honor working on the ANKZF1 project with you. Thank you for the pleasant communication about your patient with infantile-onset inflammatory bowel disease. Beste Caroline Wiegerinck, onze wekelijkse besprekingen voor het STX3 project waren altijd heel gezellig! Het was erg fijn om samen met jou aan dit onderzoek te

werken. Dear Rüdiger Adam, thank you so much for the warm welcome in Mannheim both times and for collecting intestinal biopsies from your MVID patient to generate organoids. It was a pleasure to meet you. The picture you made from me while preparing the biopsies for transport is a precious memory. Beste Hankje Escher, dankjewel voor jouw hulp bij het STX3 paper en het verzamelen van de patiëntgegevens voor het congenitale diarree paper. Beste Jorik van Rijn, het afmaken van de experimenten voor het DGAT1 paper is bij jou in goede handen. Dankjewel voor je samenwerking op dit project en je snelle reactie op mijn vragen. Beste Marielle van Gijn, heel erg bedankt voor jouw belangrijke bijdrage aan het congenitale diarree paper en je uitleg over het gebruik van next-generation sequencing als diagnostische test.

Ook iedereen die heeft meegeholpen aan de experimenten, die niet in de papers zijn opgenomen, wil ik heel erg bedanken. Beste Marco Betist, dankjewel voor alle uren die jij aan de Caenorhabditis Elegans experimenten hebt besteed. Naast dat ik heel veel van je geleerd heb, was het een feest om met je samen te werken. Beste Pien van der Burgh en Jeroen van Velzen, heel erg bedankt voor jullie hulp in de FACS facility.

Beste collega's van het Coffer lab: Marije Bartels, Ruben van Boxtel, Koen Braat, Luca Braccioli, Sandra Coenen, Inge Dokter, Sanne van Dooremalen, Veerle Fleskens, Cindy Frederiks, Catalina Gomez Puerto, Anita Govers, Evelien Kruisselbrink, Jorg van Loosdregt, Magdalena Lorenowicz, Ana Rita Lourenço, Enric Mocholi, Cornelieke Pals, Janneke Peeters, Ester Rieter, Guy Roukens, Koen Schepers, Estel Thijssen, Emily Triffaux, Liesbeth Varion en Stephin Vervoort. Een aantal jaar geleden kwam ik als arts in een laboratorium. Ik wist niets van Ficoll-Paque en had nog nooit gehoord van flowcytometrie en confocal imaging. Stap voor stap hebben jullie mij alle technieken geleerd. Zowel tijdens de wekelijkse werkbesprekingen als daarbuiten waren jullie altijd geïnteresseerd in mijn onderzoek en bereid met mij mee te denken over hoe ik experimenten kon verbeteren. Ook voor suggesties voor vervolgexperimenten kon ik altijd bij jullie terecht. Dank jullie wel voor jullie geduld en bereidheid mee te denken. Dank jullie wel dat ik altijd een beroep op jullie kon doen, als ik niet zelf mijn cellen kon doorzetten of reagentia kon toevoegen. Dear Cata and Emily, thank you so much for your friendship. I really enjoyed all our orange juices, lunches and teas! Dear roommates Ana Rita, Luca, Jessica Sigmans, Jan Gerlag and Eline van Kappel. In our room it was not only possible to share scientific successes and disappointments, but also to talk about not work-related subjects. I will never forget our conversation about spirit levels and Luca, I loved being in the committee for finding a proper partner for one of our roommates with you. Thank you for all the good times.

De behulpzaamheid en gezelligheid beperkten zich zeker niet alleen tot het Coffer lab. Ook de collega's van de groepen van Anton Martens en Madelon Maurice, de overige groepen van de celbiologie en de groepen van Berent Prakken, Marianne Boes en Jeffrey Beekman wil ik heel erg bedanken voor hun gezelligheid en dat ik altijd voor vragen en advies bij hen terecht kon. Corlinda ten Brink, dankjewel voor je hulp bij de confocal experimenten. Despina Xanthakis, dankjewel voor je hulp bij de gistexperimenten. Betty Hartgring en Wieke van der Kuijl, dank jullie wel voor jullie geduld als ik weer eens kritisch was en voor jullie interesse.

Beste Peter van Hasselt en Koos Jansen. Mijn wetenschappelijke carrière begon tien jaar geleden met ons onderzoek naar de incidentie van intracraniële vitamine K deficientie bloedingen. Het was een erg leuk onderzoek, niet alleen vanwege het onderwerp, maar ook omdat we gegevens moesten verzamelen op alle kinder intensive care's van Nederland. Jullie aanstekelijke enthousiasme heeft mijn interesse in wetenschappelijk onderzoek alleen maar versterkt. Ik wil jullie heel erg bedanken hiervoor, alsmede voor jullie interesse in mijn promotieonderzoek de afgelopen jaren.

Beste Janneke Stapelbroek. Mijn allereerste stappen in een laboratorium deed ik samen met jou, toen ik als student onderzoek deed naar *ATP8B1* mutaties. Dankjewel voor je fijne begeleiding, geduldige uitleg en gezelligheid. Mede door dit onderzoek heb ik mijn voorliefde voor pathofysiologie en pediatrische aandoeningen met een genetische oorzaak ontdekt. Ik vond het erg leuk om onze samenwerking tijdens het STX3 project voort te zetten.

Inmiddels is het alweer anderhalf jaar geleden, dat ik Utrecht verruild heb voor Rotterdam voor de volgende stap in mijn carrière. Geachte prof. dr. M. de Hoog, beste Matthijs. Ik ben je zeer dankbaar, dat je mij de kans hebt gegeven om mijn droom om kinderarts te worden te verwezenlijken. Dankjewel voor je vertrouwen. Beste collega's uit het Maasstad Ziekenhuis. Toen ik anderhalf jaar geleden mijn opleiding tot kinderarts bij jullie begon, had ik net enkele jaren onderzoek achter de rug. Hoewel ik anderhalf jaar ervaring had als ANIOS, was die ervaring lang geleden. Jullie hebben mij geholpen mijn kennis en vaardigheden weer op peil te brengen. Inmiddels heb ik mijn plek helemaal gevonden. Dankjewel voor jullie begeleiding en jullie interesse in mijn onderzoek en mij als persoon. Ik kijk uit naar het tweede deel van mijn perifere stage.

Ik kan nog zo blij zijn met mijn werk en mijn collega's, echt gelukkig word ik van de personen die ik thuis om mij heen heb staan.

Lieve Saskia, Caroline, Maartje, Joyce, Susanne, Anke, Gijs, Anouska, Remko, Sara, Bart en Rachel. Wat begon met weekendjes weg en etentjes wordt langzaam aangevuld met spelen in de speeltuin en wandelen in het bos met de kinderen. Dank jullie wel voor jullie gezelligheid, de ontspanning naast het werk en jullie interesse in mijn onderzoek. Ik hoop dat onze vriendschap nog lang zal blijven bestaan.

Lieve paranimfen Melvin en Anita. Ik ben heel blij, dat jullie op deze bijzondere dag aan mijn zijde willen staan. Melvin, ik kan me de tijd bijna niet meer herinneren, dat wij elkaar niet kenden. Wat is begonnen met stijldansen toen we op de middelbare school zaten, is uitgegroeid tot een hele waardevolle vriendschap. Onze hele studie hebben we samen doorlopen. Het was altijd heel gezellig, niet alleen tijdens de colleges, maar ook in de trein (of we nou naar de Uithof gingen of naar de Barteljorisstraat) en tijdens onze etentjes (ongeacht welke film we keken). We hebben heel veel mooie momenten meegemaakt samen, waarvan onze reis naar Zuid-Afrika zonder twijfel de meest waardevolle is. Heel erg bedankt voor je onvoorwaardelijke vriendschap. Ik hoop dat onze vriendschap nog vele jaren zal blijven bestaan. Anita, enkele jaren geleden zijn wij tegelijkertijd aan ons promotieonderzoek begonnen. Wat was het fijn om samen dit traject te doorlopen. Jij was degene bij wie ik altijd terecht kon, als een experiment gelukt was, als een experiment mislukt was, als ik de kliniek miste of als ik over mijn kinderen wilde praten. Dankjewel dat je altijd voor me klaarstaat. Dankjewel voor je gezelligheid en dat je altijd bereid was me te helpen met mijn experimenten. Ik weet zeker, dat de afgelopen jaren slechts het begin waren van een lange vriendschap.

Lieve Christian, Janneke, Benjamin, Sanne, Andrea, Ad, Jolanda, Jorim, Dicole, Patrick en Laura. Dankjewel dat ik bij jullie kan zijn, wie ik ben. Ik ben heel blij met jullie als (schoon)familie.

Lieve pappie en memme. Ik ben zielsgelukkig, dat jullie mijn ouders zijn. Dank jullie wel voor jullie onvoorwaardelijke vertrouwen en liefde. Paps, dankjewel dat ik altijd bij je terecht kan voor adviezen en voor je oprechte interesse in mijn onderzoek. Ik ben uitermate trots op wat jij allemaal hebt bereikt. Mam, heel erg bedankt voor je warmte en voor alles wat je doet voor ons en de kinderen. Dankjewel dat de deur altijd voor ons openstaat.

Lieve Micha en Elin, er is niets fijner dan bij jullie en papa te zijn. Jullie maken mama de allergelukkigste van de hele wereld. Door jullie heeft het leven een gouden randje. Mama houdt oneindig veel van jullie.

Lieve Semya, er zijn geen woorden voor om te zeggen, hoe gelukkig ik met je ben. Dankjewel dat jij me laat zijn, wie ik ben en dat je er altijd voor me bent. Zonder jou zou ik niet de arts kunnen zijn, die ik wil zijn, en had ik dit onderzoek niet kunnen uitvoeren, zoals ik het heb uitgevoerd. Ons leven samen heeft ons al veel moois gebracht, maar dit is pas het begin. Dankjewel dat je mijn man bent. Ik hou van je.

Curriculum vitae

Désirée van Haaften-Visser was born on January 22nd 1985 in Den Helder, the Netherlands. In 2003 she graduated with honors from the 'Christelijke Scholengemeenschap De Goudse Waarden' grammar school and started her study medicine at the University Utrecht. During her study she performed an internship in gynecology in South-Africa and an internship in social medicine at the naval base at Curaçao. Furthermore she performed two scientific internships, both in the Wilhelmina Children's Hospital in Utrecht. The first research project was supervised by dr. Peter van Hasselt and focused on the incidence of late intracranial bleeding due to vitamin K deficiency. The second was entitled 'The effect of one mutation in the *ATP8B1* gene on hearing' and was supervised by prof. Roderick Houwen. In 2009 she obtained her medical degree with honors, after which she worked as research physician in the Wilhelmina Children's Hospital for a few months, where she continued her research on ATP8B1 deficiency, and also studied Wilson disease. In 2010 she started as resident in pediatrics at the Sint Antonius Hospital in Nieuwegein (supervisor dr. Walter Balemans), after which she continued a residency in pediatrics at the Wilhelmina Children's Hospital in Utrecht (supervisor dr. Joost Frenkel). In 2011 she started as PhD student in the Wilhelmina Children's Hospital under supervision of prof. Roderick Houwen and prof. Paul Coffer, where she studied genes associated with congenital intestinal diseases. This research has resulted in this thesis. Both as medical student and as PhD student she also participated as teacher in several courses for medical students at the University Utrecht. In 2016 she started her pediatric residency at the Maasstad Hospital in Rotterdam (supervisor dr. Michael Groeneweg). From July 2018 she will continue her residency in the Sophia Children's Hospital in Rotterdam (supervisor prof. Matthijs de Hoog). Désirée is married with Semya and has two children: Micha (2014) and Elin (2016).

List of publications

This thesis

Désirée Y. van Haaften-Visser, Magdalena Harakalova*, Enric Mocholi*, Joris M. van Montfrans, Abdul Elkadri, Ester Rieter, Karoline Fiedler, Peter M. van Hasselt, Emily M.M. Triffaux, Mieke M. van Haelst, Isaac J. Nijman, Wigard P. Kloosterman, Edward E.S. Nieuwenhuis, Aleixo M. Muise, Edwin Cuppen, Roderick H.J. Houwen, Paul J. Coffer. Ankyrin repeat and zinc-finger domain-containing 1 mutations are associated with infantile-onset inflammatory bowel disease. *J Biol Chem* 2017;292:7904–7920
* These authors contributed equally

Désirée Y. van Haaften–Visser*, Caroline L. Wiegerinck*, Andreas R. Janecke*, Kerstin Schneeberger*, Georg F. Vogel*, Johanna C. Escher, Rüdiger Adam, Cornelia E. Thöni, Kristian Pfaller, Alexander J. Jordan, Cleo-Aron Weis, Isaac J. Nijman, Glen R. Monroe, Peter M. van Hasselt, Ernest Cutz, Judith Klumperman, Hans Clevers, Edward E.S. Nieuwenhuis, Roderick H.J. Houwen, Gijs van Haaften, Michael W. Hess[#], Lukas A. Huber[#], Janneke M. Stapelbroek[#], Thomas Müller[#], Sabine Middendorp[#]. Loss of syntaxin 3 causes variant microvillus inclusion disease. *Gastroenterology* 2014;147:65–68
*[#] These authors contributed equally

Désirée Y. van Haaften – Visser, Caroline L. Wiegerinck, Charlotte I. de Bie, Johanna C. Escher, Janneke M. Stapelbroek, Peter M. van Hasselt, Roderick H.J. Houwen, Marielle E. van Gijn. Next-generation sequencing as a novel tool in the diagnosis of monogenetic GI disease: congenital diarrhea as an example. Submitted

Désirée Y. van Haaften – Visser*, Jorik M. van Rijn*, Freddy T.M. Kokke, Klaske D. Lichtenbelt, Maarten P.G. Massink, Karen J. Duran, Peter J.G. Nikkels, Edward E.S. Nieuwenhuis, Paul J. Coffer, Roderick H.J. Houwen, Gijs van Haaften, Sabine Middendorp. Loss of function of DGAT1 is associated with fat intolerance. Manuscript in preparation
* These authors contributed equally

Other publications

Wendy L. van der Woerd, **Désirée Y. van Haaften-Visser**, Stan F. J. van de Graaf, Claude Férec, Emmanuelle Masson, Janneke M. Stapelbroek, Peter Bugert, Heiko Witt, Roderick H.J. Houwen. Mutational analysis of ATP8B1 in patients with chronic pancreatitis. *PLoS ONE* 2013;8:e80553

Désirée Y. Visser, Nicolaas J. Jansen, Marloes M. IJland, Tom J. de Koning, Peter M. van Hasselt. Intracranial bleeding due to vitamin K deficiency: advantages of using a pediatric intensive care registry. *Intensive Care Med* 2011;37:1014–1020

Désirée Y. Visser, Anke L. Bootsma, Olle Th.J. ten Cate. Kennis, inzicht en toepassing: welke typen toetsvragen passen hierbij? *Tijdschrift voor Medisch Onderwijs* 2010;29(6):337-346

Désirée Y. Visser. Een maand naar de West. De marinearts op Curaçao. *Nederlands Militair Geneeskundig Tijdschrift* 2008;61(4):139-141